

SUPPORTING INFORMATION

Probing the Efficiency of Electron Transfer Through Porphyrin-Based Molecular Wires

Mikael U. Winters, Emma Dahlstedt, Holly E. Blades, Craig J. Wilson,
Michael J. Frampton, Harry L. Anderson, Bo Albinsson

Table of Contents for Supporting Information

(1) Ground State Absorption Spectra	page S2–S3
(2) Spectroelectrochemistry	page S3–S6
(3) Electrochemistry and Measurement of Redox Potentials	page S6
(4) Semi-Empirical PM3 Calculations	page S6–S7
(5) Calculation of State Energies	page S7–S8
(6) Pump-Probe Time-Resolved Absorption and Fluorescence	page S8–S12
(7) Synthetic Procedures	page S13–S23
(8) NMR spectra	page S24–S35
(9) MALDI mass spectra	page S36–S44
(10) References	page S45

Department of Chemical and Biological Engineering
Physical Chemistry
Kemivägen 3
SE - 412 96 Göteborg (Sweden)
Fax: (+46) 31 772 38 58
E-mail: balb@chalmers.se

and

Department of Chemistry, University of Oxford
Chemistry Research Laboratory
Mansfield Road
Oxford OX1 3TA (United Kingdom)
Fax: (+44) 1865 285 002
E-mail: harry.anderson@chem.ox.ac.uk

Section 1: Ground State Absorption Spectra

(1a) Monomer Series ($n = 1$). Figure S1 shows the absorption spectra of the porphyrin monomer triad (**Fc-P₁-C₆₀**) and the four related reference compounds (**Fc-P₁-Si**, **Si-P₁-C₆₀**, **Si-P₁-Si** and **Bu-P₁-Bu**). The spectra of **Fc-P₁-C₆₀** and **Bu-P₁-Bu** are similar, and red-shifted compared to the other compounds, demonstrating that the main change on adding the donor and acceptor groups to the porphyrin bridge are due to conjugation with the *para*-phenylene linker, rather than direct ground state interaction with the terminals. The absorption of the Fc donor and C₆₀ acceptor are primarily in the region below 300 nm, but both species have low-intensity bands stretching far into the visible region.^{1,2}

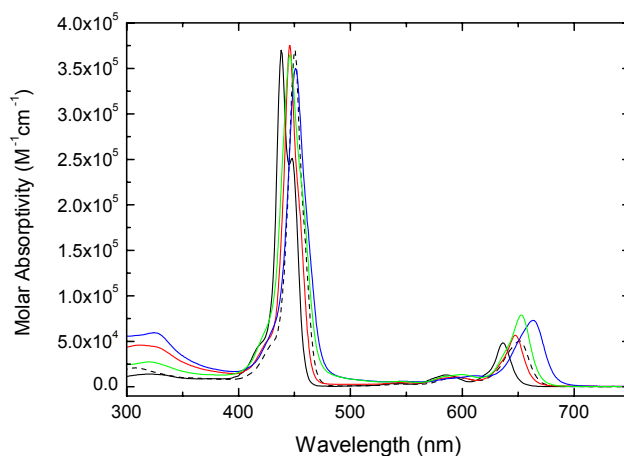


Figure S1. Ground-state absorption spectra of **Fc-P₁-C₆₀** (blue line) and the relevant reference compounds in THF (black line is **Si-P₁-Si**, dashed black line is **Bu-P₁-Bu**, red line is **Si-P₁-C₆₀**, and the green line is **Fc-P₁-Si**).

(1b) Dimer Series ($n = 2$). The ground-state absorption spectrum of **Si-P₂-Si** is significantly red-shifted relative to **Si-P₁-Si** due to the stabilization of the excited state of a larger conjugated system, and the peaks of the B- and Q-bands are split (Figure S2).

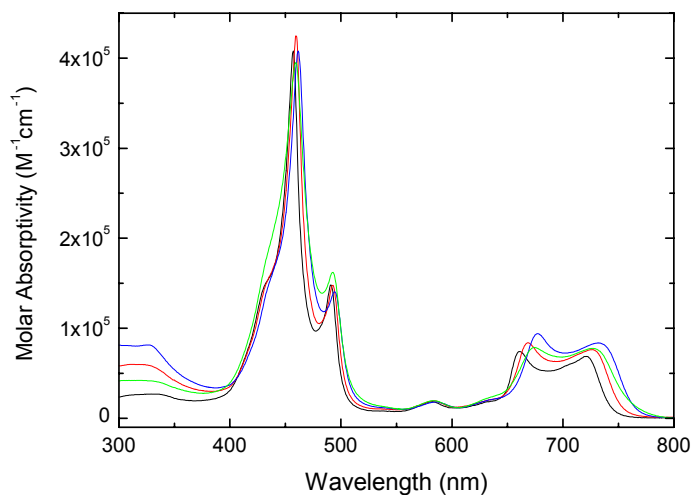


Figure S2. Absorption spectra of the dimer systems in THF. The black line is **Si-P₂-Si**, the red line is **Si-P₂-C₆₀**, the green line is **Fc-P₂-Si**, and the blue line is **Fc-P₂-C₆₀**.

(1c) Tetramer Series ($n = 4$). The ground-state absorption spectrum of **Si-P₄-Si** is significantly broadened compared to that of **Si-P₂-Si** and slightly shifted to the red (Figure S3). The coupling between the porphyrin constituents of this oligomer gives rise to several new transitions that together make up broad B- and Q-bands.^{3,4} The already quite large conjugated system is not affected much by the addition of the donor and acceptor, which is evident by the relatively small changes that occur between the tetramer and the various substituted systems (**P₄-C₆₀**, **Fc-P₄-Si** and **Fc-P₄-C₆₀**).

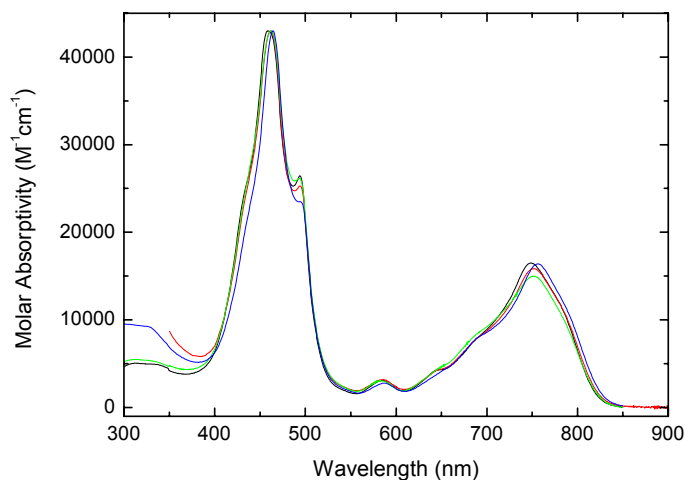


Figure S3. Ground-state absorption spectra of the tetramer systems in THF. The black line is **Si-P₄-Si**, the red line is **Si-P₄-C₆₀**, the green line is **Fc-P₄-Si**, and the blue line is **Fc-P₄-C₆₀**.

Section 2: Spectroelectrochemistry

(2a) General Experimental Details. The spectroelectrochemistry was performed using a modified 1 mm quartz cuvette with a platinum mesh (82×82 wires/inch, 65 % open area) functioning as working electrode for the electrolysis. An ordinary non-aqueous Ag/Ag⁺ electrode was used for reference and a Pt wire served as counter electrode. The solvents used (DCM and THF) were carefully purified and dried. Tetrabutylammonium perchlorate was used as supporting electrolyte (TBAP, 0.1 M), and this solution was used to record a baseline spectrum and subsequently deoxygenated by argon bubbling for approximately 60 min before the sample was introduced. The spectrometer used was set to the scan rate 4000 nm/min, which was fast enough for the time-scale on which the electrolysis took place. A spectrum was recorded every 30, 20 or 10 seconds and the scan was done in the wavelength region of primary interest for transient absorption (500–1100 nm).

(2b) Monomer Series ($n = 1$). In order to be able to interpret transient absorption data, spectra of the radicals **Si-P₁⁺-Si**, **Fc⁺** and **C₆₀⁻** were recorded by spectroelectrochemical means. The spectra were recorded between 500 and 1100 nm, which is the region of primary interest for transient absorption. The spectrum of the zinc porphyrin radical cation (**Si-P₁⁺-Si**) is shown in Figure S4. The sharp peak at 650 nm exhibited by the neutral species is less intense and shifted to shorter wavelengths (630 nm). New peaks are formed at 580, 716, 800, and 900 nm, which make the resulting spectrum rather broad. In a transient absorption experiment, the peak at 716 nm ($\epsilon \sim 13\,000\text{ M}^{-1}\text{cm}^{-1}$) is a good signature for **P₁⁺** as the 630 nm peak overlap with a strong negative peak due to ground-state bleaching (*vide infra*).

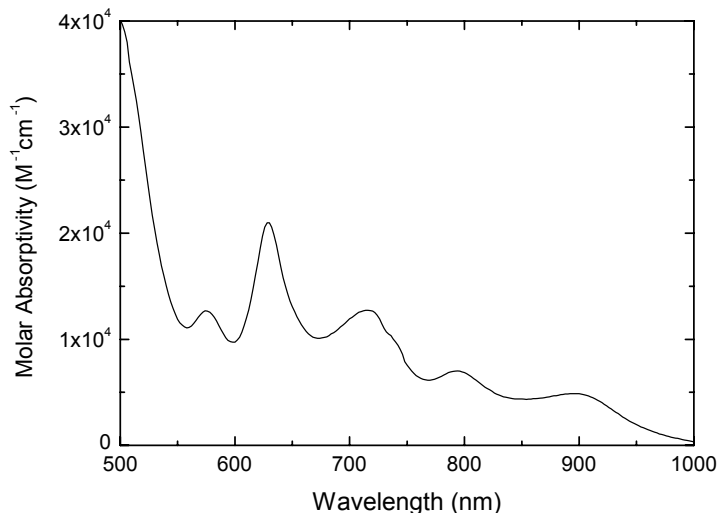


Figure S4. The spectrum of the porphyrin radical cation $\text{Si-P}_1^+\text{-Si}$, measured in THF with 0.1 M Bu_4NClO_4 .

The radical cation of the ferrocene donor has a broad absorption band centered at 750 nm (Figure S5), which is in a region where neutral ferrocene has no optical transitions. Sharp isosbestic points in the UV suggest that only one new species is formed. The molar absorptivity at 750 nm is approximately $2800 \text{ M}^{-1}\text{cm}^{-1}$. When the fullerene radical anion was generated, new peaks were formed at 920 and 1070 nm, and again isosbestic points in the UV show that these peaks are from the formation of a single new species, *i.e.* the anion radical (Figure S6). The molar absorptivity at 1070 nm was approximately $12000 \text{ M}^{-1}\text{cm}^{-1}$, a value similar to earlier reports.⁵

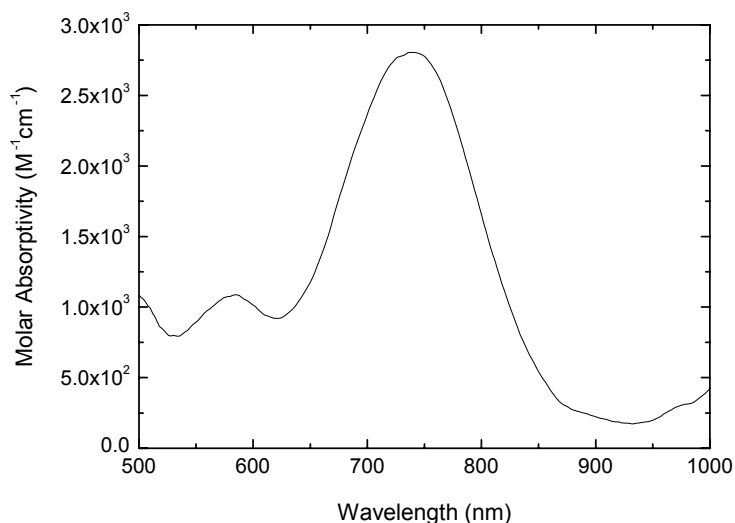


Figure S5. The spectrum of the ferrocene donor radical cation recorded in THF (0.1 M Bu_4NClO_4).

If it is assumed that the spectra of the species $\text{Fc-P}_1^+\text{-C}_{60}^-$ as well as $\text{Fc}^+\text{-P}_1\text{-C}_{60}^-$ are equivalent to the appropriately weighted linear combination of the component spectra, it is evident that the sum spectra has only one prominent peak between 800 and 1100 nm, *i.e.* at 1070 nm, and are otherwise broad with few sharp peaks. It is also clear that above 1000 nm, the absorption is dominated by the C_{60} anion radical. The peak at 1070 nm could not be detected with transient absorption due to limitations in the experimental set-up (white-light continuum generation) for which the measurable wavelength region is 450–1050 nm. Probing at or above 1000 nm should however result in a kinetic trace describing the formation and decay of C_{60}^- , and, as mentioned earlier, probing at 716 nm will give the same information about the porphyrin cation radical.

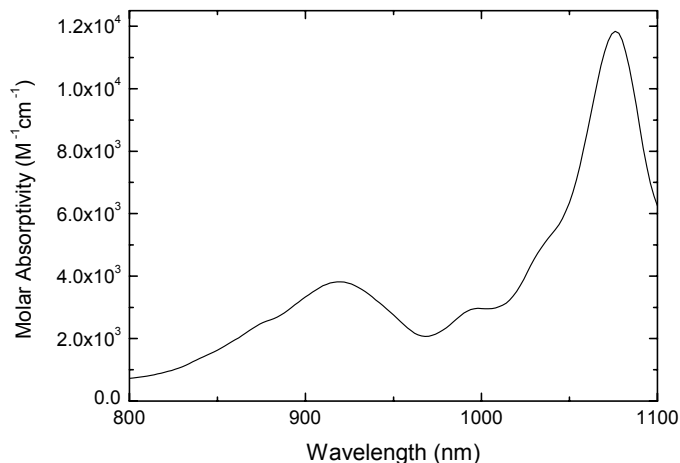


Figure S6. Absorption spectrum of the fullerene radical anion C_{60}^- in DCM (0.1 M Bu_4NClO_4).

(2c) Dimer Series ($n = 2$). When the mono-cation of **Si-P₂-Si** was generated, it was found that this species exhibits a very intense band with peak absorption at 964 nm ($\epsilon \sim 120\,000\text{ M}^{-1}\text{cm}^{-1}$) but an otherwise broad and less structured absorption in the studied region (500–1100 nm, Figure S7).⁶⁻⁸ During the electrolysis there were clean isosbestic points at 641 and 744, indicating that only the mono-cation is formed. The fact that this strong absorption partly overlap with the much weaker C_{60} anion absorption, makes it nearly impossible to detect a distinct spectroscopic signal from the anion. However, at longer times the porphyrin dimer cation formed from the first charge separation has returned to its ground-state, either by porphyrin-fullerene charge recombination or by accepting an electron from ferrocene. For the triad it is thus possible to assign any long-lived absorption above 1000 nm to the fullerene anion, which is then part of the fully charge separated system.

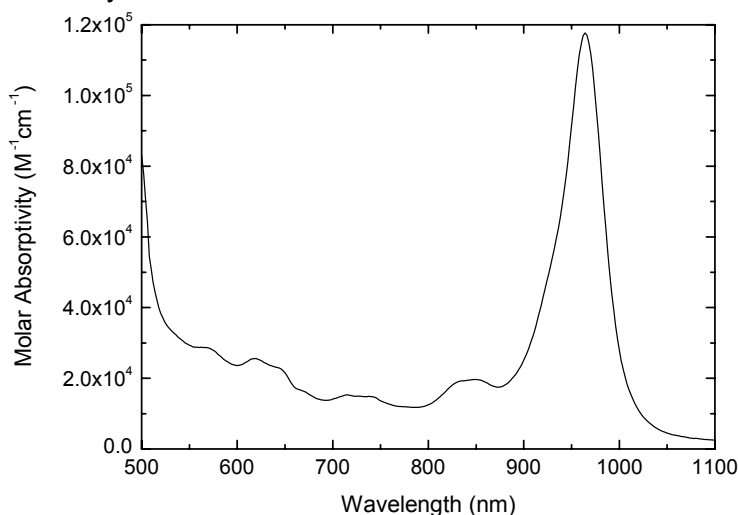


Figure S7. Absorption spectrum of the porphyrin dimer cation radical, exhibiting a very intense absorption band above 900 nm. The spectrum was recorded in THF with 0.1 M Bu_4NClO_4 .

(2d) Tetramer Series ($n = 4$). The electrolysis of the porphyrin tetramer was inefficient, but approximately 10% of the material was oxidized to the mono-cation radical, which was enough to get a rough spectrum but the molar absorptivity cannot be estimated with any accuracy (1×10^4 – $2 \times 10^4\text{ M}^{-1}\text{cm}^{-1}$). Compared to the neutral species, a new absorption band is formed at 1020 nm that completely overlaps with the absorption of C_{60}^- (Figure S8) and makes it impossible to detect unique signal from this anion radical when **Si-P₄-C₆₀** is investigated. For the

triad system, the charge shift that takes place means that the porphyrin tetramer cation radical decay to ground-state long before C_{60}^- and thus a unique signal can be detected from this species at longer delay times (Figure 3).

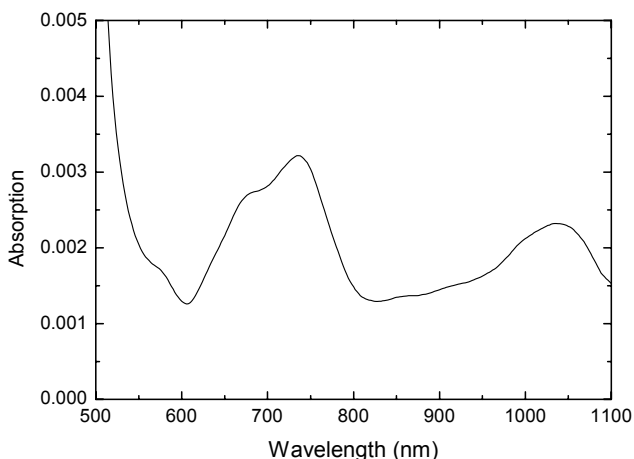


Figure S8. Approximate absorption spectrum of P_4^+ in THF with 0.1 M Bu_4NClO_4 .

Section 3: Electrochemistry and Measurement of Redox Potentials

Electrochemical experiments were performed using an Autolab PGSTAT12 potentiostat. Compounds were dissolved in THF containing Bu_4NBF_4 (0.1 M), under argon. A 3 mm glassy carbon working electrode was used with a Pt wire counter electrode and a $Ag/AgNO_3$ pseudo-reference electrode. The redox potentials of all the compounds synthesized during this study were measured using square-wave voltammetry (Table S1) and the reversibility of the redox waves was checked by cyclic voltammetry. Typical results are shown in Figures 2 and 3. In the case of **Si-P₁-Si**, **Bu-P₁-Bu**, **Bu-P₂-Bu** and **Bu-P₄-Bu** the potentials were referenced directly to internal ferrocene, but **Fc-P-C₆₀**, **Fc-P₂-C₆₀** and **Fc-P₄-C₆₀** were referenced to ferrocene via internal hexamethylferrocene to avoid overlap with the Fc/Fc^+ waves of the compounds.

Table S1: Summary of Redox Potentials^a

	Fc/Fc^+	P_n^+/P_n^+	P_n^+/P_n^{2+}	P_n^{2+}/P_n^{3+}	C_{60}/C_{60}^-	P_n^-/P_n^-	P_n^-/P_n^{2-}	P_n^{2-}/P_n^{3-}
Si-P₁-Si		0.53 V				-1.61 V		
Bu-P₁-Bu		0.44 V				-1.64 V		
Bu-P₂-Bu		0.40 V	0.56 V			-1.50 V	-1.62 V	
Bu-P₄-Bu		0.37 V	0.47 V	0.61 V		-1.43 V	-1.50 V	-1.66 V
Fc-P-C₆₀	0.04 V	0.45 V			-1.00 V	-1.60 V		
Fc-P₂-C₆₀	0.04 V	0.43 V	0.58 V		-1.00 V	-1.50 V	-1.63 V	
Fc-P₄-C₆₀	0.04 V	NR ^b	–	–	-1.00 V	-1.44 V	-1.59 V	-1.77 V

^a All redox potentials relative to internal ferrocene or decamethylferrocene ($E_{1/2}^{ox}$ -0.410 V vs Fc/Fc^+); electrolyte: 0.1 M Bu_4NBF_4 in THF (distilled over $LiAlH_4$); carbon working electrode, Pt counter electrode, $Ag/AgNO_3$ reference electrode.

^b Broad peak 0.33–0.62 V.

Section 4: Semi-Empirical PM3 Calculations

Energy-minimized molecular geometries were obtained using the semi-empirical PM3 method in Hyperchem 5.1 Pro. The distance R_{Fc-C60} was chosen to be the shortest distance between the closest sp^2 carbon connecting the C_{60} sphere to the oligomer and the first carbon of the cyclopentadienyl ring connected to the oligomer chain. The distances R_{P-C60} and R_{Fc-P} were taken between the centers of the P_n moieties and the carbons of C_{60} and Fc used above.

Table S2: Distances from PM3 calculations (Å)

compound	R_{P-C60}	R_{Fc-P}	R_{Fc-C60}
Fc-P-C₆₀	12.4	11.8	24.2
Fc-P₂-C₆₀	19.2	18.5	37.7
Fc-P₄-C₆₀	32.8	32.1	64.9

Section 5: Calculation of State Energies

The state energies presented in Figure 4 were estimated from Equations S1a-d by using redox potentials (Section 3 above) as well as absorption and emission spectra of the compounds in THF. A Coulomb stabilization term was included for the charged species ($\epsilon_s = \epsilon(\text{THF}@295\text{ K}) = 7.52$). The distances R_{P-C60} , R_{Fc-P} and R_{Fc-C60} , were estimated as specified above (Section 4). The driving forces for electron transfer presented in Table 2 could then be calculated from the relevant state energies. The energies of the triplet states of the porphyrin oligomers were determined from phosphorescence spectra measured at 80 K in 2-MTHF.⁹

$$E(\text{Fc-P}_n^*-\text{C}_{60}) = E_{00} \quad (\text{S1a})$$

$$E(\text{Fc-P}_n^+-\text{C}_{60}^-) = E(\text{P}_n/\text{P}_n^+) - E(\text{C}_{60}/\text{C}_{60}^-) - \frac{e}{4\pi\epsilon_0\epsilon_s R_{P-C60}} \quad (\text{S1b})$$

$$E(\text{Fc}^+-\text{P}_n-\text{C}_{60}) = E(\text{Fc}/\text{Fc}^+) - E(\text{P}_n/\text{P}_n^-) - \frac{e}{4\pi\epsilon_0\epsilon_s R_{Fc-P}} \quad (\text{S1c})$$

$$E(\text{Fc}^+-\text{P}_n-\text{C}_{60}^-) = E(\text{Fc}/\text{Fc}^+) - E(\text{C}_{60}/\text{C}_{60}^-) - \frac{e}{4\pi\epsilon_0\epsilon_s R_{Fc-C60}} \quad (\text{S1d})$$

E_{00} values were estimated from the intersection of the normalized Q-band absorption and emission spectra, to 1.87, 1.68, 1.59 eV for $n = 1, 2$ and 4 , respectively. Distances R_{P-C60} , R_{Fc-P} and R_{Fc-C60} were used from Table S2. $E(\text{Fc}/\text{Fc}^+)$ and $E(\text{C}_{60}/\text{C}_{60}^-)$ are the redox potentials from Table S1 (0.04 eV and -1.00 eV respectively); these redox potentials do not change with the length of the porphyrin oligomer bridge. The redox potentials $E(\text{P}_n/\text{P}_n^+)$ and $E(\text{P}_n/\text{P}_n^-)$ were taken from the values of **Bu-P_n-Bu** (Table S1); these values are better than those measured directly for **Fc-P_n-C₆₀** because (a) it is easier to measure the redox potentials for the bridge in the absence of redox active end groups and (b) values for **Bu-P_n-Bu** provide a better estimate of the energy required to charge the bridge of **Fc-P_n-C₆₀** when the terminals are not charged.

Section 6: Time-Resolved Fluorescence and Pump-Probe Transient Absorption

(6a) General Experimental Details. The solvent used for all spectroscopic experiments was tetrahydrofuran (THF, LABSCAN, HPLC grade), distilled immediately before the experiments.

Fluorescence lifetimes were determined using time-correlated single photon counting. The sample was excited in the B-band by the frequency-doubled output from a mode-locked Ti:Sapphire laser (Tsunami, Spectra Physics). A pulse selector (Model 3980, Spectra Physics) was used to achieve a 4 MHz repetition rate. The photons were collected by a micro channel plate photo multiplier tube (MCP-PMT R3809U-50, Hamamatsu) and fed into a multi-channel analyzer with 4096 channels. The detector response limited the time-resolution to approximately 20 ps. A minimum of 12 000 counts were recorded in the top channel. The intensity data was fitted by iteratively reconvoluting a two-exponential expression with the instrument response signal using the software package F900 (Edinburgh Instruments).

A pump-probe set up was used to record transient absorption spectra and transient absorption decays. A Ti:Sapphire oscillator (Tsunami, Spectra Physics) generating pulses approximately 90 fs broad (FWHM) was used to seed a Ti:Sapphire regenerative amplifier (Spitfire, Spectra Physics) that was pumped by a frequency-doubled diode-pumped Nd:YLF laser (Evolution-X, Spectra Physics) and produced pulses approximately 110 fs long (FWHM). The amplified laser

beam (790 nm) was divided by a 70/30 beam-splitter and the two beams were subsequently used as pump and probe. The pump beam was manipulated by an OPA (TOPAS, Light Conversion Ltd) to yield 450, 495 or 660 nm and was delayed relative to the probe pulse by either one of two available optical delay lines. The probe beam was obtained by focusing the remaining IR on a 1 mm sapphire plate, which generated a continuum from 450-1050 nm. The probe was subsequently divided into a reference beam and a probe beam, and the latter of these was overlapped by the pump at the sample. When spectra and decays were measured in the near-infrared, a combination of long-wave pass filters were used in order to completely block out visible light, otherwise the detected signal was dominated by secondary diffraction maxima from the monochromator used (TRIAX 180, ISA Instruments). All porphyrins have strong triplet absorption at approximately 500 nm, which without appropriate filters give strong, long-lived transient absorption signals at 1000 nm. The samples were dissolved in freshly distilled THF that was deoxygenated by argon bubbling and the optical density was approximately 1 at the excitation wavelength. The samples were contained in a moving 1 mm cuvette and excited at a 500 Hz repetition rate. The recorded traces were fitted individually and globally to a sum of exponentials convoluted with the cross-correlated pump and probe pulse (simulated by Gaussian pulse profiles) with home-made routines (MATLAB, Mathworks Inc.).

Excitation pulses for the nano-second transient absorption measurements were provided by a pulsed Nd:YAG laser (Continuum Surelite II-10, pulse width <7 ns) pumping an OPO giving a tuneable light source in the wavelength region between 400 and 700 nm. The probe light was provided by a Xenon arc lamp and was at a 90 degree angle relative to the excitation light. After hitting the sample, the probe light intensity was detected in two different ways. It was either passed through a monochromator and detected by a five-stage Hamamatsu R928 photomultiplier tube (for collecting decays) or collected by a CCD camera (ANDOR Technology). All samples were degassed by multiple freeze-pump-thaw cycles.

(6b) Monomer Series ($n = 1$). Steady state fluorescence measurements confirmed a very high degree of quenching of the porphyrin emission (>99 %) for the reference system containing the fullerene acceptor (**Si-P₁-C₆₀**) and the triad (**Fc-P₁-C₆₀**). However, when the second reference system (**Fc-P₁-Si**) was examined, it was found that the porphyrin fluorescence was also quenched very efficiently by ferrocene, probably by an energy transfer process. The transient absorption spectrum of **Fc-P₁-Si** did not disclose any formation of new species, which makes electron transfer (forming **Fc⁺-P₁⁻-Si**) a less likely competing deactivation pathway. Instead, low-lying excited states of ferrocene^{1,2,10} are believed to function as excitation energy acceptors that quench the porphyrin excited state. The competition that arises from this parallel quenching pathway becomes less important with increasing oligomer length, also indicating energy transfer as the likely cause of quenching since the gradual red-shift in oligomer absorption means smaller overlap between the transitions that are supposedly involved in this process and moreover, larger **Fc-P** distance.

Transient absorption measurements on the reference system **Si-P₁-C₆₀** show a clear build-up in excited state absorption at wavelengths indicative of the relevant porphyrin cation radical (716 nm) as well as at 900 and above 1000 nm, indicative of the anion radical (Figure S9). The data were accurately fitted to a two-exponential expression, and the life times found are related to the rate constants of Scheme 1 as described by the equations below (Equation S2). From these expressions, the rate constant for charge separation (k_{CS}) as well as for the subsequent recombination (k_{CR1}) were determined. The rate constant for charge separation calculated in this fashion agree with that estimated by fluorescence experiments (Table 1).

$$\tau_{21} = (k_f + k_{nr} + k_{CS})^{-1} \tag{S2}$$

$$\tau_{22} = (k_{CR1})^{-1}$$

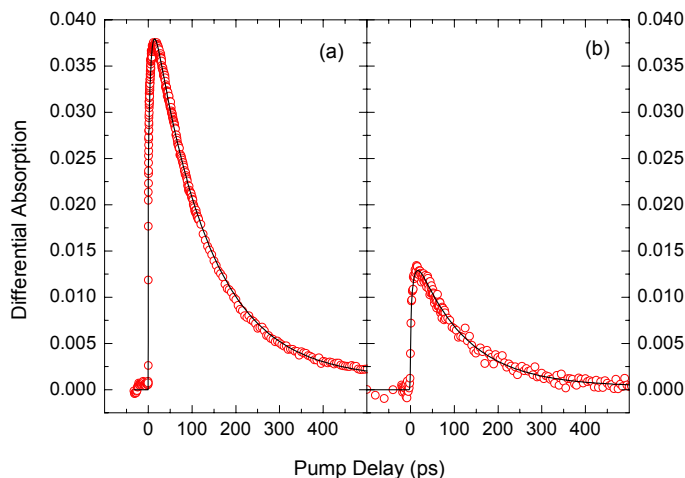


Figure S9. The left pane (a) shows the transient absorption rise and decay of **Si-P₁-C₆₀** at 716 nm, whereas the right pane (b) shows the transient absorption rise and decay at 1000 nm. In both cases a biexponential fit with $\tau_{21} = 6.1$ ps (rise-time) and $\tau_{22} = 130$ ps (decay) could be made successfully.

In the transient absorption spectra of **Fc-P₁-C₆₀**, the most long-lived absorption is formed at 1000 nm (Figures 6 and S10), and corresponds to the fullerene radical anion. Data from several wavelengths could successfully be fit in a global fashion to a three exponential expression, which is expected, as solving the differential equations describing the kinetics of the proposed model yield the three lifetimes (Equation S3):

$$\begin{aligned} \tau_{31} &= (k_f + k_{nr} + k_Q + k_{CS})^{-1} \\ \tau_{32} &= (k_{CR1} + k_{CSh})^{-1} \\ \tau_{33} &= k_{CR2}^{-1} \end{aligned} \quad (\text{S3})$$

The rate constant for quenching due to the ferrocene donor (k_Q) was determined by transient absorption measurements on the reference system **Fc-P₁-Si** (Table 1). If it is assumed that this rate and the rate for charge separation found for the **Si-P₁-C₆₀** system (k_{CS1}) does not change in the triad, Equation S3 can be used to calculate the expected value of τ_{31} . When the calculated value was compared to the lifetime found from experiments on **Fc-P₁-C₆₀**, perfect agreement was found. The lifetime determined for the long range charge separated state was approximately 640 ps, which is surprisingly short and indicate a strong electronic communication between donor and acceptor. The quantum yield for the primary charge separated state (**Si-P₁⁺-C₆₀⁻**) is approximately 37 %, whereas the overall quantum yield was about 29 % for the charge shifted state, as $k_{CSh} > k_{CR1}$ (Table 1).

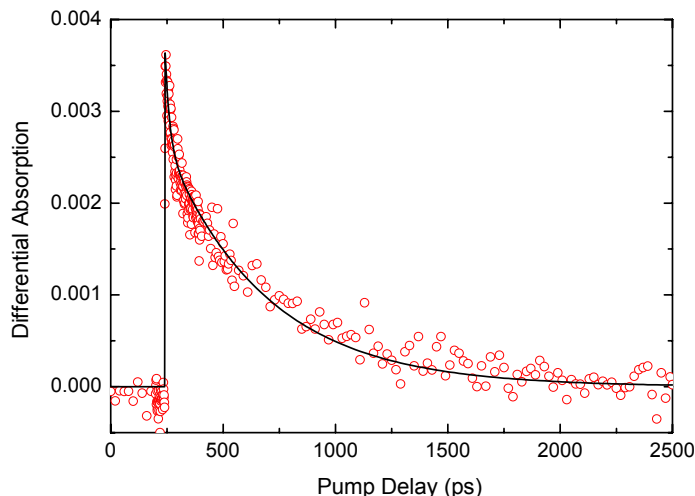


Figure S10. Transient absorption rise and decay for **Fc-P₁-C₆₀** recorded at 1000 nm with triexponential fit, $\tau_{31} = 2.7$ ps (rise), $\tau_{32} = 30$ ps (decay), and $\tau_{33} = 640$ ps (decay).

(6c) Dimer Series ($n = 2$). Steady-state fluorescence showed that the emission of the porphyrin dimer is quenched to a large extent for the systems **Si-P₂-C₆₀**, **Fc-P₂-Si** and **Fc-P₂-C₆₀**. However, the quenching efficiencies calculated from steady-state fluorescence indicate the presence of minute traces of a fluorescent impurity, as they are lower than those determined from rate constants determined by transient absorption. TCSPC measurements yielded a short lifetime coupled to the quenched excited state, but also a longer one similar to an unquenched porphyrin dimer and it is thus likely that there are traces of **Si-P₂-Si** in the samples.

Transient absorption measurements on **Si-P₂-C₆₀** yielded two lifetimes when decay traces from wavelengths characteristic of the involved radicals as well as of $S_1 \rightarrow S_n$ transitions and ground-state recovery were fitted in a global fashion. Further, an intense absorption peak is formed at 960 nm (Figure S11) as well as a much weaker absorption band above 1020 nm as was anticipated from the spectroelectrochemical measurements. These observations are consistent with the formation of the charge separated state **Si-P₂⁺-C₆₀⁻**. It should be noted however, that the charge separation behavior of **Si-P₂-C₆₀** is more complicated than described above, because of the rotational flexibility of the porphyrin-porphyrin linker, which leads to two spectroscopically distinct excited states. This introduces a wavelength dependent driving force for charge separation that is the subject of a separate study (manuscript in preparation).

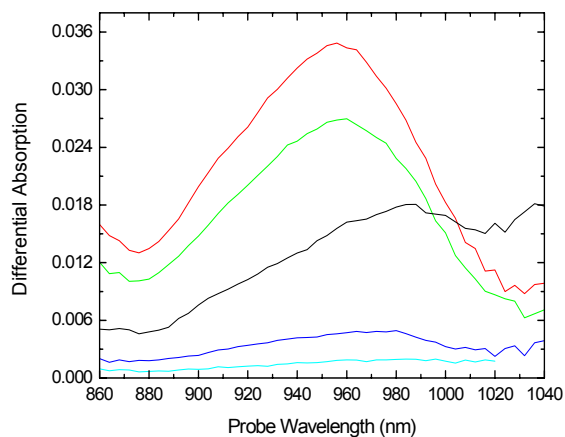


Figure S11. Near-infrared spectrum of **Si-P₂-C₆₀** at 0–5 ps (black line), 50 ps (red line), 100 ps (green line), 500 ps (blue line), and 1 ns (cyan line). The sample is in THF and was excited at 490 nm.

The transient absorption of **Fc-P₂-C₆₀** also exhibits the formation of strong absorption in the near infrared, centered at 980 nm. In the spectra there are also indications of a peak forming above 1000 nm and there is a long-lived absorption in this region (Figure 6). The decay of the porphyrin dimer cation radical is faster in the triad than in the dyad (Table 1), indicating that the charge shift forming the fully charge separated state takes place. This is also suggested by the transient signal formed at 760 nm after the porphyrin dimer ground-state recovery, which corresponds to the ferrocene radical cation and has a lifetime similar to that at 1000 nm (Figure S13). The fully charge separated state has a lifetime which is approximately 7.1 ns. This triad system was also investigated with a nano-second transient absorption set-up, but as this system had an approximate time resolution of 10 ns, no decay could be accurately determined.

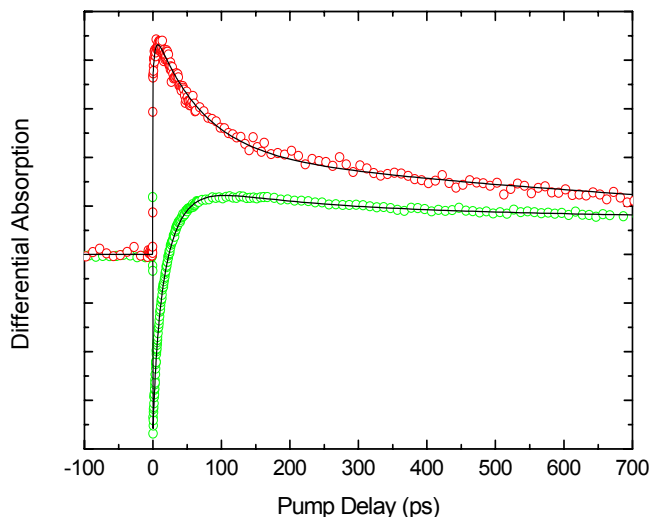


Figure S12. Transient absorption traces of **Fc-P₂-C₆₀** in THF measured at 1000 nm (red trace) and at 760 nm (green trace), as well as triexponential fits ($\tau_{31} = 5.9$ ps, $\tau_{32} = 41$ ps, and $\tau_{33} = 7100$ ps).

(6d) Tetramer Series ($n = 4$). The conformational heterogeneity of the porphyrin oligomers has several effects on the photophysics of the systems as well as on the charge transfer dynamics of the triads and reference systems. The fluorescence spectrum of **Si-P₄-Si** is excitation wavelength dependent, and shows that the conformational flexibility available to this molecule introduces a continuous distribution of states of different energies. This means that the quenching efficiency exhibits excitation wavelength dependence, as the driving force for electron transfer changes with the relative energy of the state excited. This behavior is treated in detail in a separate work and for the present study the porphyrin tetramer was excited at 495 nm for best comparison with **Si-P₂-Si**. Steady-state fluorescence quenching showed that the **Si-P₄-Si** fluorescence is quenched in all systems and this was confirmed by TCSPC measurements. However, the TCSPC measurements did not only yield quenched fluorescence lifetimes that roughly agree with those found by transient absorption, but also revealed traces of unquenched porphyrin tetramer.

When the transient absorption spectrum of **Si-P₄-C₆₀** in the visible region is compared to that of **Si-P₄-Si**, it is evident that the differential absorption decays faster for the dyad but no new peak from the formation of a cation is apparent due to the strong ground-state bleaching that overlaps with the absorption of the radical cation (Figure S3 & S8). Above 850 nm a transient absorption is built up (Figure 6 and S13), with a maximum at approximately 1010 nm, which shows that charge separation does take place in the system. Decay traces between 500 and 1000 nm were fitted globally to a two-exponential expression on the form:

$$\Delta A(t) = \alpha_1 \exp\{-t/\tau_1\} + \alpha_2 \exp\{-t/\tau_2\} + \alpha_3 \quad (\text{S4})$$

where α_3 is a constant included because of a higher triplet yield for this system compared to that for **Si-P-C₆₀** and **Si-P₂-C₆₀**. The lifetimes found were interpreted in terms of the kinetic model proposed for these systems (Equation S2, Table 1).

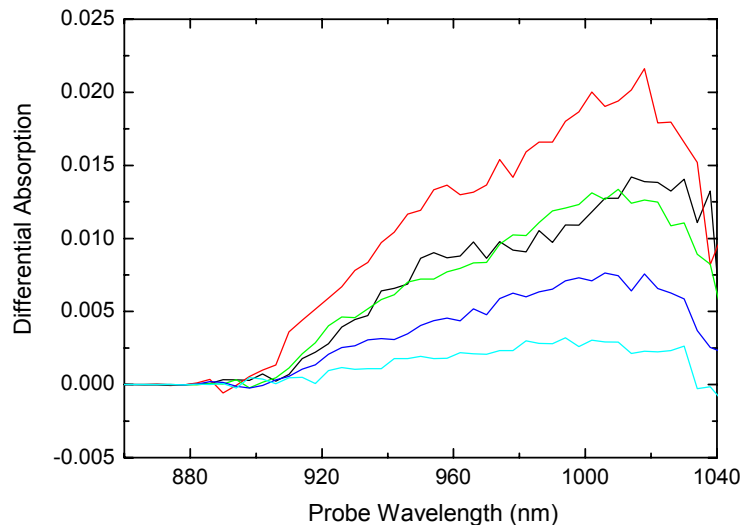


Figure S13. Differential absorption spectra of **Si-P₄-C₆₀** in the near IR at 1 ps (black line), 25 ps (red line), 250 ps (green line), 500 ps (blue line), and 1 ns (cyan line). The pump wavelength was 495 nm and the sample was dissolved in THF.

The fluorescence studies showed that the ferrocene donor also quenches the tetramer, but the rate of quenching of **Fc-P₄-Si** is slower than that for **Fc-P₁-Si** and **Fc-P₂-Si**. The lifetimes found when decay data was fitted correlated to the fluorescence lifetimes (Table 1). In the transient absorption spectrum of **Fc-P₄-C₆₀**, strong absorption is formed in the near-infrared. After 2 ns only two features remain in the spectrum, that is, absorption above 1000 nm and also a weak band centered at approximately 810 nm (Figure S14). These absorption bands are characteristic of **C₆₀⁻** and **Fc⁺** and show that the fully charge separated state is produced also for the tetramer triad. The lifetime for this state was estimated to 7.8 ns. Measurements on this system were also performed with nano-second transient absorption, but no accurate decay could be determined.

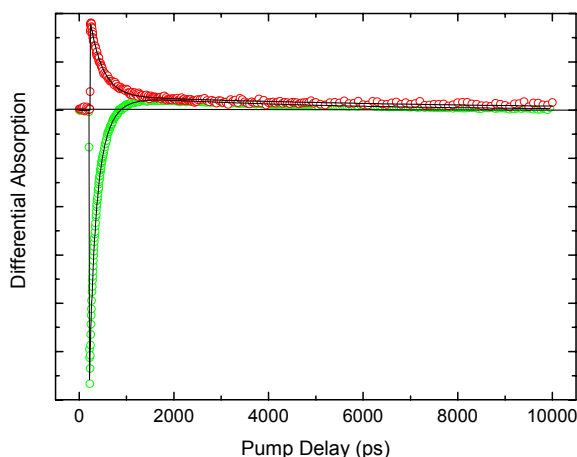
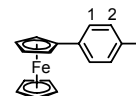


Figure S14. Transient absorption formed at 810 nm (green trace) and 1000 nm (red trace) when **Fc-P₄-C₆₀** in THF is excited at 495 nm. Also shown are triexponential fits ($\tau_{31} = 18$ ps, $\tau_{32} = 175$ ps, and $\tau_{33} = 7800$ ps).

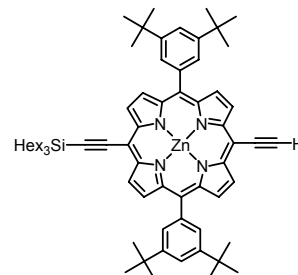
Section 7: Synthetic Procedures

General. When required, solutions were degassed by boiling under reduced pressure followed by saturating with argon; this cycle was repeated twice. Dry NEt_3 was distilled from CaH_2 . Dried THF, CH_2Cl_2 and toluene were obtained by passing through alumina under N_2 pressure. All other reagents were used as commercially supplied. Flash column chromatography was carried out on silica gel 60 under positive pressure. TLC was carried out on aluminium backed silica gel 60 F254 plates. Where mixtures of solvents were used ratios are reported by volume. NMR spectra were recorded at ambient probe temperature on Bruker instruments. All chemical shifts are given in parts per million relative to residual protonated solvent. The majority of MALDI-ToF spectra were recorded on a Micromass ToF Spec 2E at Oxford. Fast atom bombardment (FAB) mass spectrometry was conducted at the EPSRC National Mass Spectrometry Service Centre at Swansea on a Finnigan MAT900. MALDI-ToF MS conducted at Swansea used a Voyager-DE-STR. Only molecular ions and major peaks are reported. Elemental analysis was performed by Elemental Microanalysis Ltd., Okehampton or I.C.L. Analytical Services, Oxford.

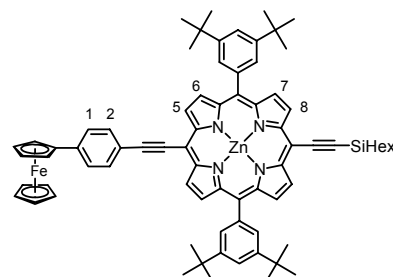
4-Iodophenylferrocene: This known compound was prepared by following a procedure of Ambroise et al.¹¹ 4-Iodoaniline (4.38 g, 20.0 mmol) was suspended in a mixture of conc. HCl (12 mL) and H_2O (45 mL). The suspension was stirred in an ice bath and solution of NaNO_2 (3.04 g, 44.0 mmol) in H_2O (10 mL) was added drop wise, while carefully maintaining a temperature of 0–5 °C. After the addition, the reaction was stirred for 30 min at 0 °C. The resulting diazonium salt solution was then added slowly to a solution of ferrocene (3.395 g, 18.25 mmol) in toluene (180 mL) at 0 °C. Instantaneous evolution of gas was observed. The reaction was stirred at 0 °C for 1 h, and then allowed to warm to 20 °C with stirring for 16 h. The aqueous and organic layers were separated and the aqueous layer was extracted with toluene. The combined organic layers were washed with saturated aqueous NaHCO_3 and brine. The solvents were removed and column chromatography (40–60 petroleum ether/0–1% CH_2Cl_2), followed by layer precipitation (40–60 petroleum ether/ CH_2Cl_2) gave orange crystals (1.33 g, 19 %). mp 122.7–123.6 °C. ^1H NMR (400 MHz, CDCl_3) δ = 7.60 (d, 2H, J = 7.5 Hz, Ar- H^2), 7.27 (br. s, 2H, Ar- H^1), 4.65 (br. s, 2H, Fc- H), 4.37 (br. s, 2H, Fc- H), 4.07 (s, 5H, Fc- H). As lit.¹¹



Zinc 5, 15-bis-(3,5-di-*tert*-butyl-phenyl)-10-ethynyl-20-trihexylsilyl-ethynylporphyrin; Si-P₁-H: Porphyrin **Si-P₁-Si** (1.54 g, 1.13 mmol) was dissolved in a 1:1 mixture of $\text{CH}_2\text{Cl}_2/\text{CHCl}_3$ (565 ml). TBAF (1.7 ml of a 1.0 M solution in THF) was added to the stirred solution. The reaction was monitored by TLC (40–60 petroleum ether/EtOAc/pyridine 10:1:1) until an optimal product mixture had been reached. After 40 min HOAc (0.21 mL) was added to quench the reaction. The volume was reduced and the mixture passed through a short silica plug (CH_2Cl_2). Column chromatography (40–60 petroleum ether/EtOAc/pyridine 100:1:1) gave pure zinc 5,15-bis-(3,5-di-*tert*-butyl-phenyl)-10-ethynyl-20-trihexylsilyl-ethynylporphyrin **Si-P₁-H** (474 mg, 37 %). R_f (40–60 petroleum ether/EtOAc/pyridine 10:1:1) = 0.65. ^1H NMR (200 MHz, CDCl_3) δ = 9.66 (m, 4H, $\beta\text{-H}^1$, $\beta\text{-H}^4$), 8.98 (m, 4H, $\beta\text{-H}^2$, $\beta\text{-H}^3$), 8.00 (d, 4H, J = 1.9 Hz, Ar- H^{ortho}), 7.78 (br. s, 2H, Ar- H^{para}), 4.12 (s, 1H, C \equiv C- H), 1.75 (m, 6H, hexyl- CH_2), 1.50–0.88 (m, 54H, 18 hexyl- CH_2 , 36 $^t\text{Bu-CH}_3$), 0.91 (m, 15H, hexyl- CH_2). Bis-protected zinc 5, 15-bis-(3,5-di-*tert*-butyl-phenyl)-10,20-bis-ethynylporphyrin **H-P₁-H** (312 mg, 33 %). R_f (40–60 petroleum ether/EtOAc/pyridine 10:1:1) = 0.56. ^1H NMR (200 MHz, CDCl_3) δ = 9.79 (d, 4H, $\beta\text{-H}$), 8.89 (d, 4H, $\beta\text{-H}$), 7.99 (d, 4H, J = 1.7 Hz, Ar- H^{ortho}), 7.78 (br. s, 2H, Ar- H^{para}), 4.12 (s, 2H, C \equiv C- H), 1.52 (s, 36H, $^t\text{Bu-CH}_3$). Recovered starting zinc 5, 15-bis-(3,5-di-*tert*-butyl-phenyl)-10,20-bistrihexylsilyl-ethynylporphyrin **Si-P₁-Si** (481 mg, 30 %).

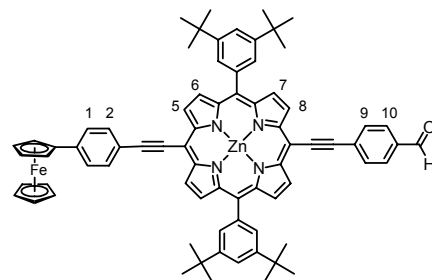


Fc-P₁-Si: $\text{Pd}_2(\text{dba})_3$ (1 mg, 1.56 μmol), CuI (1 mg, 6.2 μmol), PPh_3 (3 mg, 12.4 μmol), **Si-P₁-H**, (50 mg, 0.047 mmol) and 4-iodophenylferrocene (36 mg, 0.094 mmol) were placed in a dried flask and under argon. Toluene (2 mL) and NEt_3 (2 mL) were added and the reaction mixture degassed. The reaction mixture was stirred at 40 °C for 1.5 h. The reaction was monitored by TLC (40–60 petroleum ether/EtOAc/pyridine 20:1:1). When the reaction was complete, the

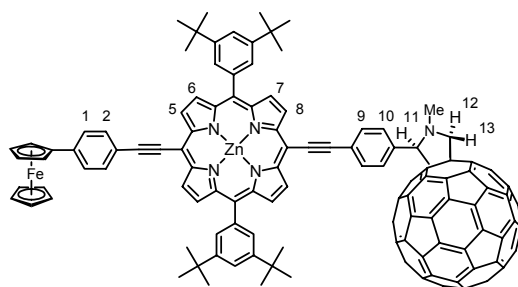


volume was reduced and the mixture passed through a short silica plug (CH₂Cl₂). Column chromatography (40-60 petroleum ether/EtOAc/pyridine 100:1:1 increasing the polarity to 100:4:1), followed by layer precipitation (CH₂Cl₂/MeOH) gave a green powder (47 mg, 75 %). *R_f* (40-60 petroleum ether/EtOAc/Pyridine 20:1:1) = 0.4. λ_{max} (CH₂Cl₂)/nm (log ϵ) 443 (5.77), 536 (4.27), 584 (4.35), 640 (4.99), 694 (4.05). ¹H NMR (400 MHz, CDCl₃) δ = 9.74 (d, 2H, *J* = 4.4 Hz, β -H⁵), 9.65 (d, 2H, *J* = 4.6 Hz, β -H⁶), 8.92 (d, 2H, *J* = 4.4 Hz, β -H⁶), 8.88 (d, 2H, *J* = 4.6 Hz, β -H⁷), 8.03 (d, 4H, *J* = 1.8 Hz, Ar-H^{ortho}), 7.94 (d, 2H, *J* = 8.4 Hz Ar-H²), 7.80 (t, 2H, *J* = 1.8 Hz, Ar-H^{para}), 7.65 (d, 2H, *J* = 8.4 Hz Ar-H¹), 4.78 (t, 2H, *J* = 1.8 Hz, Fc-H), 4.42 (t, 2H, *J* = 1.8 Hz, Fc-H), 4.13 (s, 5H, Fc-H), 1.81–1.75 (m, 6H, hexyl-CH₂), 1.58 - 1.51 (m, 42H, 6 hexyl-CH₂, 36 ^tBu-CH₃), 1.44–1.34 (m, 12H, hexyl-CH₂), 1.03–0.99 (m, 6H, hexyl-CH₂), 0.90 (t, 9H, *J* = 7.1 Hz, hexyl-CH₃). ¹³C NMR (63 MHz, CDCl₃) δ = 152.8, 152.2, 150.9, 150.8, 149.9, 143.9, 142.1, 140.4, 136.2, 133.2, 132.0, 131.3, 131.0, 130.3, 126.6, 124.4, 122.8, 122.0, 121.3, 109.8, 101.9, 101.3, 99.9, 97.3, 93.9, 84.9, 77.7, 77.4, 77.2, 70.2, 69.9, 67.0, 35.5, 33.8, 32.2, 32.1, 24.8, 23.1, 14.6, 14.4. *m/z* (MALDI ToF MS⁺): 1340.2 (C₈₆H₁₀₂N₄SiZnFe, [M]⁺, requires 1341.66).

Fc-P₁-CHO: TBAF (247 μ L of a 1.0 M solution in THF, 0.247 mmol) was added to a stirred solution of **Fc-P₁-Si** (221 mg, 0.165 mmol) in CH₂Cl₂ (56 mL). The reaction was monitored by TLC (40-60 petroleum ether/EtOAc/pyridine 10:1:1). After quenching with HOAc, the reaction mixture was passed through a short silica plug (CH₂Cl₂), and the solvents removed. *R_f* (40-60 petroleum ether/EtOAc/pyridine 10:1:1) = 0.4. 4-Bromobenzaldehyde (305 mg, 1.65 mmol), Pd(PPh₃)₄ (38 mg, 3.2 mmol), CuI (8 mg, 0.043 mmol), were added under argon. Toluene (6 mL) and NEt₃ (4 mL) were added and the reaction mixture degassed. The reaction mixture was stirred at 40 °C for 20 h. The reaction was monitored by TLC (40-60 petroleum ether/EtOAc/pyridine 10:1:1). When the reaction was complete, the volume was reduced and the mixture passed through a short silica plug (CH₂Cl₂). Column chromatography (40-60 petroleum ether/EtOAc/pyridine 100:1:1 increasing the polarity to 100:4:1), followed by layer precipitation (CH₂Cl₂/MeOH) gave a green powder (106 mg, 55 %). *R_f* (40-60 petroleum ether/EtOAc/pyridine 10:1:1) = 0.3. ν_{max} /cm⁻¹ 2962 (C–H), 2188 (C≡C), 1700 (C=O), 881 (C–H Arom.), 821 (C–H Arom.). ¹H NMR (400 MHz, CDCl₃) δ = 10.10 (s, 1H, CHO), 9.70 (d, 2H, *J* = 4.6 Hz, β -H⁸), 9.69 (d, 2H, *J* = 4.6 Hz, β -H⁵), 8.93 (d, 2H, *J* = 4.6 Hz, β -H⁷), 8.90 (d, 2H, *J* = 4.6 Hz, β -H⁶), 8.13 (d, 2H, *J* = 8.1 Hz, Ar-H¹⁰), 8.05–8.03 (m, 6H, 4 Ar-H^{ortho}, 2 Ar-H₉), 7.92 (d, 2H, *J* = 8.1 Hz, Ar-H²), 7.80 (t, 2H, *J* = 1.6 Hz, Ar-H^{para}), 7.60 (d, 2H, *J* = 8.1 Hz, Ar-H¹), 4.76 (d, 2H, *J* = 1.5 Hz, Fc-H), 4.41 (d, 2H, *J* = 1.5 Hz, Fc-H), 4.12 (s, 5H, Fc-H), 1.55 (s, 36H, ^tBu-CH₃). *m/z* (MALDI ToF MS⁺): 1163.3 (C₇₅H₆₉N₄SiZnFe, [M+H]⁺, requires 1163.41).



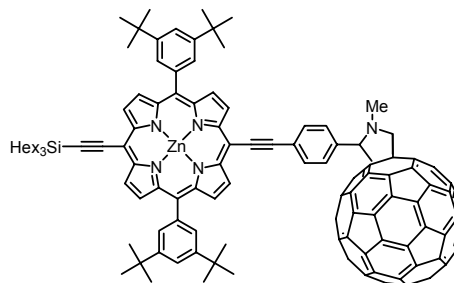
Fc-P₁-C₆₀: A mixture of **Fc-P₁-CHO** (91 mg, 0.078 mmol), sarcosine (350 mg, 3.90 mmol), and C₆₀ (283 mg, 0.390 mmol) were dissolved in toluene (295 mL). The reaction mixture was degassed and refluxed for 18 h under argon. Solvents were removed and column chromatography (petroleum ether/toluene 1:1, gradually increasing the polarity to 3:7 to pure toluene), followed by layer precipitation (CH₂Cl₂/MeOH) gave a green powder (93 mg, 62 %). *R_f* (petroleum ether/toluene 3:7) = 0.7. λ_{max} (CH₂Cl₂)/nm (log ϵ) 452 (5.77), 673 (4.82). ¹H NMR (400 MHz, CDCl₃) δ = 9.74 (d, 2H, *J* = 4.4 Hz, β -H⁵) 9.72 (d, 2H, *J* = 4.6 Hz, β -H⁸), 8.92–8.89 (m, 4H, β -H⁶, β -H⁷), 8.10–8.06 (m, 2H, Ar-H⁹), 8.04–8.02 (m, 4H, Ar-H^{ortho}), 7.99–7.92 (m, 4H, 2 Ar-H², 2 Ar-H¹⁰), 7.81–7.79 (m, 2H, Ar-H^{para}), 7.65 (d, 2H, *J* = 8.8 Hz, Ar-H¹), 5.02–4.98 (m, 2H, H¹² or H¹³, H¹¹), 4.78 (br.s, 2H, Fc-H), 4.42 (br.s, 2H, Fc-H), 4.27 (d, 1H, *J* = 9.7 Hz, H¹² or H¹³), 4.13 (br. s, 5H, Fc-H), 2.91 (s, 3H, N-CH₃), 1.56 (s, 36H, ^tBu-CH₃). *m/z* (MALDI ToF MS⁺): 1909.5 (C₁₃₇H₇₃N₅SiZnFe, [M]⁺, requires 1909.46).



Si-P₁-CHO: TBAF (1.0 M in THF, 0.550 mL, 0.550 mmol) was added to a solution of **Si-P₁-Si** (500 mg, 0.367 mmol) in CH₂Cl₂/CHCl₃ (1:1, 68 mL) and the solution stirred for 30 min, with monitoring by TLC. Granular CaCl₂ (ca. 200 mg) was added and the mixture filtered through a plug of silica (CH₂Cl₂) and then

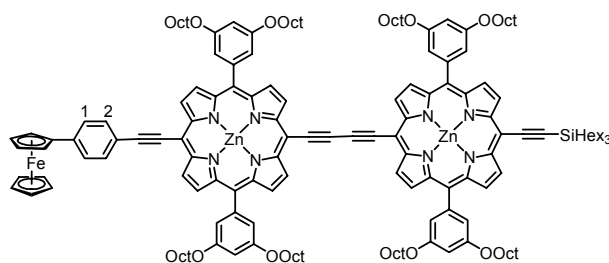
the solvent was removed. 4-bromobenzaldehyde (678 mg, 3.6 mmol), CuI (18 mg, 0.095 mmol), Pd(PPh₃)₄ (85 mg, 0.073 mmol), toluene (15 mL) and Et₃N (10 mL) were added, the solution purged with nitrogen then heated under argon at 60 °C for 20 h. The solvent was removed and the residue purified by column chromatography over silica (40-60 petroleum ether/EtOAc/pyridine 10:1:1) to give the desired mono-aldehyde product (149 mg, 34%). ¹H NMR (400 MHz, CDCl₃) δ = 10.02 (s, 1H, CHO), 8.98 (d, 2H, *J* = 4.5 Hz, β-*H*), 9.03 (d, 2H, *J* = 4.5 Hz, β-*H*), 9.74 (d, 2H, *J* = 4.5 Hz, β-*H*), 9.76 (d, 2H, *J* = 4.5 Hz, β-*H*), 8.06 & 8.13 (m, 4H, Ar-*H*), 8.05 (d, 4H, *J* = 2.0 Hz, Ar-*H*^{ortho}), 7.86 (d, 2H, *J* = 2.0 Hz, Ar-*H*^{para}), 1.81–1.72 (m, 6H, hexyl-CH₂), 1.61–1.50 (m, 6H, hexyl-CH₂), 1.56 (36 H, s, *t*-butyl-*H*), 1.45–1.34 (m, 12H, hexyl-CH₂), 1.03 (m, 6H, hexyl-CH₂), 0.91 (t, 9H, *J* = 7.0 Hz, hexyl-CH₃). *m/z* (MALDI ToF MS⁺): 1187.9 (C₇₇H₉₄N₄O₅SiZn, [M]⁺, requires 1184.6).

Si-P₁-C₆₀: A solution of **Si-P₁-CHO** (149 mg, 0.123 mmol), C₆₀ (453 mg, 0.629 mmol) and sarcosine (560 mg, 629 mmol) in toluene (480 mL) was heated under argon at reflux for 20 h. The solvent was removed and the residue purified by column chromatography over silica (40-60 petroleum ether/toluene 1:1), then layered reprecipitated (CH₂Cl₂/MeOH) to give a dark green solid (156 mg, 64%). *R_f* (40-60 petroleum ether/toluene 1:1) = 0.4. ¹H NMR (400 MHz, CDCl₃/CS₂ 1:1) δ = 9.15 (d, 2H, *J* = 4.5 Hz, β-*H*), 9.05 (d, 2H, *J* = 4.5 Hz, β-*H*), 8.35 (d, 2H, *J* = 4.6 Hz, β-*H*), 8.31 (d, 2H, *J* = 4.6 Hz, β-*H*), 7.43–7.41 (m, 6H, Ar-*H*), 7.20 (s, 4H, Ar-*H*), 4.08 (d, 1H, *J* = 9 Hz, NCHH), 4.03 (s, 1H, NCH), 3.27 (d, 1H, *J* = 9 Hz, NCHH), 2.22 (s, 3H, N-CH₃), 1.22–1.13 (m, 6H, hexyl-CH₂), 0.97–0.93 (m, 42H, 6 hexyl-CH₂, 36 ^tBu-CH₃), 0.86–0.76 (m, 12H, hexyl-CH₂), 0.45–0.41 (m, 6H, Si-CH₂), 0.34 (t, 9H, *J* = 7 Hz, hexyl-CH₃). *m/z* (MALDI ToF MS⁺): 1931.7 (C₈₉H₄₉NSi, [M]⁺, requires 1931.7).



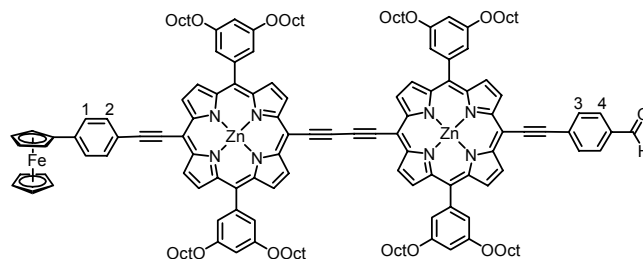
Si-P₂-H: **Si-P₂-Si** (0.490 g, 0.18 mmol) was dissolved in a 1:1 mixture of CH₂Cl₂/CHCl₃ (60 mL). TBAF (0.27 mL of a 1.0 M solution in THF) was added to the stirred solution. The reaction was monitored by TLC (40-60 petroleum ether/EtOAc/pyridine 10:1:1) until an optimal product mixture had been reached. After 40 min HOAc (25 μL) was added to quench the reaction. The volume was reduced and the mixture passed through a short silica plug (CH₂Cl₂). Column chromatography (40-60 petroleum ether/EtOAc/pyridine 10:1:1) gave **Si-P₂-H** (0.285 g, 65 %). *R_f* (40-60 petroleum ether/EtOAc/pyridine 10:1:1) = 0.52. ¹H NMR (400 MHz, CDCl₃/5% *d*₅-pyridine) δ = 9.90 (d, 2H, *J* = 4.6 Hz, β-*H*), 9.88 (d, 2H, *J* = 4.6 Hz, β-*H*), 9.66 (t, 4H, *J* = 4.6 Hz, β-*H*), 9.09 (d, 2H, *J* = 4.6 Hz, β-*H*), 9.08 (d, 2H, *J* = 4.6 Hz, β-*H*), 9.00 (d, 2H, *J* = 4.6 Hz, β-*H*), 8.98 (d, 2H, *J* = 4.6 Hz, β-*H*), 7.39 (d, 8H, *J* = 2.4 Hz, Ar-*H*^{ortho}), 6.92 (br. t, 4H, *J* = 2.0 Hz, Ar-*H*^{para}), 4.21–4.15 (m, 17H, C≡C-*H*, 16 O-CH₂), 1.94–1.87 (m, 16H, octyl-CH₂), 1.83–1.76 (m, 6H, hexyl-CH₂), 1.61–1.51 (m, 24H, hexyl-CH₂), 1.47–1.26 (m, 80 H, octyl-CH₂), 1.06–1.02 (m, 6H, hexyl-CH₂), 0.95–0.91 (m, 9H, hexyl-CH₃), 0.90–0.87 (m, 24H, octyl-CH₃). *m/z* (MALDI ToF MS⁺) 2450.3 (C₁₅₄H₂₀₄N₈O₈Si₂Zn₂, [M]⁺, requires 2449.42).

Fc-P₂-Si: Pd₂(dba)₃ (2 mg, 2.03 μmol), **Si-P₂-H** (150 mg, 0.061 mmol) and 4-iodophenylferrocene (48 mg, 0.122 mmol) were placed in a dried flask under argon. Toluene (6 mL) and Et₃N (6 mL) were added and the reaction mixture degassed. The reaction mixture was stirred at 40 °C for 1.5 h. The reaction was monitored by TLC (40-60 petroleum ether/EtOAc/pyridine 20:1:1). When the reaction was complete, the volume was reduced and the mixture passed through a short silica plug (CH₂Cl₂). Column chromatography (40-60 petroleum ether/EtOAc/pyridine 100:1:1, increasing the polarity accordingly) gave a green solid (84 mg, 51 %). *R_f* (40-60 petroleum ether/EtOAc/pyridine 20:1:1) = 0.4. λ_{max} (CH₂Cl₂)/nm (log ε) 458 (5.32), 489 (5.10), 577 (4.21), 658 sh (4.61), 709 (4.79). ¹H NMR (400 MHz, CDCl₃/5% *d*₅-pyridine). δ = 9.89 (m, 4H, β-*H*), 9.75 (d, 2H, *J* = 4.5 Hz, β-*H*), 9.66 (d, 2H, *J* = 4.5 Hz, β-*H*), 9.08 (m, 4H, β-*H*), 9.01 (d, 2H, *J* = 4.5 Hz, β-*H*), 8.98 (d, 2H, *J* = 4.5 Hz, β-*H*), 7.97 (d, 2H, *J* = 7.8 Hz, Ar-



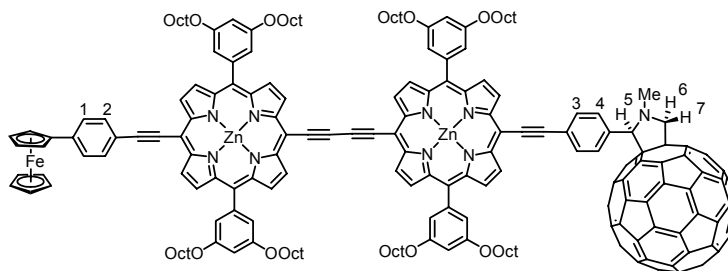
H^2), 7.69 (d, 2H, $J = 7.8$ Hz, Ar- H^2), 7.14 (d, 8H, $J = 2.0$ Hz, Ar- H^{ortho}), 6.93 (br. s, 4H, Ar- H^{para}), 4.80 (d, 2H, $J = 1.3$ Hz, Fc- H), 4.44 (d, 2H, $J = 1.3$ Hz, Fc- H), 4.19–4.15 (m, 21H, 16 O- CH_2 , 5 Fc- H), 1.92 (m, 16H, octyl- CH_2), 1.80 (m, 6H, hexyl- CH_2), 1.57–1.27 (m, 98H, 80 octyl- CH_2 , 18 hexyl- CH_2), 0.95–0.73 (m, 39H, 24 octyl- CH_3 , 15 hexyl- CH_2/CH_3). m/z (MALDI ToF MS+) 2715.4 ($C_{170}H_{216}FeN_8O_8SiZn_2$, $[M]^+$, requires 2715.45).

Fc-P₂-CHO: TBAF (29 μ L of a 1.0 M solution in THF, 0.029 mmol) was added to a stirred solution of **Fc-P₂-Si** (53 mg, 0.019 mmol) in CH_2Cl_2 (7.5 mL). The reaction was monitored by TLC (40-60 petroleum ether/EtOAc/pyridine 10:1:1). After quenching with HOAc, the reaction mixture was passed through a short silica plug (CH_2Cl_2), and the solvents removed. R_f (40-60 petroleum ether/EtOAc/pyridine 10:1:1) = 0.5. Adapting a published procedure, 4-



iodobenzaldehyde (44 mg, 0.19 mmol), $Pd_2(dba)_3$ (1 mg, 0.6 μ mol), CuI (1 mg, 2.4 μ mol), PPh_3 (1 mg, 4.8 μ mol) were added under argon to the **Fc-P₂-H**. Toluene (2 mL) and Et_3N (2 mL) were added and the reaction mixture degassed. The reaction was stirred at 20 $^\circ C$. for 1 hr under argon. The reaction was monitored by TLC (40-60 petroleum ether/EtOAc/pyridine 10:1:1). When the reaction was complete, the volume was reduced and the resulting residue passed through a short silica plug (CH_2Cl_2). Column chromatography (40-60 petroleum ether/EtOAc/pyridine 20:1:1) gave a green solid (27 mg, 55 %). R_f (40-60 petroleum ether/EtOAc/pyridine 10:1:1) = 0.6. ν_{max}/cm^{-1} 2923 (C-H), 2853 (C-H) 1700 (C=O), 794 (C-H Ar). 1H NMR (400 MHz, $CDCl_3/5\%$ d_5 -pyridine) $\delta = 10.01$ (s, 1H, CHO), 9.88 (d, 2H, $J = 4.6$ Hz, β -H), 9.86 (d, 2H, $J = 4.6$ Hz, β -H), 9.73 (d, 2H, $J = 4.6$ Hz, β -H), 9.70 (d, 2H, $J = 4.6$ Hz, β -H), 9.08–9.06 (m, 4H, β -H), 9.03 (d, 2H, $J = 4.6$ Hz, β -H), 9.00 (d, 2H, $J = 4.5$ Hz, β -H), 8.13 (d, 2H, $J = 8.1$ Hz, Ar- H^4), 8.04 (d, 2H, $J = 8.1$ Hz, Ar- H^3), 7.95 (d, 2H, $J = 8.1$ Hz, Ar- H^2), 7.66 (d, 2H, $J = 8.1$ Hz, Ar- H^1), 7.39 (d, 8H, $J = 1.9$ Hz, Ar- H^{ortho}), 6.92 (br. s, 4H, Ar- H^{para}), 4.78 (d, 2H, $J = 1.5$ Hz, Fc- H), 4.44 (d, 2H, $J = 1.5$ Hz, Fc- H), 4.17 (t, 16H, $J = 6.3$ Hz, O- CH_2), 4.14 (s, 5H, Fc- H), 1.90 (m, 16H, octyl- CH_2), 1.57–1.32 (m, 80H, octyl- CH_2), 0.87 (t, 24H, $J = 6.6$ Hz, octyl- CH_3). m/z (MALDI ToF MS+) 2537.9 ($C_{159}H_{182}FeN_8O_9Zn_2$, $[M]^+$, requires 2536.21).

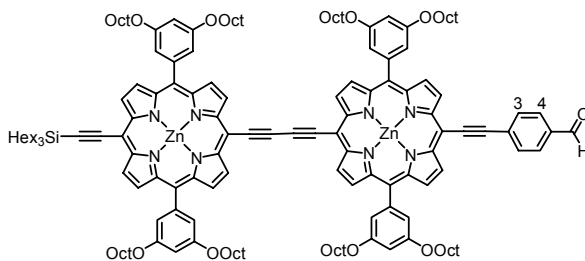
Fc-P₂-C₆₀: A mixture of **Fc-P₂-CHO** (27 mg, 0.012 mmol), sarcosine (48 mg, 0.53 mmol), and C_{60} (39 mg, 0.053 mmol) were dissolved in toluene (40 mL). The reaction mixture was degassed and refluxed for 18 h under argon. Solvents were removed and column chromatography (petroleum ether/toluene 1:1, gradually increasing the polarity to



3:7 to pure toluene), followed by layer precipitation ($CH_2Cl_2/MeOH$) gave a very dark green powder (23 mg, 65 %). R_f (petroleum ether/toluene 3:7) = 0.3. λ_{max} (CH_2Cl_2)/nm (log ϵ) 460 (5.61), 490 (5.37), 578 (4.44), 661 sh (4.93), 716 (5.13). 1H NMR (400 MHz, $CDCl_3/5\%$ d_5 -pyridine) $\delta = 9.86$ (m, 4H, β -H), 9.73 (d, 2H, $J = 4.4$ Hz, β -H), 9.70 (d, 2H, $J = 4.4$ Hz, β -H), 9.04 (m, 4H, β -H), 8.97 (m, 4H, β -H), 8.06 (d, 2H, $J = 7.9$ Hz, Ar- H^3), 7.99–7.89 (m, 4H, 2 Ar- H^2 , 2 Ar- H^4), 7.67 (d, 2H, $J = 8.0$ Hz, Ar- H^1), 7.38 (br.s, 4H, Ar- H^{ortho}), 7.36 (br.s, 4H, Ar- H^{ortho}), 6.91 (br. s, 4H, Ar- H^{para}), 4.91–4.86 (m, 2H, H^6 or H^7 , H^5), 4.79 (br. s, 2H, Fc- H), 4.43 (br. s, 2H, Fc- H), 4.18–4.11 (m, 22H, 1 H^6 or H^7 , 16 O- CH_2 , 5 Fc- H), 2.88 (s, 3H, N- CH_3), 1.93–1.85 (m, 16H, octyl- CH_2), 1.56–1.48 (m, 16H, octyl- CH_2), 1.43–1.21 (m, 64H, octyl- CH_2), 0.88–0.84 (m, 24H, octyl- CH_3). m/z (MALDI ToF MS+) 3283.3 ($C_{221}H_{187}FeN_9O_8Zn_2$, $[M]^+$, requires 3283.25).

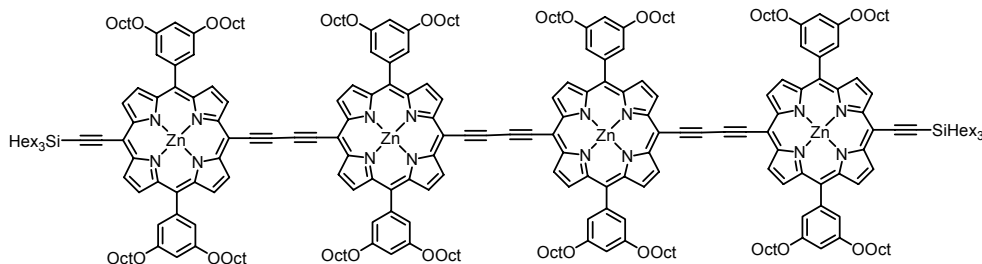
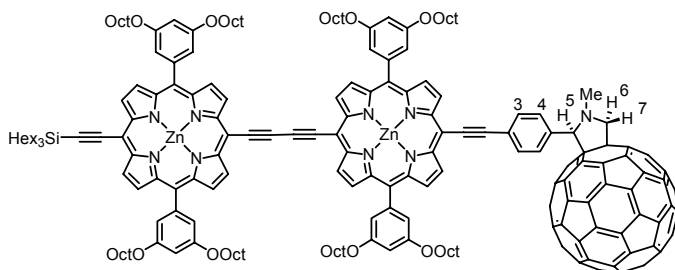
Si-P₂-CHO: 4-Iodobenzaldehyde (58 mg, 0.25 mmol), Pd₂(dba)₃ (1 mg, 0.83 μmol), CuI (1 mg, 3.1 μmol), PPh₃ (2 mg, 6.3 μmol) and **Si-Por₂-H** (61 mg, 0.025 mmol) were placed in a dried flask under argon. Toluene (2.5 mL) and Et₃N (2.5 mL) were added and the reaction mixture degassed. The reaction mixture was stirred at 40 °C and left for 20 h under argon. The reaction was monitored by TLC (40-60 petroleum ether/EtOAc/pyridine 10:1:1).

When the reaction was complete, the volume was reduced and the mixture passed through a short silica plug (CH₂Cl₂). Column chromatography (40-60 petroleum ether/EtOAc/pyridine 20:1:1) gave a very dark green solid (51 mg, 81 %). *R_f* (40-60 petroleum ether/EtOAc/pyridine 10:1:1) = 0.6. ν_{\max} /cm⁻¹ 2923 (C–H), 2853 (C–H) 1701 (C=O) 793 (C–H Arom.). ¹H NMR (400 MHz, CDCl₃/5% *d*₅-pyridine) δ = 10.06 (s, 1H, CHO), 9.88 (m, 4H, β -H), 9.69 (d, 2H, *J* = 4.5 Hz, β -H), 9.65 (d, 2H, *J* = 4.5 Hz, β -H), 9.07 (m, 4H, β -H), 9.03 (d, 2H, *J* = 4.5 Hz, β -H), 9.00 (d, 2H, *J* = 4.5 Hz, β -H), 8.10 (d, 2H, *J* = 8.1 Hz, Ar-*H*⁴), 8.00 (d, 2H, *J* = 8.1 Hz, Ar-*H*³), 7.38 (m, 8H, Ar-*H*^{ortho}), 6.92 (m, 4H, Ar-*H*^{para}), 4.17 (t, 16H, *J* = 6.3 Hz, O-CH₂), 1.91–1.86 (m, 16H, octyl-CH₂), 1.80–1.74 (m, 6H, hexyl-CH₂), 1.57–1.28 (m, 98H, 80 octyl-CH₂, 18 hexyl-CH₂), 1.05–0.85 (m, 39H, 24 octyl-CH₃, 15 hexyl-CH₂/CH₃). *m/z* (MALDI ToF MS+) 2558.0 (C₁₆₁H₂₀₈N₈O₉SiZn₂, [M]⁺, requires 2557.44).



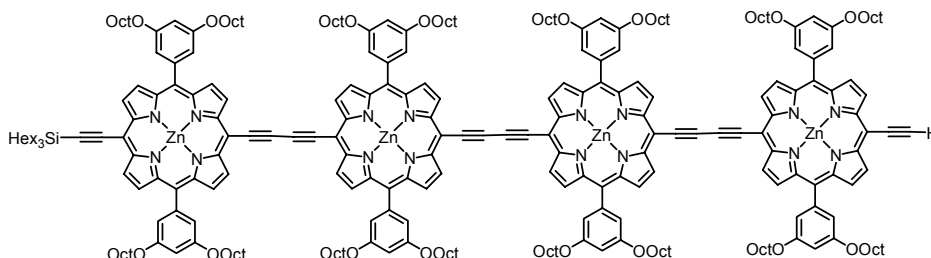
Si-P₂-C₆₀: A mixture of the **Si-P₂-CHO** (53 mg, 0.02 mmol), sarcosine (90 mg, 1.0 mmol) and C₆₀ (73 mg, 0.10 mmol) were dissolved in toluene (75 mL). The reaction mixture was degassed and refluxed for 18 h under argon. Solvents were removed and column chromatography (petroleum ether/toluene 1:1, gradually increasing the polarity to 3:7 to pure toluene), followed by layer precipitation (CH₂Cl₂/MeOH) gave a very dark green powder (37 mg, 71 %).

R_f (petroleum ether/toluene 3:7) = 0.3 (streaky). λ_{\max} (CH₂Cl₂)/nm (log ϵ) 458 (5.63), 489 (5.39), 577 (4.44), 653 sh (4.86), 707 (5.08). ¹H NMR (400 MHz, CDCl₃/5% *d*₅-pyridine) δ = 9.86 (t, 4H, *J* = 4.4 Hz, β -H), 9.70 (d, 2H, *J* = 4.4 Hz, β -H), 9.63 (d, 2H, *J* = 4.4 Hz, β -H), 9.06 (d, 2H, *J* = 4.4 Hz, β -H), 9.04 (d, 2H, *J* = 4.4 Hz, β -H), 8.96 (t, 4H, *J* = 4.4 Hz, β -H), 8.07 (d, 2H, *J* = 8.4 Hz, Ar-*H*³), 7.94 (br. s, 2H, Ar-*H*⁴), 7.37 (m, 8H, Ar-*H*^{ortho}), 6.91 (m, 4H, Ar-*H*^{para}), 4.91–4.87 (m, 2H, H⁶ or H⁷, H⁵), 4.18–4.12 (m, 17H, H⁶ or H⁷, 16 O-CH₂), 2.87 (s, 3H, N-CH₃), 1.93–1.84 (m, 16H, octyl-CH₂), 1.82–1.74 (m, 6H, hexyl-CH₂), 1.59–1.24 (m, 98H, 80 octyl-CH₂, 18 hexyl-CH₂), 1.05–1.01 (m, 6H, hexyl-CH₂), 0.94–0.84 (m, 33H, 24 octyl-CH₃, 9 hexyl-CH₃). *m/z* (MALDI ToF MS+) 3304.5 (C₂₂₃H₂₁₃N₉O₈SiZn₂, [M]⁺, requires 3304.49).

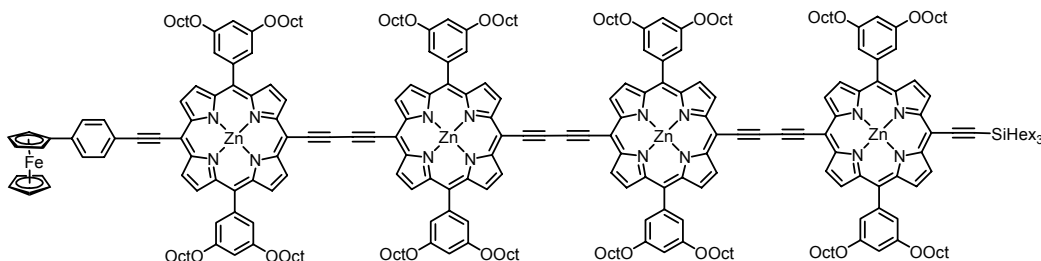


Si-P₄-Si: Porphyrin **Si-P₄-H** (0.285 g, 0.12 mmol) was dissolved in dry CH₂Cl₂ (80 mL) and stirred vigorously under air for 20 min. CuCl (0.345 g, 3.5 mmol) and TMEDA (0.53 mL, 3.5 mmol) were added and stirred for 20 minutes further, monitoring by TLC (40-60 petroleum ether/pyridine 15:1). Copper salts were removed by passing the mixture through a short silica plug (CH₂Cl₂). The product was layer precipitated (CH₂Cl₂/MeOH) to yield a dark brown powder (0.138 g, 48 %). *R_f* (40-60 petroleum ether/10% pyridine) = 0.44. λ_{\max} (CH₂Cl₂/1% Pyridine)/nm (log ϵ) 426 (5.91), 496 (5.79), 588 (4.86), 772 (5.54).

$\nu_{\max}/\text{cm}^{-1}$ 2957 (C–H), 2924 (C–H), 2854 (C–H), 2127 (C≡C). $^1\text{H NMR}$ (500 MHz, $\text{CDCl}_3/5\%$ d_5 -pyridine) δ = 9.91–9.88 (m, 12H, β -H), 9.65 (d, 4H, J = 4.4 Hz, β -H), 9.10–9.08 (m, 12H, β -H), 8.97 (d, 4H, J = 4.4 Hz, β -H), 7.43 (d, 8H, J = 2.2 Hz, Ar- H^{ortho}), 7.39 (d, 8H, J = 2.2 Hz, Ar- H^{ortho}), 6.95 (t, 4H, J = 2.2 Hz, Ar- H^{para}), 6.93 (t, 4H, J = 2.2 Hz, Ar- H^{para}), 4.17–4.23 (m, 32H, O- CH_2), 1.96–1.89 (m, 32H, octyl- CH_2), 1.83–1.77 (m, 12H, hexyl- CH_2), 1.60–1.52 (m, 44H, 32 octyl- CH_2 , 12 hexyl- CH_2), 1.47–1.27 (m, 152H, 128 octyl- CH_2 , 24 hexyl- CH_2), 1.06–1.03 (m, 12H, hexyl- CH_2), 0.93 (t, 18 H, J = 7.1 Hz, hexyl- CH_3) 0.90–0.87 (m, 48 H, octyl- CH_3). m/z (MALDI ToF MS+) 4892.0 ($\text{C}_{308}\text{H}_{406}\text{N}_{16}\text{O}_{16}\text{Si}_2\text{Zn}_4$, $[\text{M}]^+$, requires 4896.82).

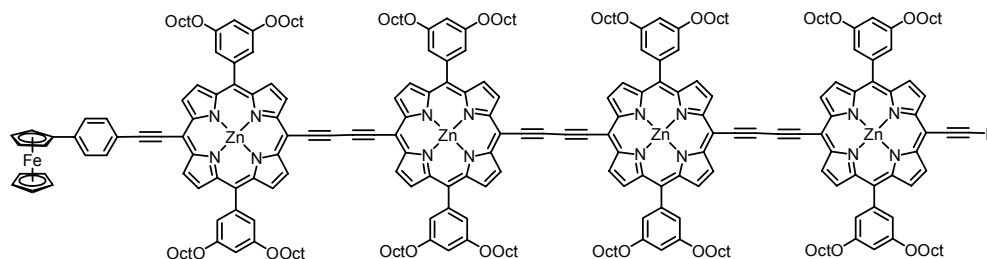


Si-P₄-H: **Si-P₄-Si** (80 mg, 16.3 μmol) was dissolved in a 1:1 mixture of $\text{CH}_2\text{Cl}_2/\text{CHCl}_3$ (16 mL). TBAF (25 μL of a 1.0 M solution in THF) was added to the stirred solution. The reaction was monitored by TLC (40-60 petroleum ether/15% pyridine) until an optimal product mixture had been reached (after 25 min), then 2 drops of HOAc was added to quench the reaction. The volume was reduced and the mixture passed through a short silica plug (CH_2Cl_2). Column chromatography (40-60 petroleum ether/9% pyridine, gradually increasing the polarity to 20%) gave the **Si-P₄-H** (34 mg, 45 %). R_f (40-60 petroleum ether/10% pyridine) = 0.41. $\nu_{\max}/\text{cm}^{-1}$ 2923 (C–H), 2853 (C–H), 2126 (C≡C). $^1\text{H NMR}$ (400 MHz, $\text{CDCl}_3/5\%$ d_5 -pyridine) δ = 9.93–9.86 (m, 12H, β -H), 9.67 (d, 2H, J = 4.4 Hz, β -H), 9.65 (d, 2H, J = 4.8 Hz, β -H), 9.09 (t, 12H, J = 3.9 Hz, β -H), 9.00 (d, 2H, J = 4.3 Hz, β -H), 8.97 (d, 4H, J = 4.3 Hz, β -H), 7.43 (d, 8H, J = 1.9 Hz, Ar- H^{ortho}), 7.39 (d, 8H, J = 2.1 Hz, Ar- H^{ortho}), 6.94 (br. s, 4H, Ar- H^{para}), 6.92 (br. s, 4H, Ar- H^{para}), 4.22–4.16 (m, 33H, C≡C-H, 32 O- CH_2), 1.96–1.87 (m, 32H, octyl- CH_2), 1.81–1.75 (m, 6H, hexyl- CH_2), 1.61–1.51 (m, 44H, 32 octyl- CH_2 , 12 hexyl- CH_2), 1.44–1.26 (m, 134H, 128 octyl- CH_2 , 6 hexyl- CH_2), 1.06–1.01 (m, 6H, hexyl- CH_2), 0.94–0.84 (m, 57 H, 48 octyl- CH_3 , 9 hexyl- CH_3). m/z (MALDI ToF MS+) 4622.0 ($\text{C}_{290}\text{H}_{368}\text{N}_{16}\text{O}_{16}\text{SiZn}_4$, $[\text{M}]^+$, requires 4614.54)

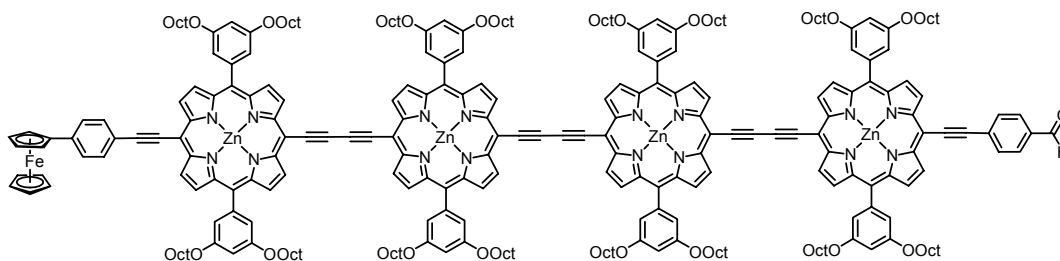


Fc-P₄-Si: $\text{Pd}_2(\text{dba})_3$ (1.7 mg, 1.8 μmol), CuI (0.7 mg, 3.7 μmol), PPh_3 (1.9 mg, 7.4 μmol) and **Si-P₄-H** (34 mg, 7.4 μmol) and 4-iodophenyl ferrocene (57 mg, 0.15 mmol) were placed in a dried flask under argon. Toluene (1 mL) and Et_3N (1 mL) were added and the reaction mixture degassed. The reaction mixture was stirred at 40 °C for 1.5 h. The reaction was monitored by TLC (40-60 petroleum ether/20% pyridine). When the reaction was complete, the volume was reduced and the mixture passed through a short silica plug (CH_2Cl_2). Column chromatography (40-60 petroleum ether/10% pyridine, increasing the polarity accordingly) followed by layer precipitation ($\text{CH}_2\text{Cl}_2/\text{MeOH}$) gave a brown solid (27 mg, 75 %). R_f (40-60 petroleum ether/20% pyridine) = 0.45. λ_{\max} ($\text{CH}_2\text{Cl}_2/1\%$ Pyridine)/nm (log ϵ) 464 (5.63), 470 (5.61), 589 (4.54), 772 (5.24). $^1\text{H NMR}$ (500 MHz, $\text{CDCl}_3/5\%$ d_5 -pyridine) δ = 9.95–9.86 (m, 12H, β -H), 9.74 (d, 2H, J = 4.4 Hz, β -H), 9.65 (d, 2H, J = 4.4 Hz, β -H), 9.12–9.07 (m, 12H, β -H), 9.00 (d, 2H, J = 4.1 Hz, β -H), 8.97 (d, 2H, J = 4.4 Hz, β -H), 7.96 (d, 2H, J = 8.2 Hz, Ar-H), 7.69 (d, 2H, J = 8.2 Hz, Ar-H), 7.43 (br. s, 8H, Ar- H^{ortho}), 7.39 (d, 8H, J = 7.9 Hz, Ar- H^{ortho}), 6.96–6.90 (m, 8H, Ar- H^{para}), 4.81 (br. s, 2H, Fc-H), 4.45 (br. s, 2H, Fc-H), 4.23–4.14 (m, 37H, 32 O- CH_2 , 5 Fc-H), 1.95–1.88 (m, 32H, octyl- CH_2), 1.82–1.76 (m, 6H, hexyl- CH_2), 1.62–1.51 (m, 38H, 32 octyl- CH_2 , 6 hexyl- CH_2), 1.46–1.27 (m, 140H, 128 octyl- CH_2 , 12 hexyl-

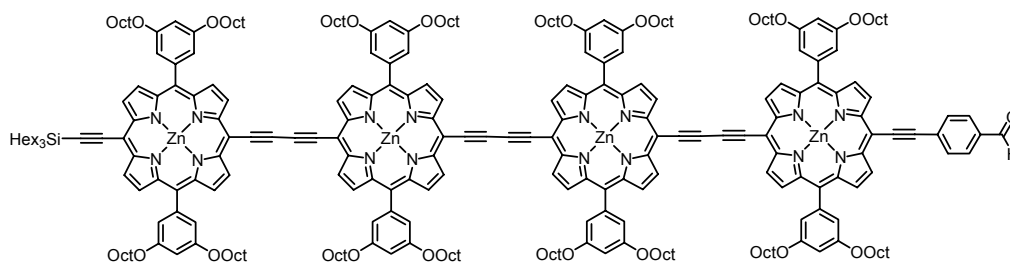
CH_2), 1.05–1.02 (m, 6H, hexyl- CH_2), 0.94–0.85 (m, 57H, 48 octyl- CH_3 , 9 hexyl- CH_3). m/z (MALDI ToF MS+) 4881.5 ($\text{C}_{306}\text{H}_{380}\text{FeN}_{16}\text{O}_{16}\text{SiZn}_4$, $[\text{M}]^+$, requires 4883.6).



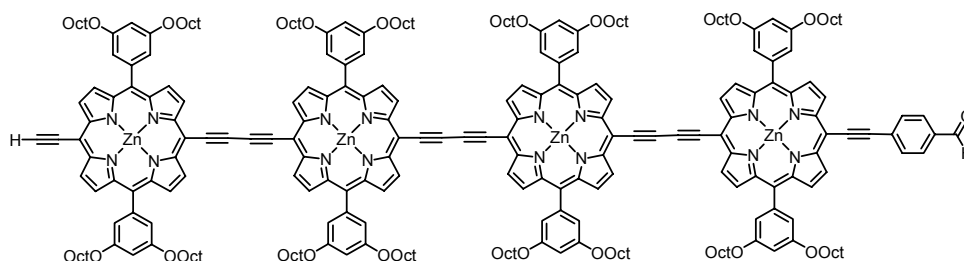
Fc-P₄-H (Route A): TBAF (14 μL of a 1.0 M solution in THF) was added to a stirred solution of **Fc-P₄-Si** (47 mg, 9.6 μmol) in CH_2Cl_2 (10 mL). The reaction was monitored by TLC (40-60 petroleum ether/10% pyridine). After quenching with HOAc, the reaction mixture was passed through a short silica plug (CH_2Cl_2), and the solvents removed yielding **Fc-P₄-H** (12 mg, 27 %). R_f (40-60 petroleum ether/5% pyridine) = 0.07. ^1H NMR (400 MHz, $\text{CDCl}_3/5\%$ d_5 -pyridine) δ = 9.93–9.85 (m, 12H, β -H), 9.74 (d, 2H, J = 4.6 Hz, β -H), 9.66 (d, 2H, J = 4.6 Hz, β -H), 9.12–9.06 (m, 12H, β -H), 9.01–8.98 (m, 4H, β -H), 7.97 (d, 2H, J = 8.0 Hz, Ar-H), 7.69 (d, 2H, J = 8.2 Hz, Ar-H), 7.43 (d, 8H, J = 2.1 Hz, Ar- H^{ortho}), 7.39 (dd, 8H, J = 6.1, 2.2 Hz, Ar- H^{ortho}), 6.96–6.90 (m, 8H, Ar- H^{para}), 4.81 (br. s, 2H, Fc-H), 4.44 (br. s, 2H, Fc-H), 4.24–4.14 (m, 38H, C=C-H, 32 O- CH_2 , 5 Fc-H), 1.95–1.89 (m, 32H, octyl- CH_2), 1.60–1.51 (m, 32H, octyl- CH_2), 1.43–1.23 (m, 128H, octyl- CH_2), 0.91–0.85 (m, 48H octyl- CH_3).



Fc-P₄-CHO: 4-iodobenzaldehyde (12 mg, 52 μmol), $\text{Pd}_2(\text{dba})_3$ (0.6 mg, 0.6 μmol), CuI (0.3 mg, 1.3 μmol), PPh_3 (0.7 mg, 2.6 μmol) and **Fc-P₄-H** (12 mg, 2.6 μmol) were added under argon. Toluene (1.5 mL) and Et_3N (1.5 mL) were added and the reaction mixture degassed. The reaction was stirred at 20 °C under argon and the reaction was monitored by TLC (40-60 petroleum ether/10% pyridine). When the reaction was complete, the volume was reduced and the resulting residue passed through a short silica plug (CH_2Cl_2). Column chromatography (40-60 petroleum ether/10% pyridine, increasing the polarity gradually to 20%) gave a green solid (13 mg, 100%). R_f (40-60 petroleum ether/20% pyridine) = 0.29. ^1H NMR (400 MHz, $\text{CDCl}_3/5\%$ d_5 -pyridine) δ = 10.16 (s, 1H, CHO), 9.92–9.86 (m, 12H, β -H), 9.73 (d, 2H, J = 4.4 Hz, β -H), 9.70 (d, 2H, J = 4.6 Hz, β -H), 9.10–9.06 (m, 12H, β -H), 9.03 (d, 2H, J = 4.6 Hz, β -H), 9.00 (d, 2H, J = 4.4 Hz, β -H), 8.21–8.17 (m, 2H, Ar-H), 8.10 (d, 2H, J = 8.4 Hz, Ar-H), 7.96 (d, 2H, J = 8.5 Hz, Ar-H), 7.68 (d, 2H, J = 8.0 Hz, Ar-H), 7.43 (d, 8H, J = 2.2 Hz, Ar- H^{ortho}), 7.39 (d, 8H, J = 1.7 Hz, Ar- H^{ortho}), 6.96–6.91 (m, 8H, Ar- H^{para}), 4.81 (br. s, 2H, Fc-H), 4.44 (br. s, 2H, Fc-H), 4.24–4.14 (m, 37H, 32 O- CH_2 , 5 Fc-H), 1.96–1.88 (m, 32H, octyl- CH_2), 1.69–1.51 (m, 64H, octyl- CH_2), 1.46–1.25 (m, 96H, octyl- CH_2), 0.93–0.85 (m, 48H, octyl- CH_3).



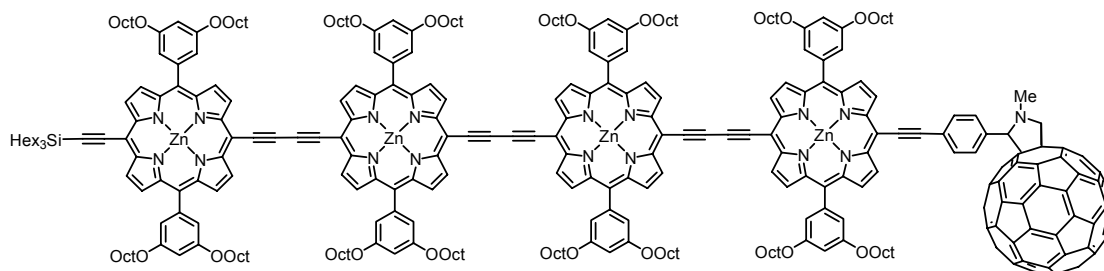
Si-P₄-CHO: **Si-P₄-Si** (100 mg, 20.3 μmol) was dissolved in a 1:1 mixture of $\text{CH}_2\text{Cl}_2/\text{CHCl}_3$ (20 mL). TBAF (31 μL of a 1.0 M solution in THF) was added to the stirred solution. The reaction was monitored by TLC (40-60 petroleum ether/EtOAc/pyridine 10:1:1) until an optimal product mixture had been reached (after 25 min), then 2 drops of HOAc was added to quench the reaction. The volume was reduced and the mixture passed through a short silica plug (CH_2Cl_2). The residue (95 mg) was combined with 4-iodobenzaldehyde (95.3 mg, 0.44 mmol), $\text{Pd}_2(\text{dba})_3$ (4.7 mg, 5.1 μmol), CuI (2.0 mg, 10.3 μmol) and PPh_3 (5.4 mg, 20.5 μmol) in a dried flask under argon. Toluene (2.5 mL) and Et_3N (2.5 mL) were added and the reaction mixture degassed. The reaction mixture was stirred at 40 $^\circ\text{C}$ and left for 2 h under argon. The reaction was monitored by TLC (40-60 petroleum ether/10% pyridine). When the reaction was complete, the volume was reduced and the mixture passed through a short silica plug (CH_2Cl_2). Column chromatography (40-60 petroleum ether/8% pyridine, increasing the polarity gradually to 20%) gave a brown solid (44 mg, 46 % overall). R_f (40-60 petroleum ether/10% pyridine) = 0.24. ^1H NMR (400 MHz, $\text{CDCl}_3/5\%$ d_5 -pyridine) δ = 10.15 (s, 1H, CHO), 9.94–9.83 (m, 12H, β -H), 9.70 (d, 2H, J = 4.4 Hz, β -H), 9.64 (d, 2H, J = 4.6 Hz, β -H), 9.08 (t, 12H, J = 3.8 Hz, β -H), 9.03 (d, 2H, J = 4.6 Hz, β -H), 8.97 (d, 2H, J = 4.6 Hz, β -H), 8.21–8.16 (m, 2H, Ar-H), 8.10 (d, 2H, J = 7.9 Hz, Ar-H), 7.46–7.34 (m, 16H, Ar- H^{ortho}), 6.97–6.87 (m, 8H, Ar- H^{para}), 4.24–4.13 (m, 32H, O- CH_2), 1.96–1.87 (m, 32H, octyl- CH_2), 1.83–1.61 (m, 38H, 32 octyl- CH_2 , 6 hexyl- CH_2), 1.59–1.50 (m, 32H, octyl- CH_2), 1.45–1.24 (m, 114H, 96 octyl- CH_2 , 18 hexyl- CH_2), 1.05–1.01 (m, 6H, hexyl- CH_2), 0.94–0.84 (m, 57H, 48 octyl- CH_3 , 9 hexyl- CH_3).



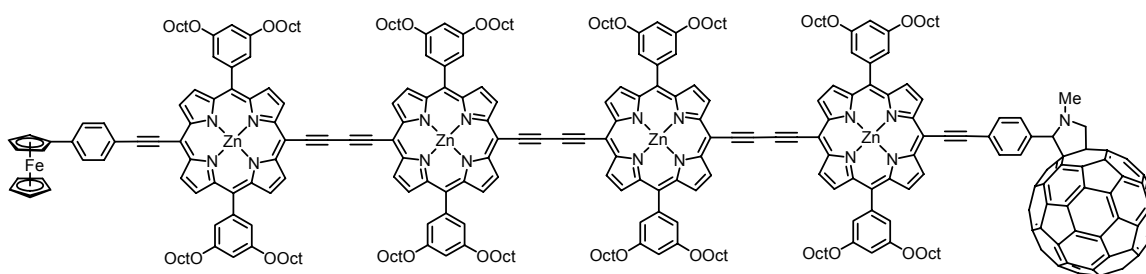
H-P₄-CHO: **Si-P₄-CHO** (40 mg, 8.4 μmol) was dissolved in CH_2Cl_2 (10 mL). TBAF (13 μL of a 1.0 M solution in THF) was added to the stirred solution. The reaction was monitored by TLC (40-60 petroleum ether/15% pyridine). 4 drops of HOAc was added after 35 min to quench the reaction. The volume was reduced and the mixture passed through a short silica plug (CH_2Cl_2). The solvent was evaporated yielding a brown solid (37 mg, 97 %). R_f (40-60 petroleum ether/15% pyridine) = 0.29. ^1H NMR (400 MHz, $\text{CDCl}_3/5\%$ d_5 -pyridine) δ = 10.15 (s, 1H, CHO), 9.93–9.86 (m, 12H, β -H), 9.70 (d, 2H, J = 4.6 Hz, β -H), 9.66 (d, 2H, J = 4.6 Hz, β -H), 9.09 (d, 12H, J = 4.4 Hz, β -H), 9.03 (d, 2H, J = 4.4 Hz, β -H), 9.00 (d, 2H, J = 4.6 Hz, β -H), 8.21–8.16 (m, 2H, Ar-H), 8.10 (d, 2H, J = 8.0 Hz, Ar-H), 7.43 (d, 8H, J = 1.9 Hz, Ar- H^{ortho}), 7.39 (dd, 8H, J = 4.7, 2.1 Hz, Ar- H^{ortho}), 6.97–6.91 (m, 8H, Ar- H^{para}), 4.24–4.14 (m, 33H, C \equiv C-H, 32 O- CH_2), 1.96–1.89 (m, 32H, octyl- CH_2), 1.59–1.51 (m, 32H, octyl- CH_2), 1.46–1.23 (m, 128H, octyl- CH_2), 0.91–0.84 (m, 48H, octyl- CH_3). m/z (MALDI ToF MS⁺) 4445.3 ($\text{C}_{279}\text{H}_{334}\text{N}_{16}\text{O}_{17}\text{Zn}_4$, $[\text{M}]^+$, requires 4445.30).

Fc-P₄-CHO (Route B): **Si-P₄-CHO** (37 mg, 8.3 μmol) was placed together with 4-iodophenyl ferrocene (65 mg, 0.166 mmol), $\text{Pd}_2(\text{dba})_3$ (1.9 mg, 2.1 μmol), CuI (0.8 mg, 4.2 μmol) and PPh_3 (2.2 mg, 8.3 μmol) in a dry flask under argon. Toluene (2 mL) and Et_3N (2 mL) were added and the reaction mixture degassed. The reaction was stirred at 40 $^\circ\text{C}$ under argon and the reaction was monitored by TLC (40-60 petroleum ether/15% pyridine). The reaction was run overnight and then an additional amount of catalyst was added since there was still some starting material according to TLC. When the reaction was complete (after 36 h), the volume was reduced and the resulting residue passed through a short silica plug (CH_2Cl_2). Column

chromatography (pure 40-60 petroleum ether, increasing the polarity gradually with pyridine to 20%) gave a brown solid (11 mg, 28%). (characterization data as above.)



Si-P₄-C₆₀: A mixture of the **Si-P₄-CHO** (20 mg, 4.2 μmol), sarcosine (38 mg, 0.42 mmol) and C₆₀ (30 mg, 42.3 μmol) were dissolved in toluene (35 mL). The reaction mixture was degassed and refluxed for 24 h under argon. The solvents were removed and the mixture passed through a silica frit (petroleum ether/toluene 1:1, gradually increasing the polarity to pure toluene) to remove most of the excess C₆₀. Column chromatography (petroleum ether/toluene 4:1, gradually increasing the polarity to 3:2 to pure toluene), followed by layer precipitation (CH₂Cl₂/MeOH) gave a very dark green powder (13 mg, 57 %). R_f (petroleum ether/toluene/pyridine 1:1:0.05) = 0.38. λ_{max} (CH₂Cl₂/1% pyridine)/nm (log ϵ) 330 (5.11), 463 (5.50), 497 (5.34), 591 (4.41), 773 (5.13). ¹H NMR (500 MHz, CDCl₃/5% d₅-pyridine) δ = 9.90–9.87 (m, 12H, β -H), 9.70 (d, 4H, J = 4.4 Hz, β -H), 9.64 (d, 4H, J = 4.4 Hz, β -H), 9.08–9.05 (m, 12H, β -H), 8.97–8.96 (m, 4H, β -H), 8.10–8.09 (m, 2H, Ar-H), 8.01–7.95 (br. s, 2H, Ar-H), 7.42 (d, 8H, J = 1.9 Hz, Ar-H^{ortho}), 7.38–7.37 (m, 8H, Ar-H^{ortho}), 6.95–6.91 (m, 8H, Ar-H^{para}), 4.96 (br. s, 1H, N-CH), 4.20–4.17 (m, 34H, N-CH₂, 32 O-CH₂), 2.93 (s, 3H, N-CH₃), 1.94–1.87 (m, 32H, octyl-CH₂), 1.83–1.76 (m, 6H, hexyl-CH₂), 1.57–1.51 (m, 38H, 32 octyl-CH₂, 6 hexyl-CH₂), 1.44–1.23 (m, 140H, 128 octyl-CH₂, 12 hexyl-CH₂), 1.05–1.02 (m, 6H, hexyl-CH₂), 0.94–0.84 (m, 57H, 48 octyl-CH₃, 9 hexyl-CH₃). m/z (MALDI ToF MS⁺) 5476.6 (C₃₅₉H₃₇₇N₁₇O₁₆SiZn₄, [M]⁺, requires 5475.6).



Fc-P₄-C₆₀: A mixture of **Fc-P₄-CHO** (13 mg, 2.8 μmol), sarcosine (25 mg, 0.28 mmol), and C₆₀ (20 mg, 19.9 μmol) were dissolved in toluene (20 mL). The reaction mixture was degassed and refluxed under argon and monitored by TLC (toluene/5% pyridine). After 24 h the solvents were removed and column chromatography (petroleum ether/toluene 1:1, gradually increasing the polarity to pure toluene and then toluene/5% pyridine to take off the product). Layer precipitation (CH₂Cl₂/MeOH) gave a dark brown powder (9 mg, 60%). R_f (toluene/5% pyridine) = 0.29. λ_{max} (CH₂Cl₂/1% pyridine)/nm (log ϵ) 329 (5.11), 467 (5.60), 497 sh (5.41), 593 (4.45), 776 (5.24). ¹H NMR (500 MHz, CDCl₃/5% d₅-pyridine) δ = 9.90–9.87 (m, 12H, β -H), 9.73 (d, 2H, J = 4.4 Hz, β -H), 9.70 (d, 2H, J = 4.1 Hz, β -H), 9.08–9.05 (m, 12H, β -H), 8.99 (d, 2H, J = 4.4 Hz, β -H), 8.97 (d, 2H, J = 4.1 Hz, β -H), 8.11–8.07 (m, 2H, Ar-H^{C60}), 7.99–7.93 (m, 4H, 2 Ar-H^{C60}, 2 Ar-H^{Fc}), 7.68 (d, 2H, J = 7.9 Hz, Ar-H^{Fc}), 7.43–7.42 (m, 8H, Ar-H^{ortho}), 7.40 (d, 4H, J = 2.2 Hz, Ar-H^{ortho}), 7.38 (d, 4H, J = 1.9 Hz, Ar-H^{ortho}), 6.95–6.91 (m, 8H, Ar-H^{para}), 4.96–4.91 (m, 2H, N-CH₂), 4.80 (br. s, 2H, Fc-H), 4.44 (br. s, 2H, Fc-H), 4.23–4.12 (m, 38H, N-CH, 32 O-CH₂, 5 Fc-H), 2.92 (s, 3H, N-CH₃), 1.95–1.88 (m, 32H, octyl-CH₂), 1.81–1.73 (m, 32H, octyl-CH₂), 1.58–1.51 (m, 32H, octyl-CH₂), 1.44–1.26 (m, 96H, octyl-CH₂), 0.91–0.84 (m, 48H, octyl-CH₃). m/z (MALDI ToF MS⁺) 5453.6 (C₃₅₇H₃₅₁FeN₁₇O₁₆Zn₄, [M]⁺, requires 5453.4).

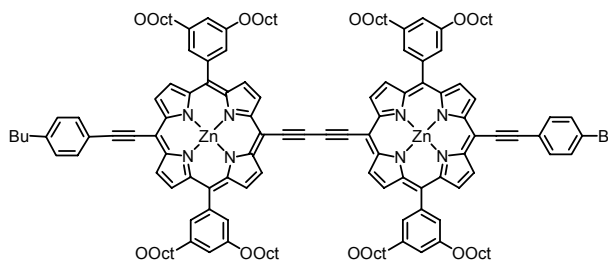
Zinc 5,15-bis-(3,5-bis-octyloxy-phenyl)-10,20-bis-(4-butyl-phenylethynyl)-porphyrin; Bu-P₁-Bu: Zinc 5,15-bis-(3,5-bis-octyloxy-phenyl)-10,20-bis-ethynyl-porphyrin **H-P₁-H** (30 mg, 28 μmol), Pd₂(dba)₃ (3.3

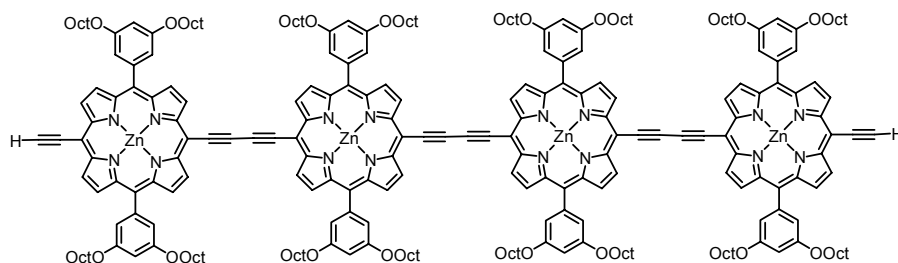
mg, 3.5 μmol), PPh_3 (6.9 mg, 26 μmol) and CuI (2.5 mg, 13 μmol) were dried under vacuum before dry Et_3N (6 mL) was added and the mixture degassed. 1-butyl-4-iodobenzene (57 mg, 222 μmol) was added and the reaction was stirred at 50 $^\circ\text{C}$ for 30 min when TLC (40-60 petroleum ether/ EtOAc /pyridine 10:1:1) showed the reaction to be complete. The volume was reduced and the mixture passed through a short silica gel column (CH_2Cl_2). Column chromatography (40-60 petroleum ether/ EtOAc /pyridine 100:1:1 to 100:3:1) followed by recrystallization by layer addition ($\text{CH}_2\text{Cl}_2/\text{MeOH}$) gave a dark green solid (35 mg, 93%). R_f (40-60 petroleum ether/ EtOAc /pyridine 10:1:1) = 0.80. λ_{max} ($\text{CH}_2\text{Cl}_2/1\%$ pyridine)/nm ($\log \epsilon$) 310 (4.58), 453 (5.39), 606 (4.23), 661 (4.88). ^1H NMR (500 MHz, $\text{CDCl}_3/5\%$ d_5 -pyridine) δ = 9.70 (d, 4H, J = 4.6 Hz, β -H), 8.98 (d, 4H, J = 4.6 Hz, β -H), 7.94 (d, 4H, J = 8.0 Hz, Ar-H), 7.38 (d, 4H, J = 8.0 Hz, Ar-H), 7.36 (d, 4H, J = 2.1 Hz, Ar- H^{ortho}), 6.91 (t, 2H, J = 2.1 Hz, Ar- H^{para}), 4.16 (t, 8H, J = 6.6 Hz, O- CH_2), 2.76 (t, 8H, J = 7.7 Hz, Ar- CH_2), 1.93–1.84 (m, 8H, CH_2), 1.76–1.69 (m, 8H, CH_2), 1.57–1.25 (m, 40H, CH_2), 1.01 (t, 6H, J = 7.4 Hz, CH_3), 0.88 (t, 12H, J = 6.7 Hz, CH_3). ^{13}C NMR (100 MHz, $\text{CDCl}_3/5\%$ d_5 -pyridine) δ = 158.14, 151.98, 149.69, 144.58, 143.46, 132.40, 131.46, 130.55, 128.80, 122.29, 121.54, 114.49, 101.57, 68.35, 31.81, 29.42, 28.26, 26.14, 22.66, 14.10, 14.01. m/z (MALDI ToF MS+) 1349.6 ($\text{C}_{88}\text{H}_{108}\text{N}_4\text{O}_4\text{Zn}$, $[\text{M}]^+$, requires 1348.76).

Zinc 5,15-bis-(3,5-bis-octyloxy-phenyl)-10,20-bis-ethynyl-porphyrin dimer; H-P₂-H: Porphyrin **Si-P₂-Si** (0.11 g, 40 μmol) was dissolved in CH_2Cl_2 (40 mL). TBAF (80 μL of a 1.0 M solution in THF) was added to the stirred solution. The reaction was monitored by TLC (40-60 petroleum ether/ EtOAc /pyridine 10:1:1). After 30 min HOAc was added to quench the reaction. The volume was reduced and the mixture passed through a short silica plug (40-60 petroleum ether and then CH_2Cl_2). Evaporation of the solvent yielded pure **H-P₂-H** (66.4 mg, 76%). R_f (40-60 petroleum ether/ EtOAc /pyridine 10:1:1) = 0.35. $\nu_{\text{max}}/\text{cm}^{-1}$ 2967 (C–H), 2934 (C–H), 2854 (C–H), 2094 (C≡C), 2150 (C≡C). ^1H NMR (400 MHz, $\text{CDCl}_3/5\%$ d_5 -pyridine) δ = 9.91 (m, 4H, β -H), 9.67 (m, 4H, β -H), 9.10 (m, 4H, β -H), 9.03 (m, 4H, β -H), 7.38 (d, 8H, J = 2.0 Hz, Ar- H^{ortho}), 6.92 (d, 2H, J = 2.0 Hz, Ar- H^{para}), 4.18 (m, 2H, C≡C-H), 4.17 (m, 16H, O- CH_2), 1.90 (m, 16H, octyl- CH_2), 1.57–1.29 (m, 80H, octyl- CH_2), 0.87 (t, 24H, J = 6.6 Hz, octyl- CH_3). m/z (MALDI ToF MS+) 2167.1 ($\text{C}_{136}\text{H}_{166}\text{N}_8\text{O}_8\text{Si}_2\text{Zn}_2$, $[\text{M}]^+$, requires 2167.14).

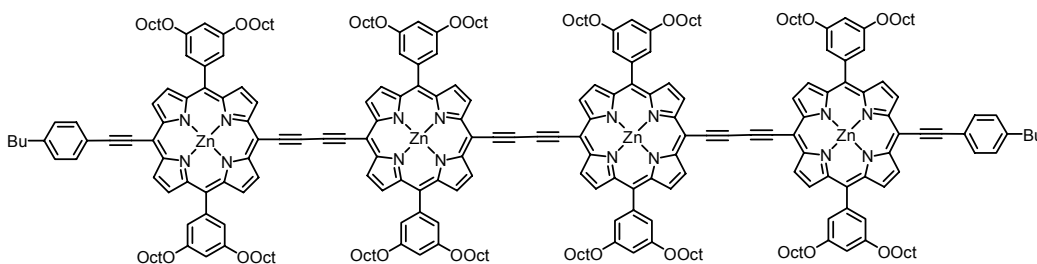
Zinc 5,15-bis-(3,5-bis-octyloxy-phenyl)-10,20-bis-(4-butyl-phenylethynyl)-porphyrin dimer;

Bu-P₂-Bu: Zinc 5,15-bis-(3,5-bis-octyloxy-phenyl)-10,20-bis-ethynyl-porphyrin dimer **H-P₂-H** (40 mg, 18 μmol), $\text{Pd}_2(\text{dba})_3$ (2.1 mg, 2.3 μmol), PPh_3 (4.4 mg, 17 μmol) and CuI (1.6 mg, 8.4 μmol) were dried under vacuum before dry Et_3N (6 mL) was added and the mixture degassed. 1-butyl-4-iodobenzene (37 mg, 140 μmol) was added and the reaction was stirred at 50 $^\circ\text{C}$ for 30 min when TLC (40-60 petroleum ether/ EtOAc /pyridine 10:1:1) showed the reaction to be complete. The volume was reduced and the mixture passed through a short silica gel column (CH_2Cl_2). Column chromatography (40-60 petroleum ether/ EtOAc /pyridine 100:1:1 to 100:3:1) followed by recrystallization by layer addition ($\text{CH}_2\text{Cl}_2/\text{MeOH}$) gave a dark green solid (39 mg, 89%). R_f (40-60 petroleum ether/ EtOAc /pyridine 10:1:1) = 0.70. λ_{max} ($\text{CH}_2\text{Cl}_2/1\%$ pyridine)/nm ($\log \epsilon$) 312 (4.69), 463 (5.67), 497 (5.29), 589 (4.35), 681 (4.98), 744 (5.10). ^1H NMR (500 MHz, $\text{CDCl}_3/5\%$ d_5 -pyridine) δ = 9.87 (d, 4H, J = 4.5 Hz, β -H), 9.72 (d, 4H, J = 4.5 Hz, β -H), 9.07 (d, 4H, J = 4.5 Hz, β -H), 8.99 (d, 4H, J = 4.5 Hz, β -H), 7.96 (d, 4H, J = 7.7 Hz, Ar-H), 7.40 (m, 12H, Ar- H^{ortho} , Ar-H), 6.93 (s, 4H, Ar- H^{para}), 4.19 (t, 16H, J = 6.4 Hz, O- CH_2), 2.77 (t, 4H, J = 7.6 Hz, Ar- CH_2), 1.95–1.87 (m, 16H, CH_2), 1.78–1.70 (m, 4H, CH_2), 1.59–1.30 (m, 84H, CH_2), 1.02 (t, 6H, J = 7.4 Hz, CH_3), 0.88 (t, 24H, J = 6.2 Hz, CH_3). m/z (MALDI ToF MS+) 2439.7 ($\text{C}_{156}\text{H}_{190}\text{N}_8\text{O}_8\text{Zn}_2$, $[\text{M}]^+$, requires 2431.33).





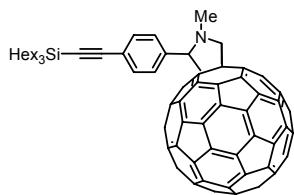
Zinc 5,15-bis-(3,5-bis-octyloxy-phenyl)-10,20-bis-ethynyl-porphyrin tetramer; H-P₄-H; Si-P₄-Si (34 mg, 6.9 μmol) was dissolved in dry CH_2Cl_2 (8 mL). TBAF (10 μL of a 1.0 M solution in THF) was added to the stirred solution. The reaction was monitored by TLC (40-60 petroleum ether/20% pyridine). After 40 min the reaction was quenched by the addition of 5 drops of HOAc. The volume was reduced and the mixture passed through a short silica plug (CH_2Cl_2 followed by THF). Evaporation of the solvent yielded **H-P₄-H** as a brown solid (30 mg, 100%). R_f (40-60 petroleum ether/20% pyridine) = 0.52. $\nu_{\text{max}}/\text{cm}^{-1}$ 2922 (C-H), 2852 (C-H), 2123 (C \equiv C). ^1H NMR (400 MHz, $\text{CDCl}_3/5\%$ d_5 -pyridine) δ = 9.94–9.85 (m, 12H, β -H), 9.68–9.62 (m, 4H, β -H), 9.12–9.05 (m, 12H, β -H), 9.01–8.97 (m, 4H, β -H), 7.42 (br. s, 8H, Ar- H^{ortho}), 7.38 (br. s, 8H, Ar- H^{ortho}), 6.93 (d, 8H, J = 7.5 Hz, Ar- H^{para}), 4.24–4.13 (m, 34H, 2 C \equiv C-H, 32 O- CH_2), 1.96–1.87 (m, 32H, octyl- CH_2), 1.60–1.50 (m, 32H, octyl- CH_2), 1.44–1.24 (m, 128H, octyl- CH_2), 0.91–0.85 (m, 80H, octyl- CH_2/CH_3). m/z (MALDI ToF MS+) 4334.7 ($\text{C}_{272}\text{H}_{330}\text{N}_{16}\text{O}_{16}\text{Zn}_4$, $[\text{M}]^+$, requires 4330.27).



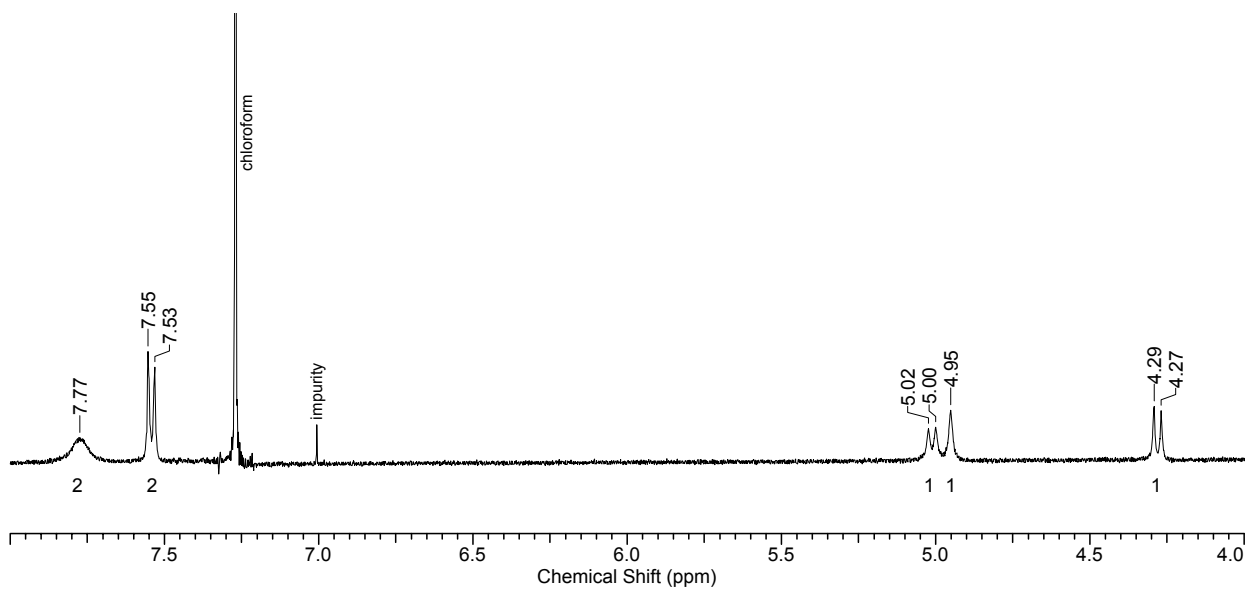
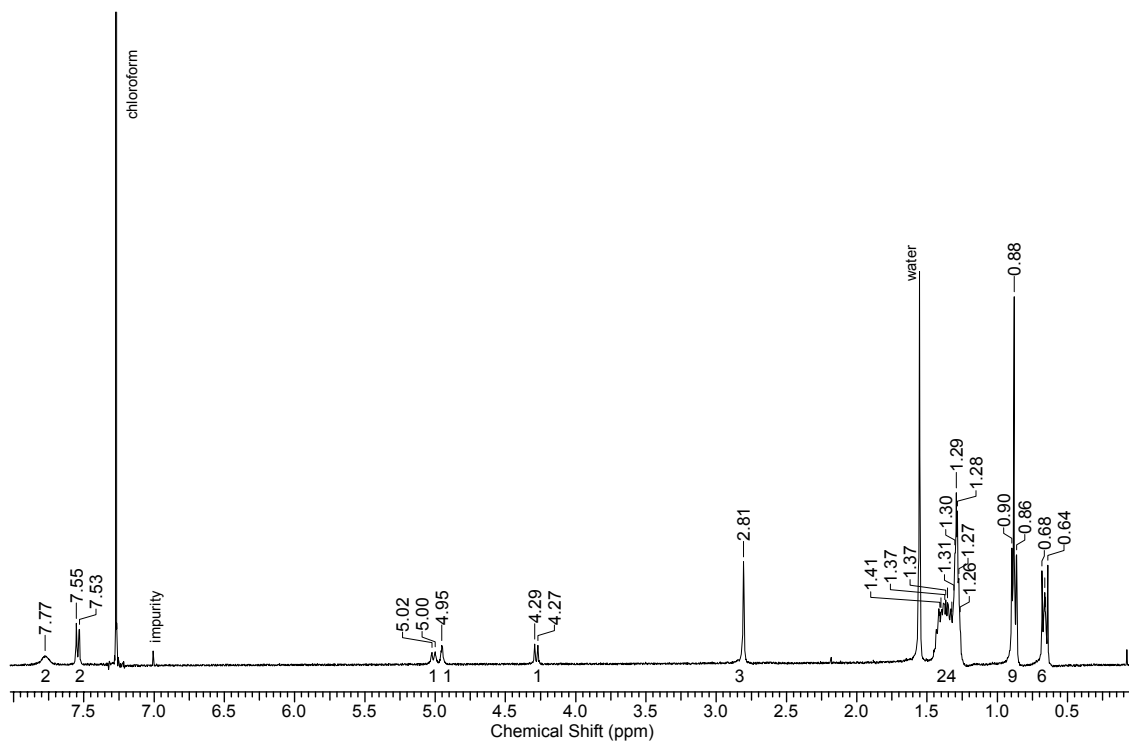
Zinc 5,15-bis-(3,5-bis-octyloxy-phenyl)-10,20-bis-(4-butyl-phenylethynyl)-porphyrin tetramer; Bu-P₄-Bu: 1-Butyl-4-iodobenzene (29 μL , 0.16 mmol), $\text{Pd}_2(\text{dba})_3$ (1.8 mg, 2 μmol), CuI (0.8 mg, 4 μmol), PPh_3 (2.1 mg, 8 μmol) and **H-P₄-H** (30 mg, 7 μmol) were added under argon. Toluene (1 mL) and Et_3N (1 mL) were added and the reaction mixture degassed and then stirred at 40°C under argon over night. The reaction was monitored by TLC (40-60 petroleum ether/10% pyridine) and when complete, the volume was reduced and the resulting residue passed through a short silica plug (CH_2Cl_2). The remaining 1-butyl-4-iodobenzene was removed by putting the sample under high vacuum (7.8×10^3 mbar) followed by layer precipitation to yield the product as a brown solid (23 mg, 71%). R_f (40-60 petroleum ether/10% pyridine) = 0.64. ^1H NMR (400 MHz, $\text{CDCl}_3/5\%$ d_5 -pyridine) δ = 9.93–9.83 (m, 12H, β -H), 9.71 (d, 4H, J = 4.6 Hz, β -H), 9.12–9.04 (m, 12H, β -H), 8.98 (d, 4H, J = 4.6 Hz, β -H), 8.01–7.92 (m, 4H, BuAr-H), 7.41 (dd, 16H, J = 6.7, 2.3 Hz, Ar- H^{ortho}), 6.97–6.90 (m, 8H, Ar- H^{para}), 4.27–4.12 (m, 32H, O- CH_2), 2.01–1.84 (m, 36H, 32 octyl- CH_2 , 4 butyl- CH_2), 1.70–1.24 (m, 136H, 128 octyl- CH_2 , 8 butyl- CH_2), 1.05–0.98 (m, 6H, butyl- CH_3), 0.93–0.83 (m, 80H, octyl- CH_2/CH_3). m/z (MALDI ToF MS+) 4605.9 ($\text{C}_{292}\text{H}_{354}\text{N}_{16}\text{O}_{16}\text{Zn}_4$, $[\text{M}]^+$, requires 4605.7).

Section 8: NMR Spectra

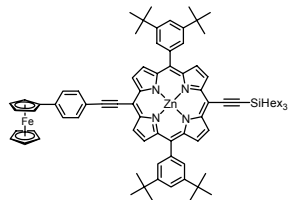
Si-C₆₀:



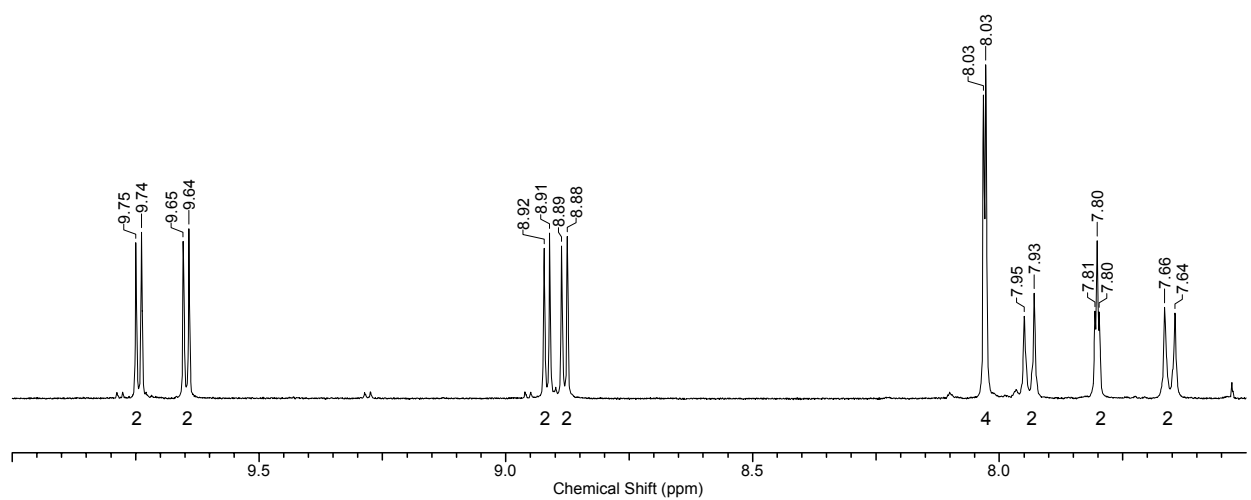
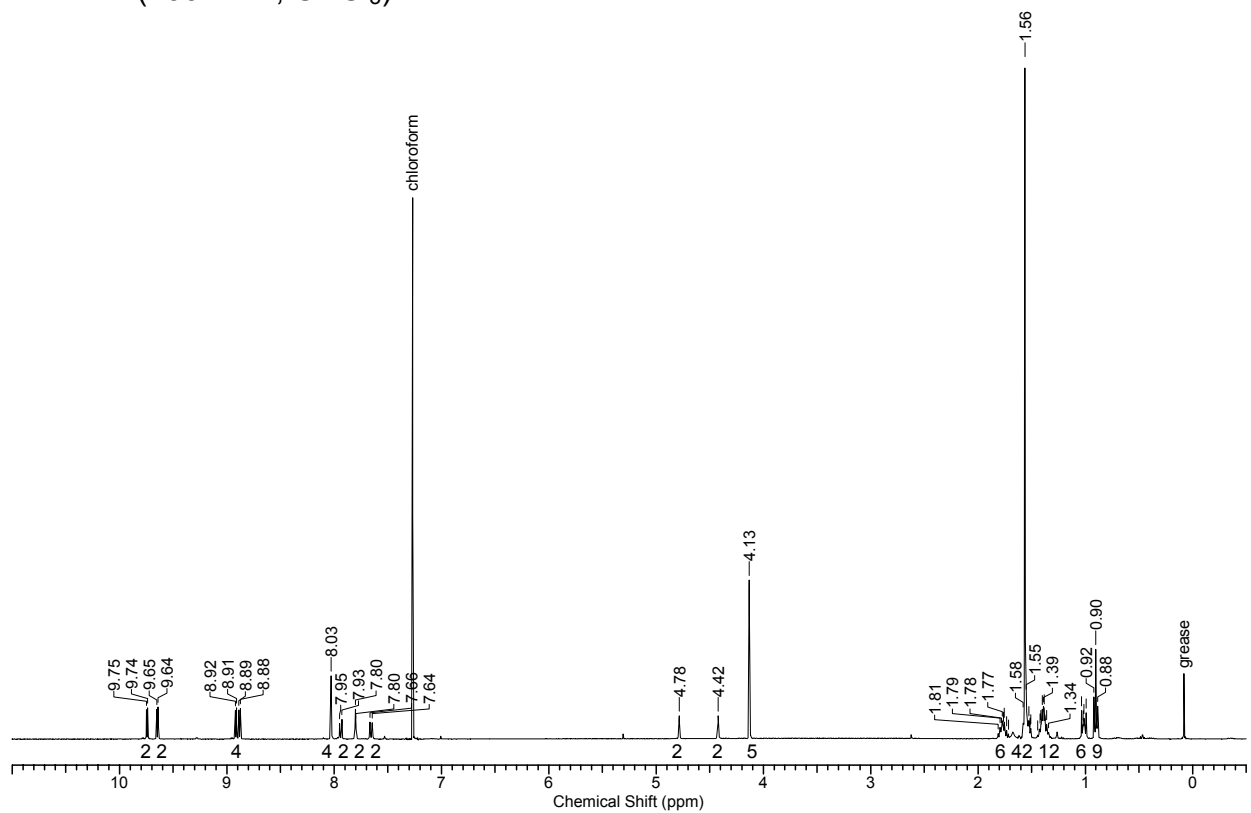
¹H NMR (400 MHz, CDCl₃)



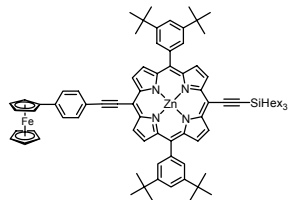
Fc-P₁-Si:



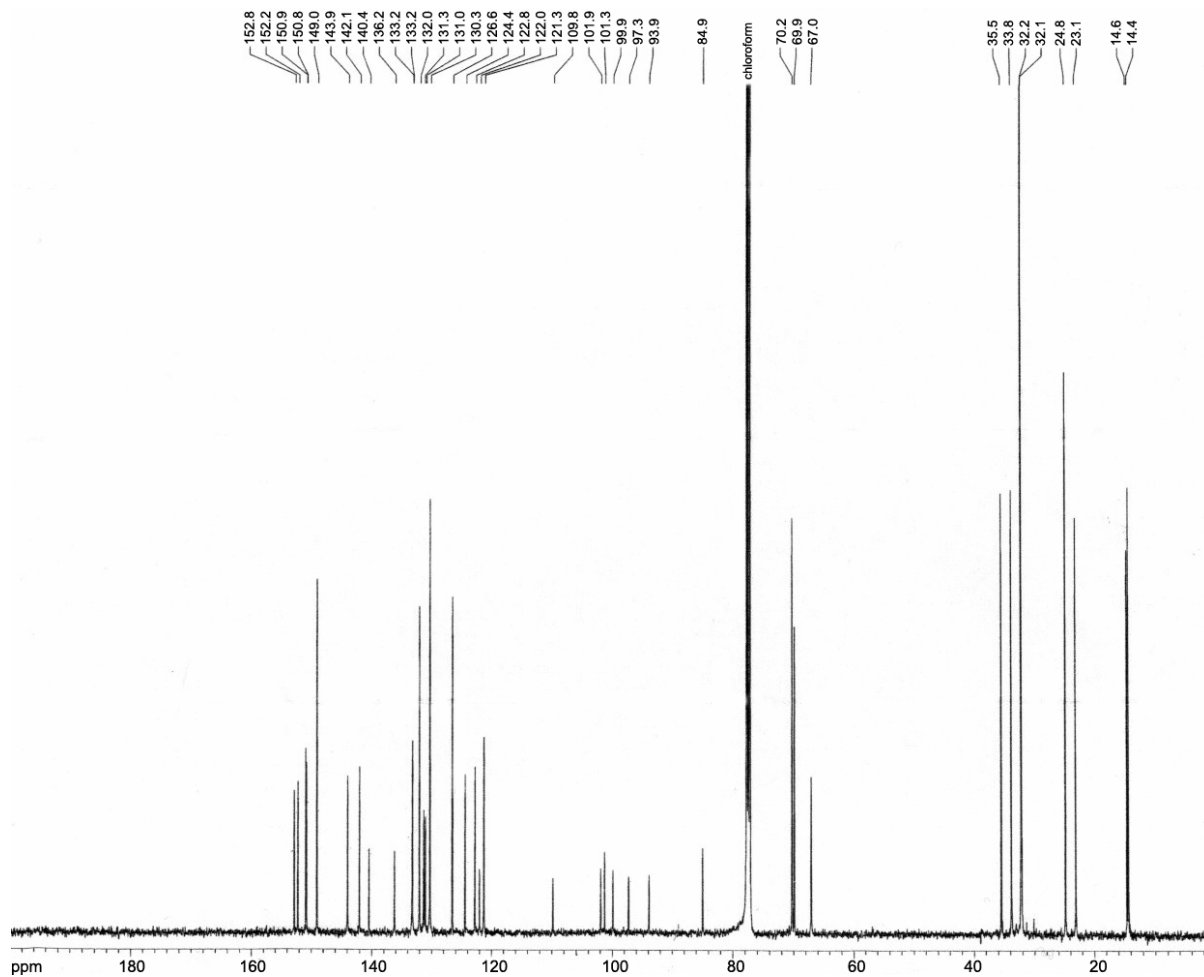
¹H NMR (400 MHz, CDCl₃)



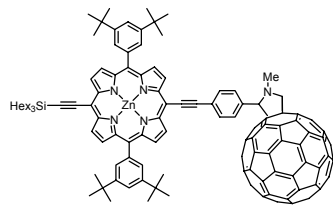
Fc-P₁-Si:



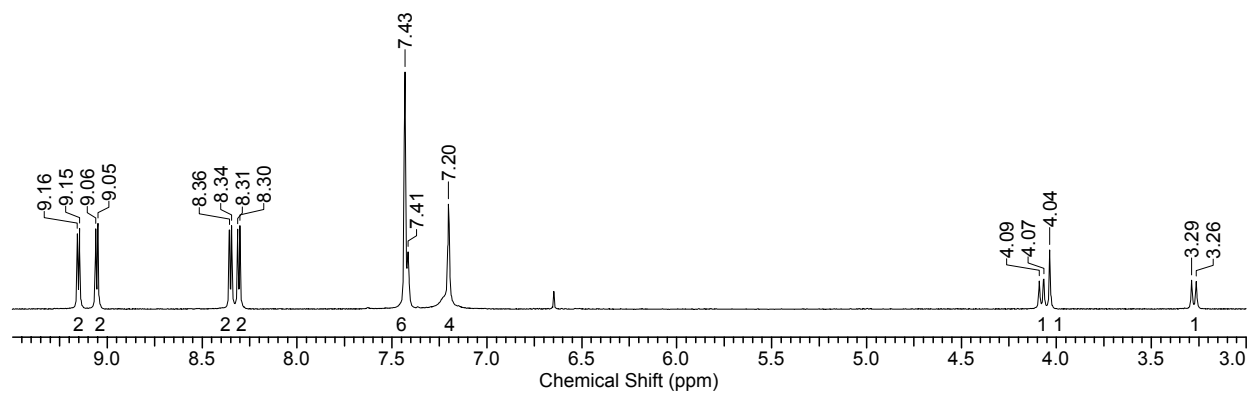
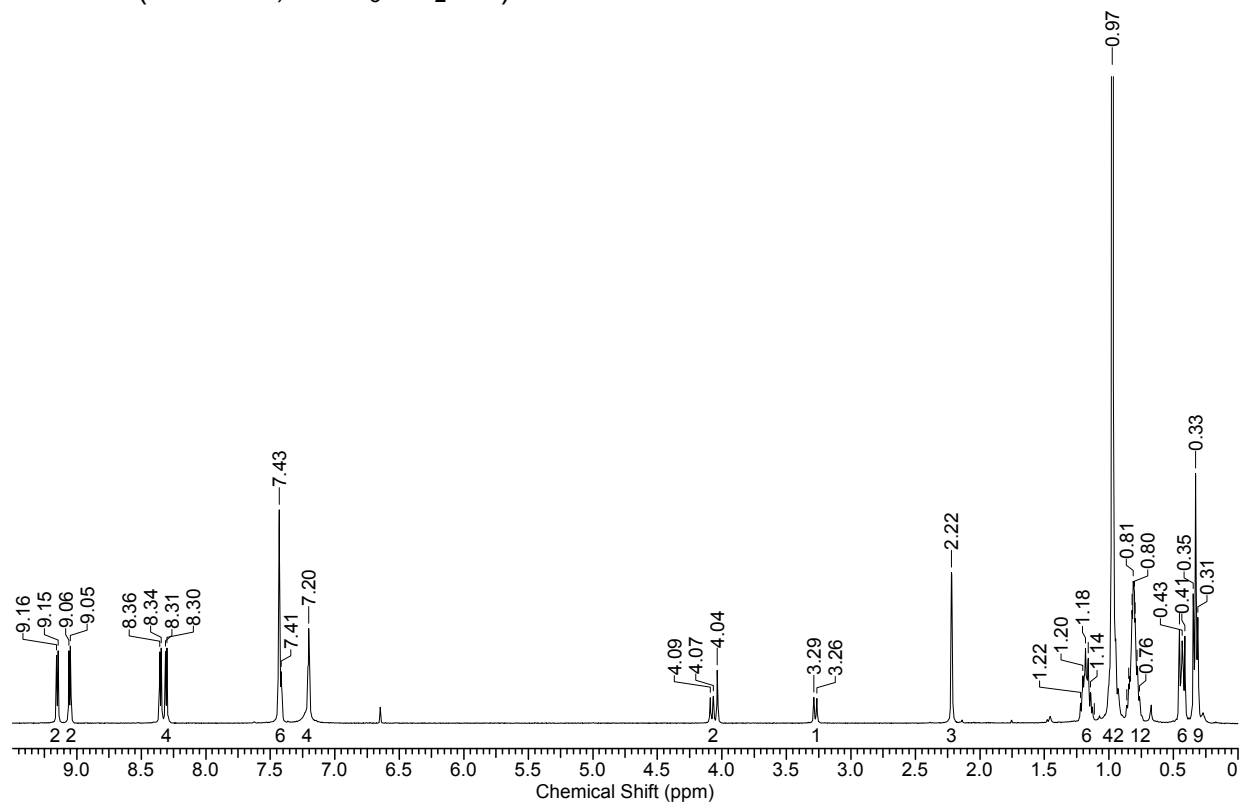
¹³C NMR (100 MHz, CDCl₃)



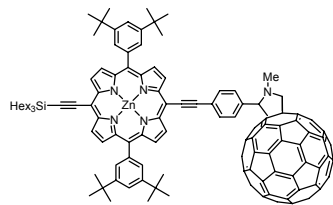
Si-P1-C60:



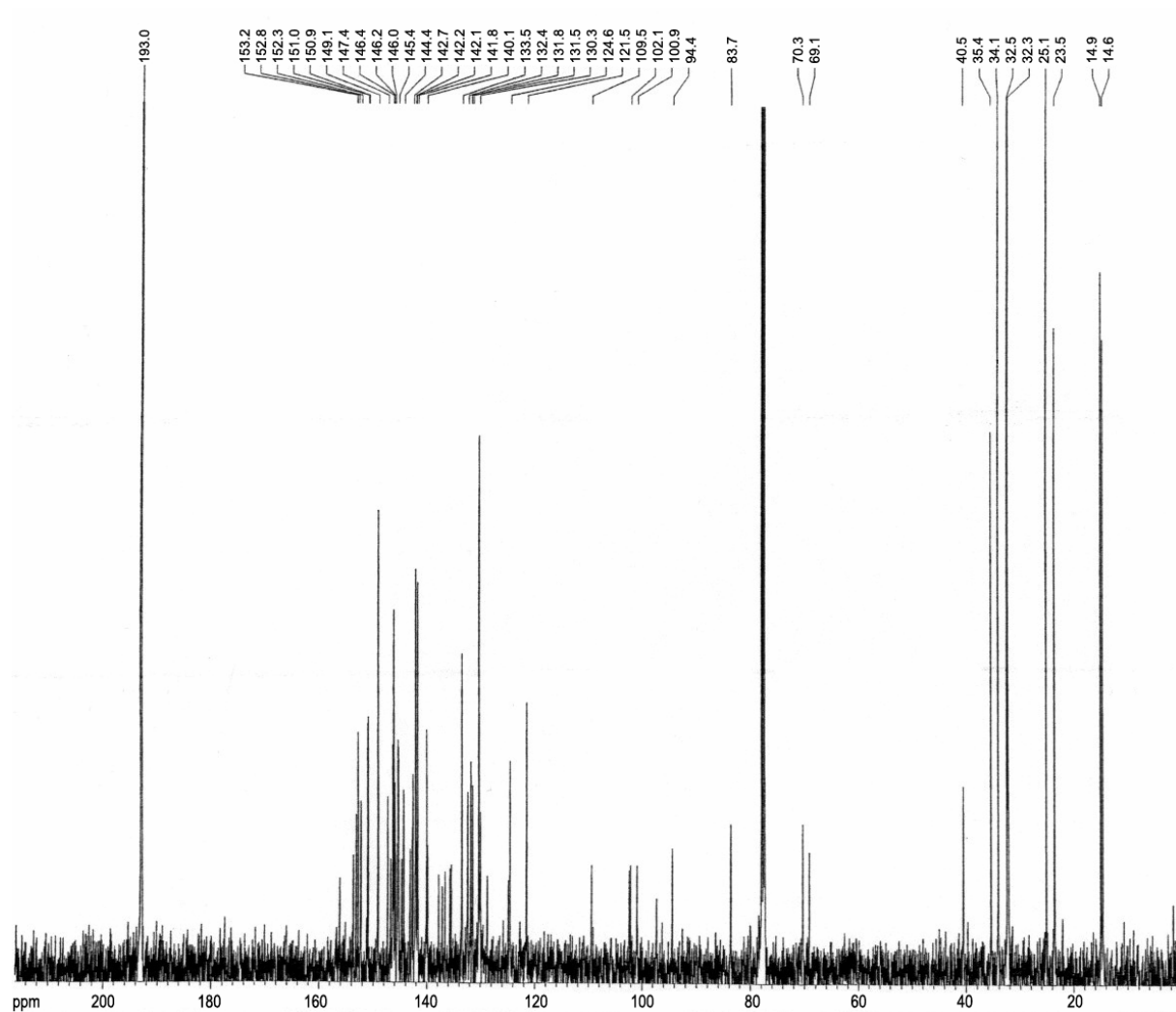
^1H NMR (400 MHz, $\text{CDCl}_3/\text{CS}_2$ 1:1)



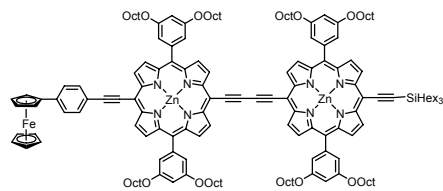
Si-P₁-C₆₀:



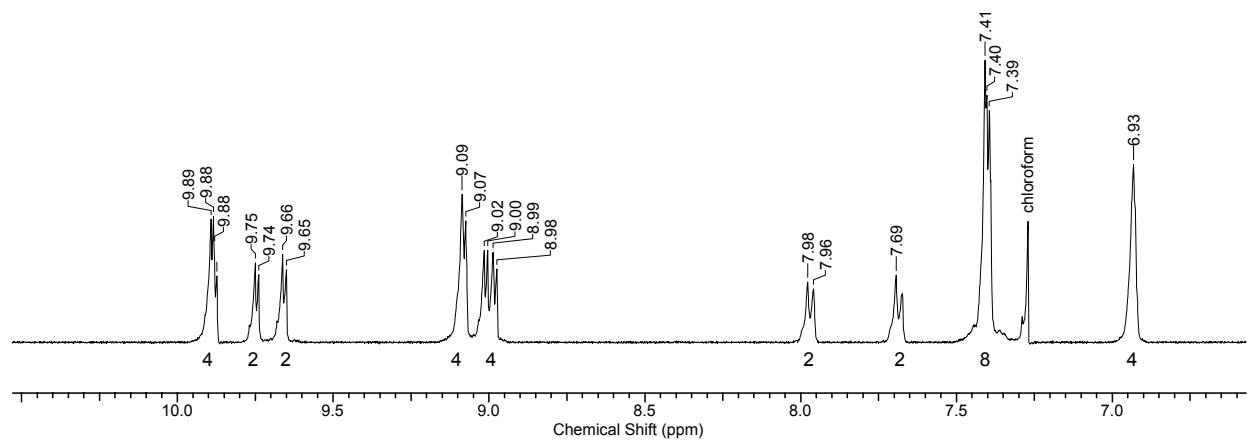
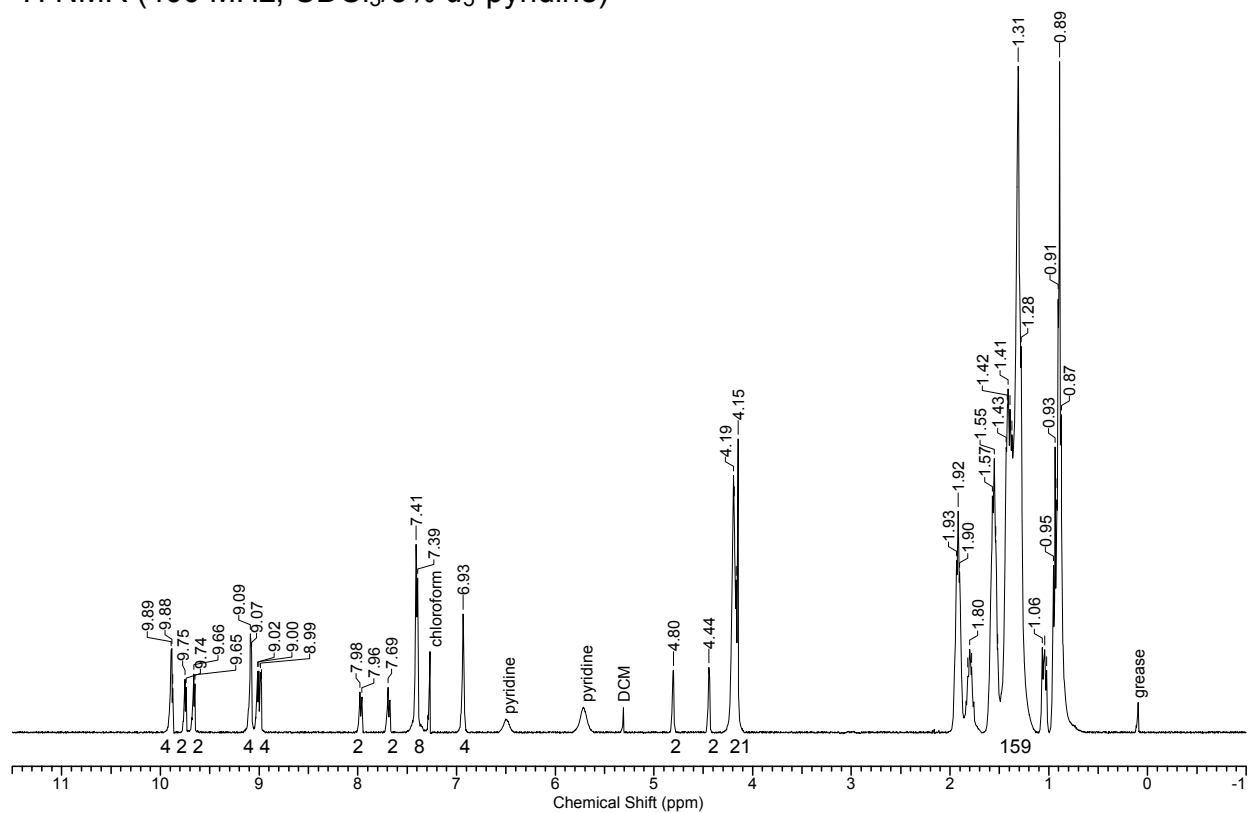
¹³C NMR (100 MHz, CDCl₃/CS₂ 1:1)



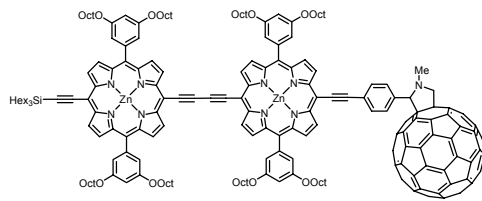
Fc-P₂-Si:



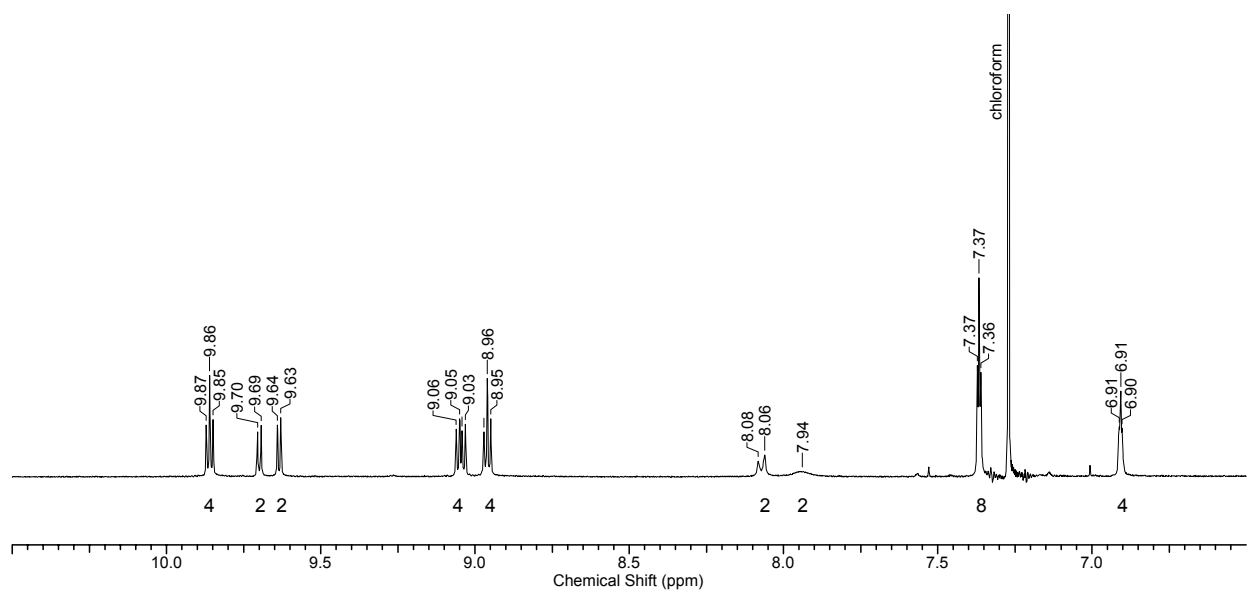
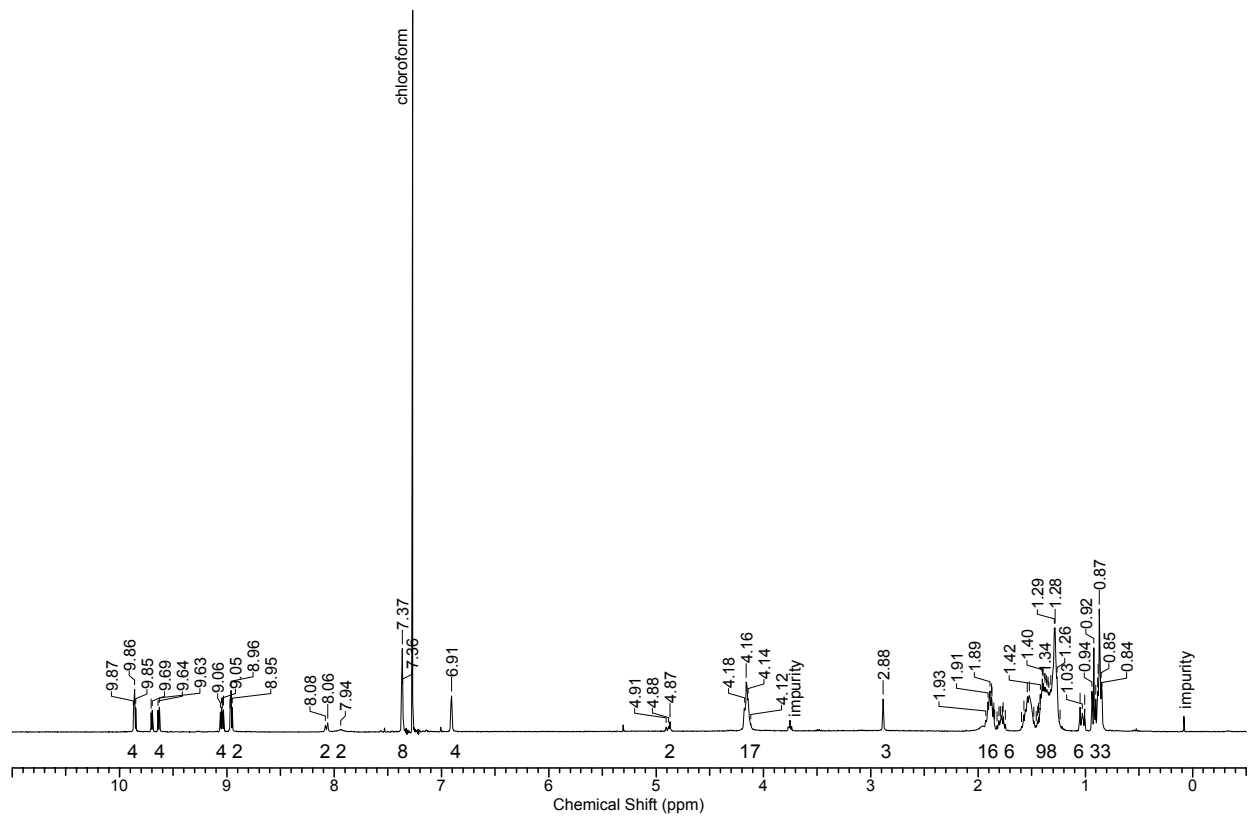
¹H NMR (400 MHz, CDCl₃/5% d₅-pyridine)



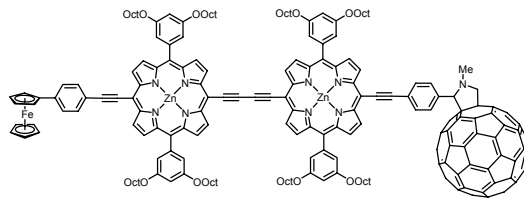
Si-P₂-C₆₀:



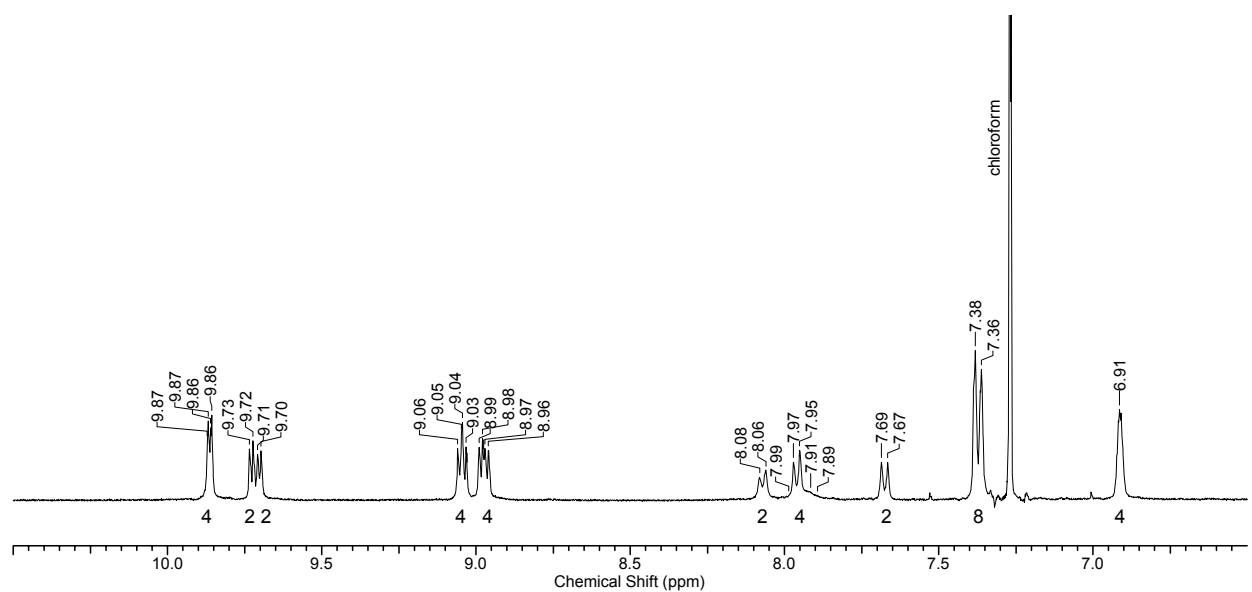
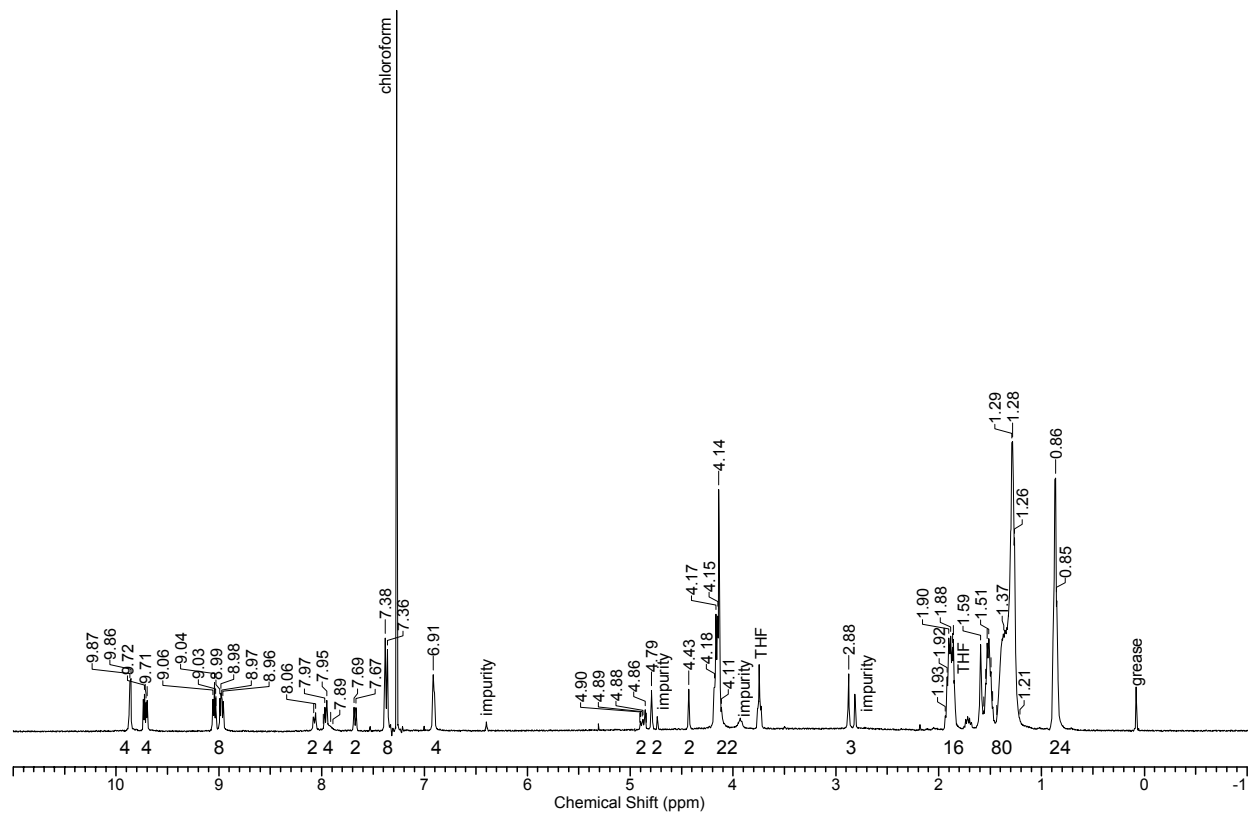
¹H NMR (400 MHz, CDCl₃/5% d₅-pyridine)



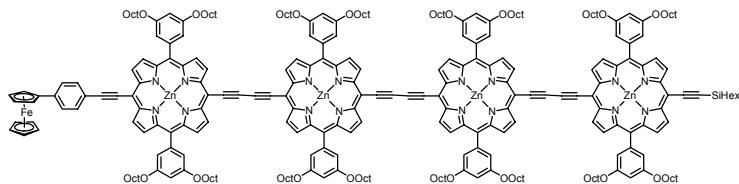
Fc-P₂-C₆₀:



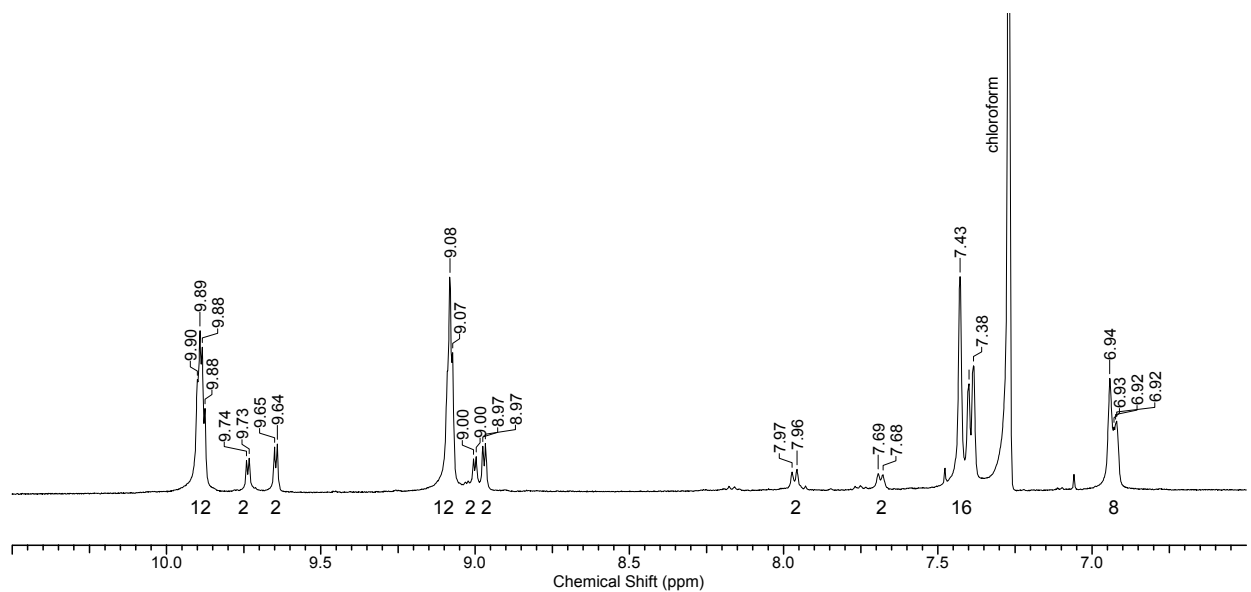
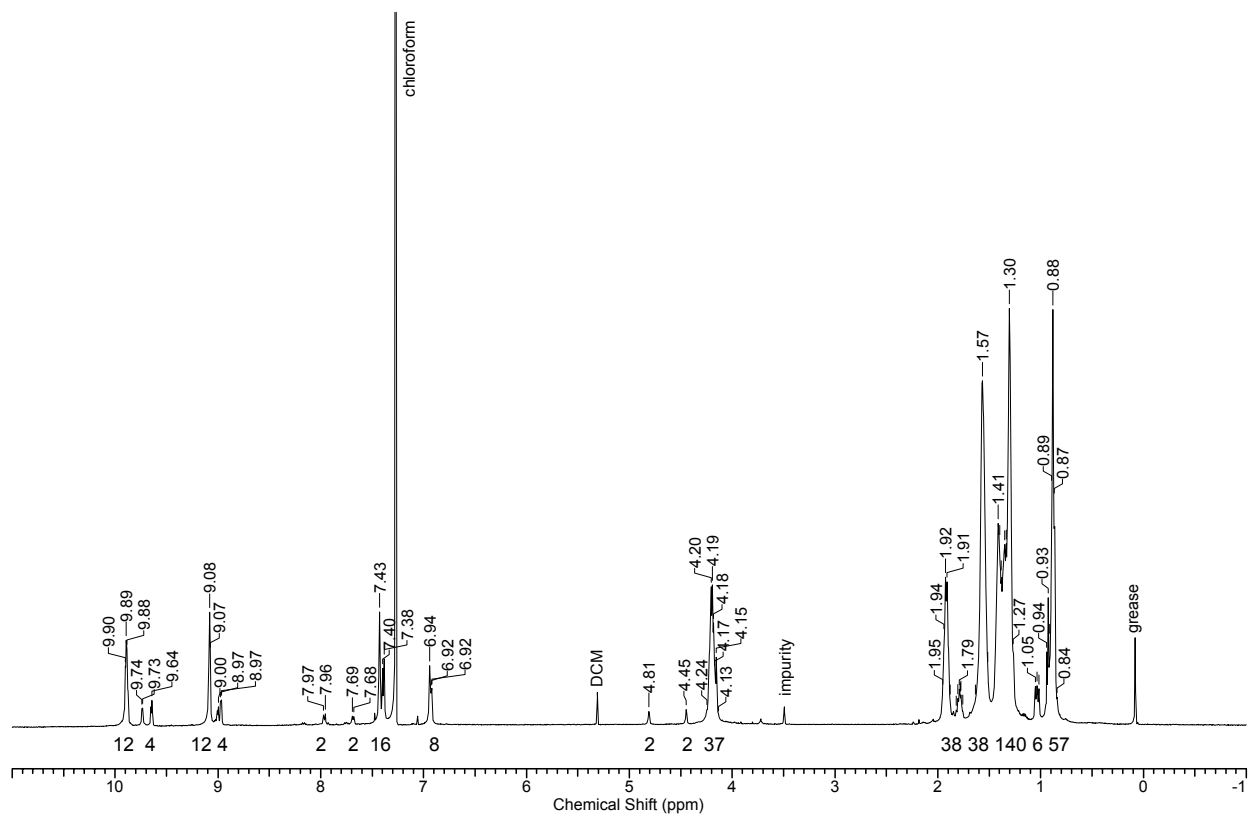
¹H NMR (400 MHz, CDCl₃/5% d₅-pyridine)



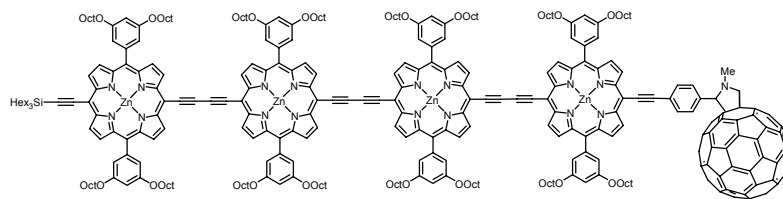
Fc-P₄-Si:



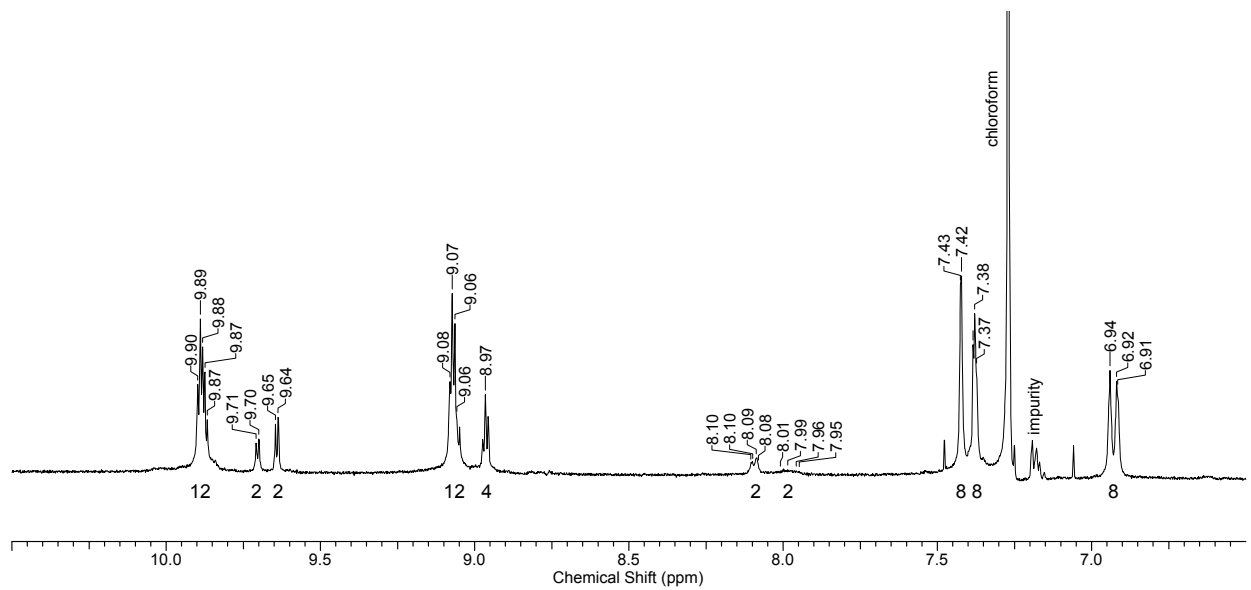
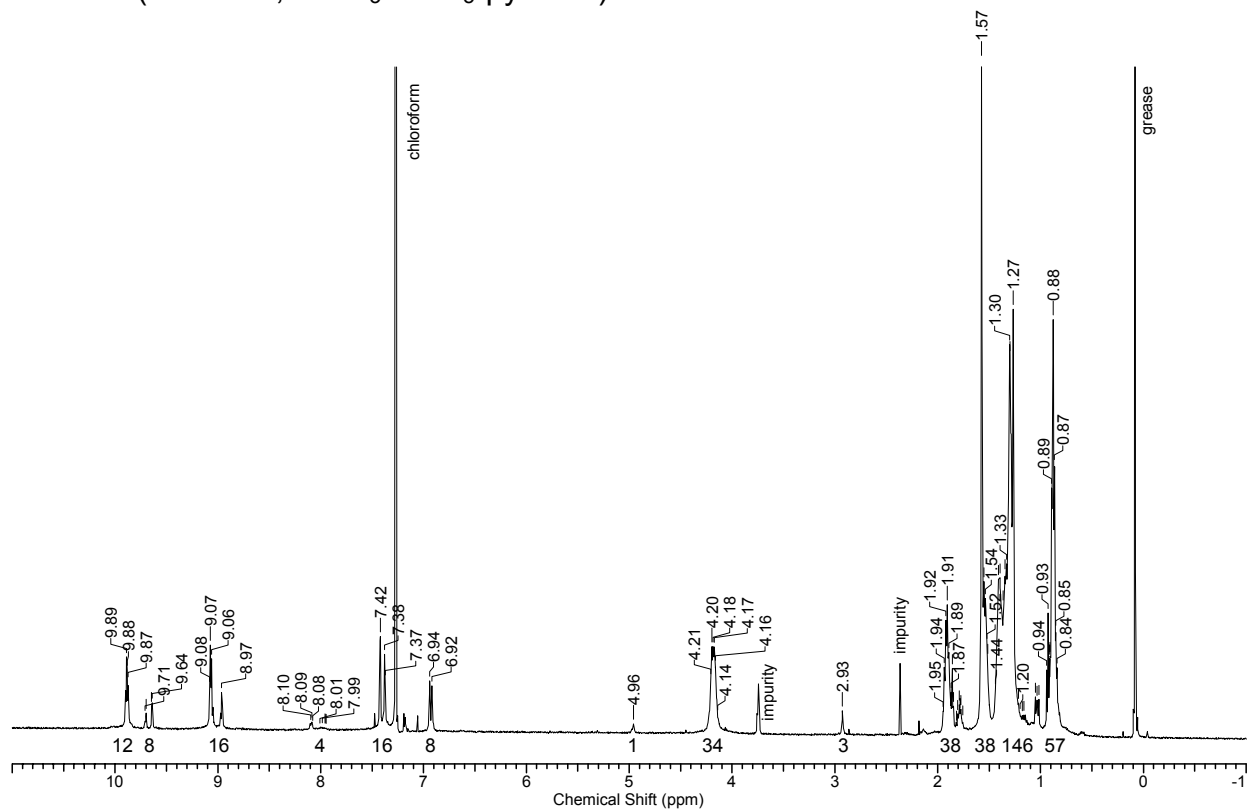
¹H NMR (500 MHz, CDCl₃/5% d₅-pyridine)



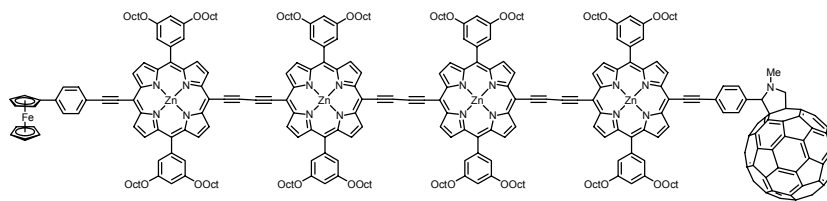
Si-P₄-C₆₀:



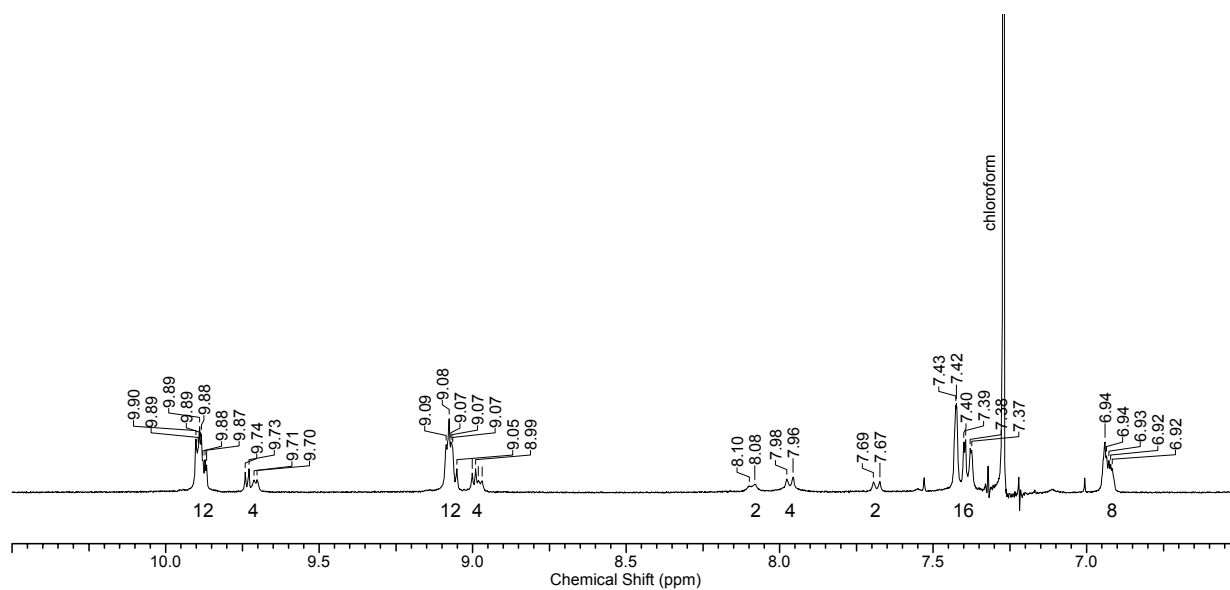
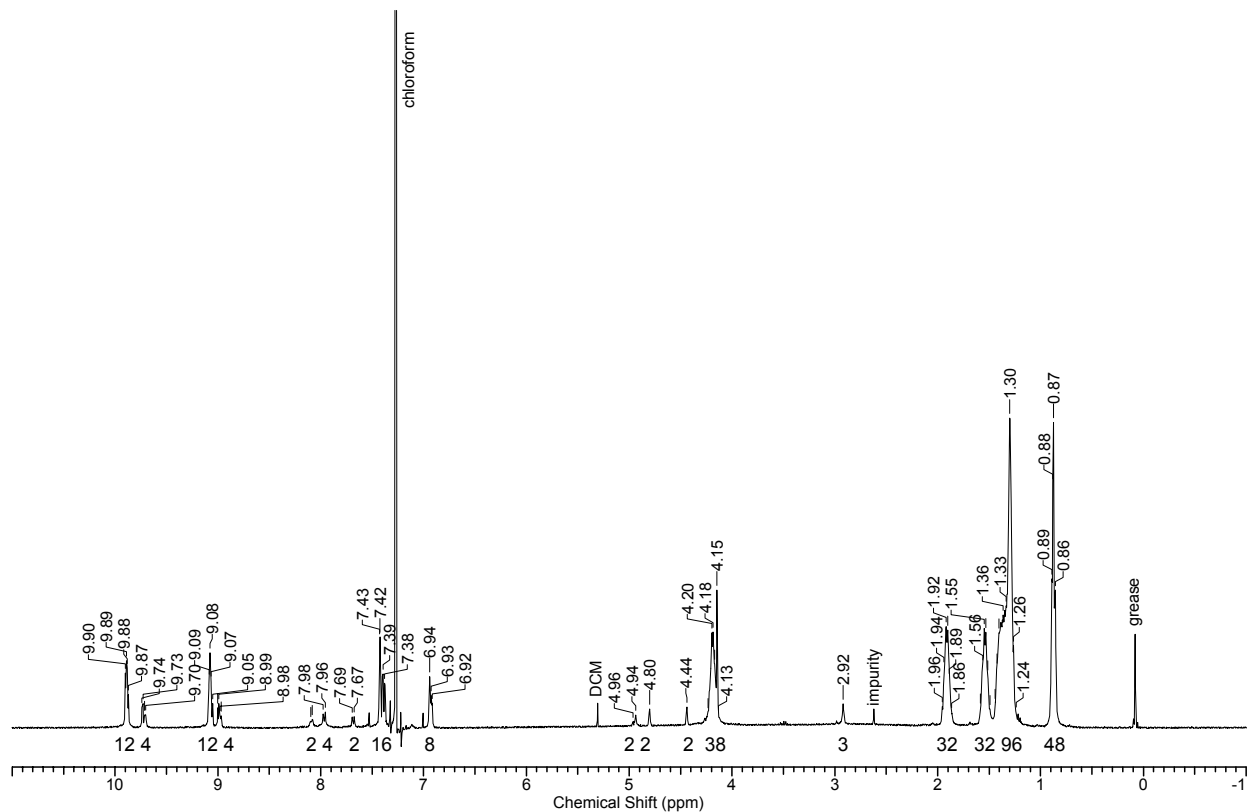
¹H NMR (500 MHz, CDCl₃/5% d₅-pyridine)



Fc-P₄-C₆₀:



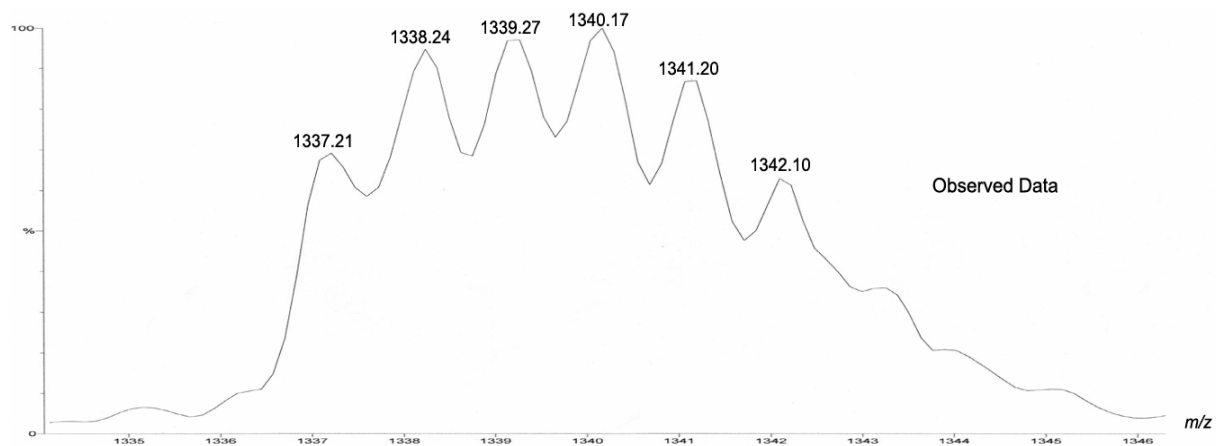
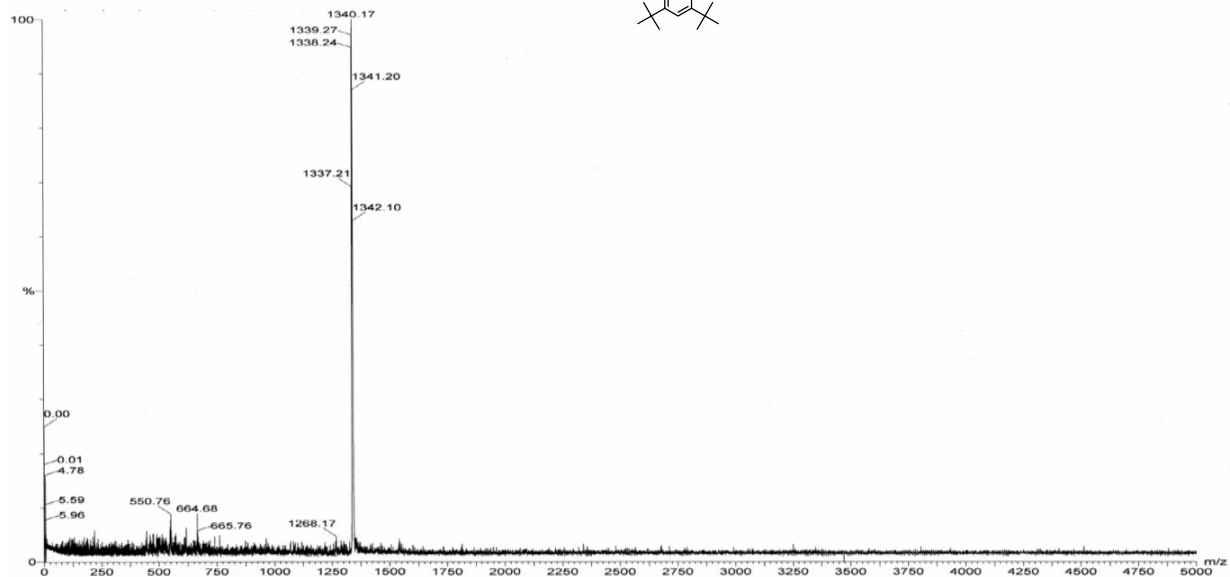
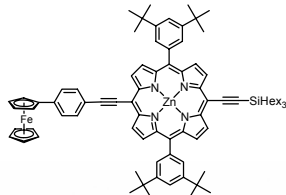
¹H NMR (500 MHz, CDCl₃/5% d₅-pyridine)



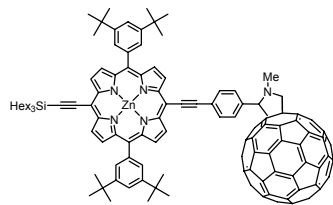
Section 9 – Mass Spectra

Fc-P₁-Si:

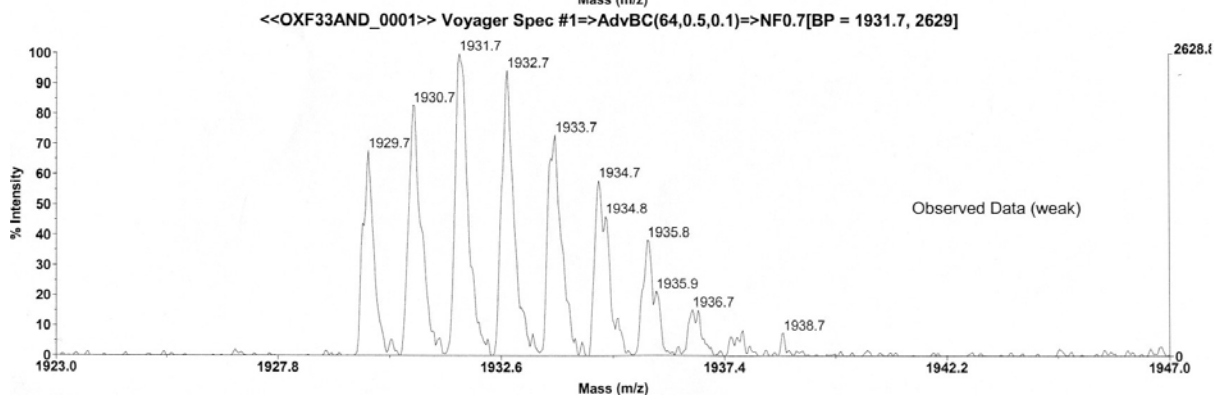
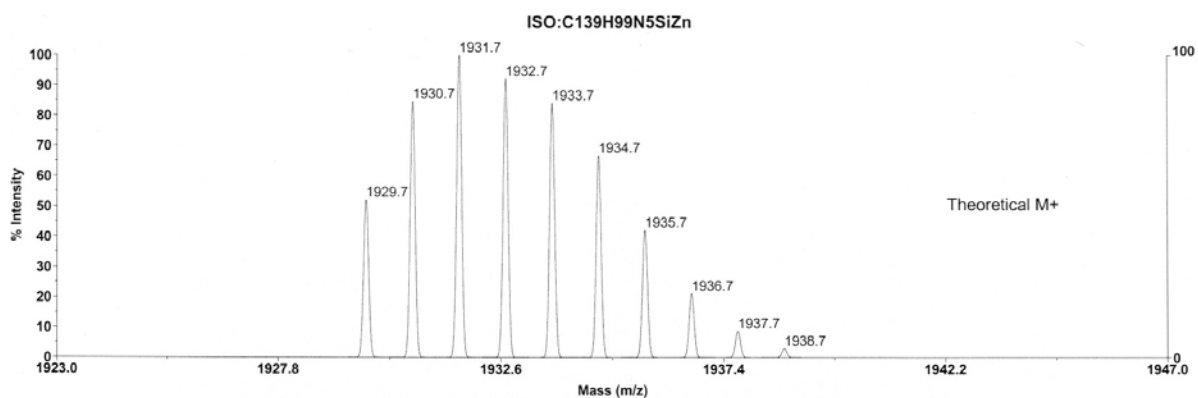
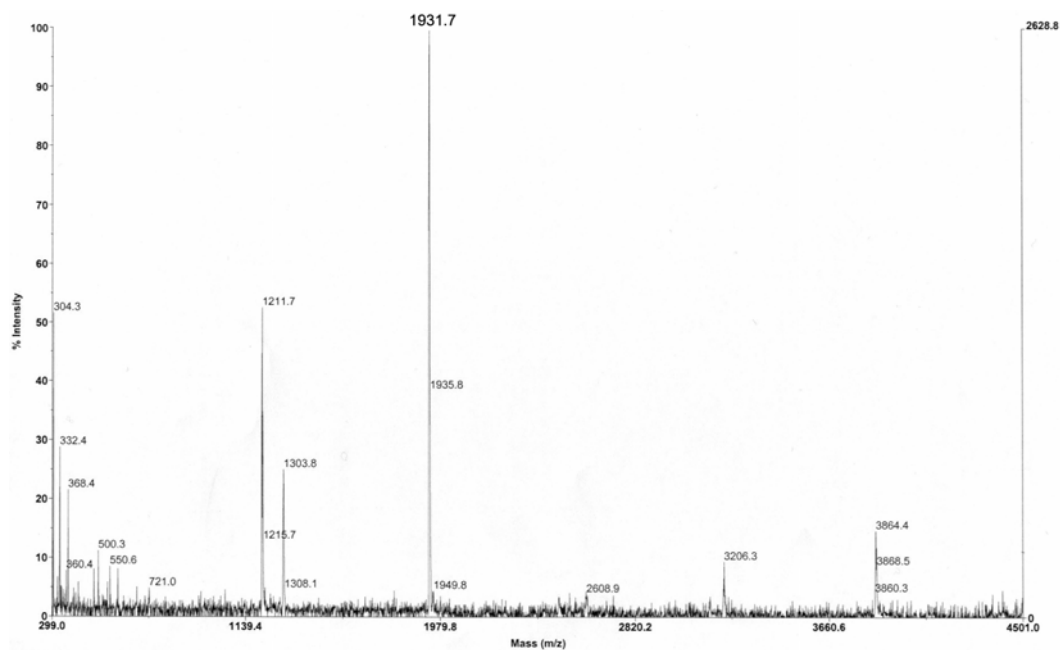
Matrix: Dithranol



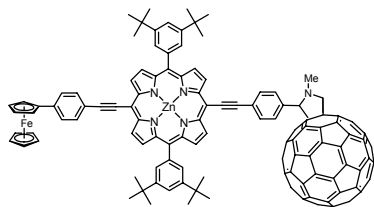
Si-P₁-C₆₀:



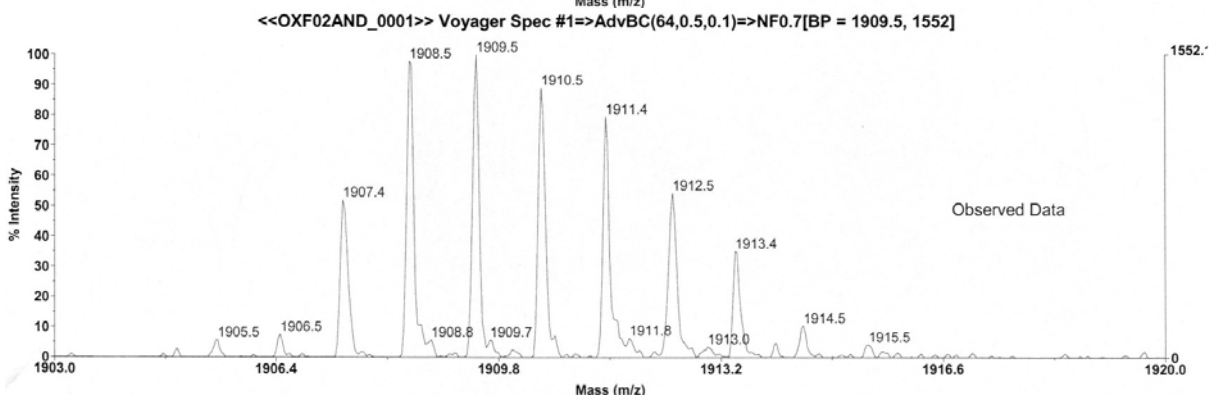
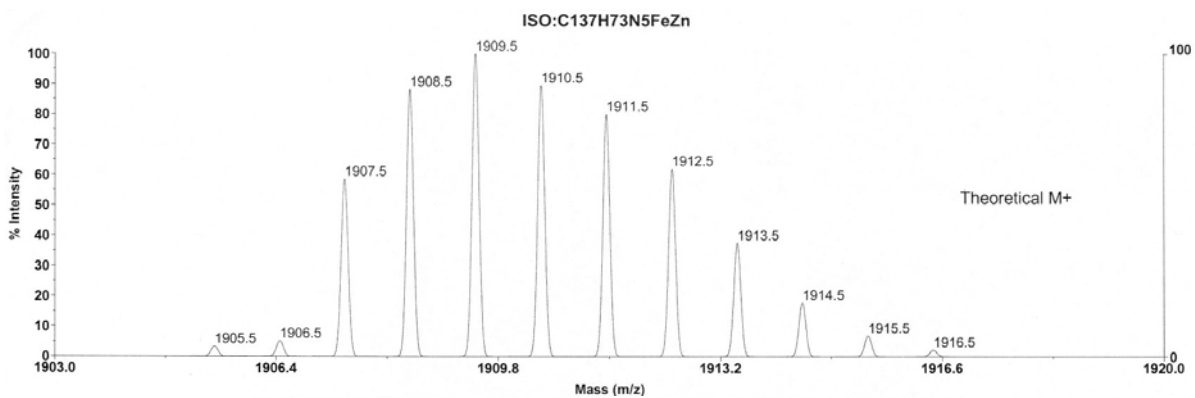
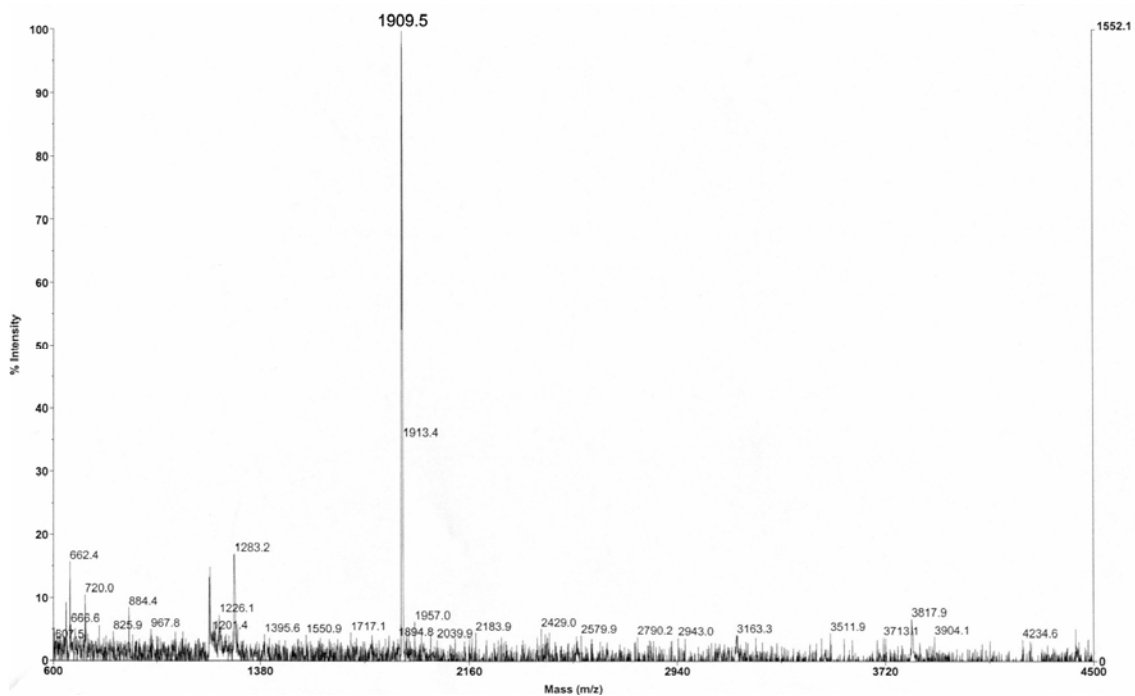
Matrix: DCTB



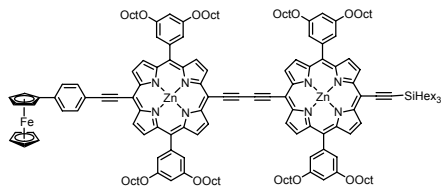
Fc-P₁-C₆₀:



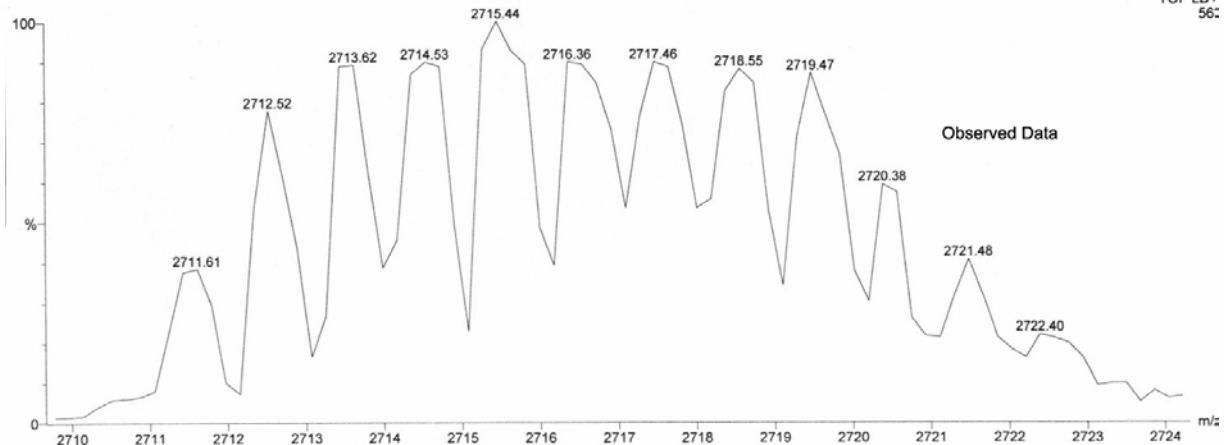
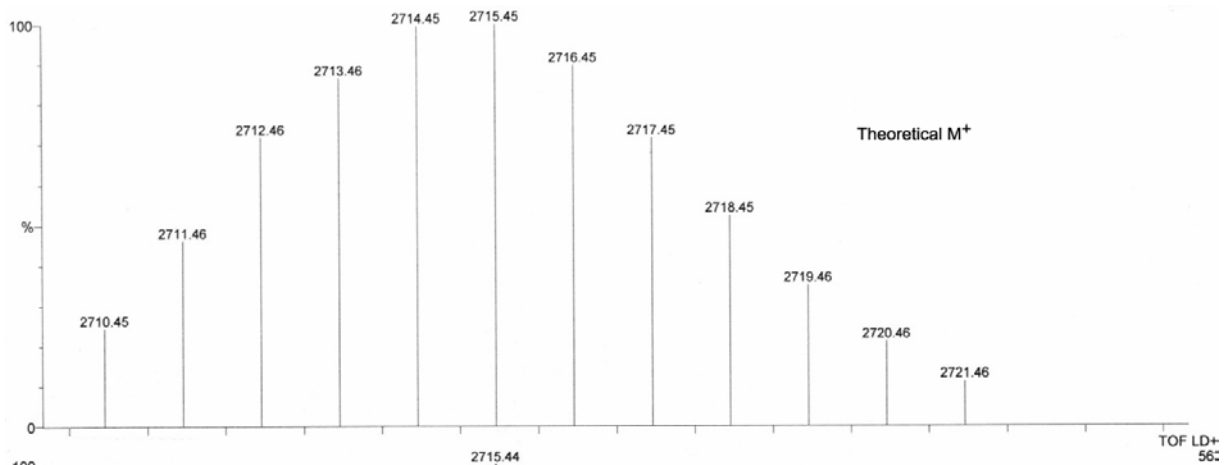
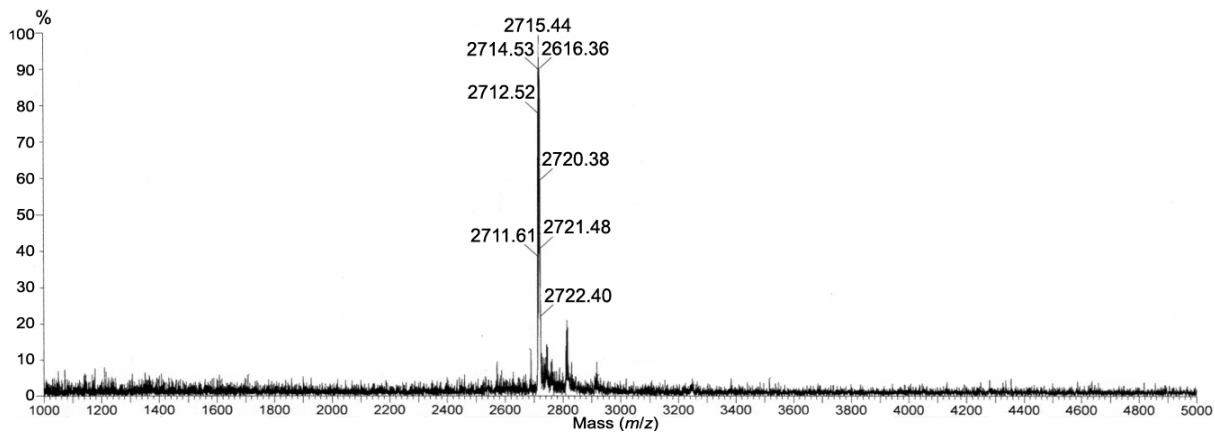
Matrix: DCTB



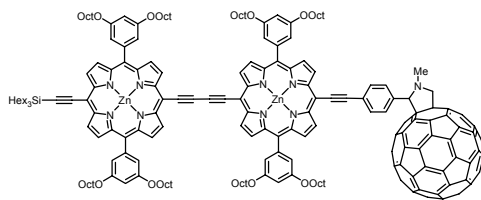
Fc-P₂-Si:



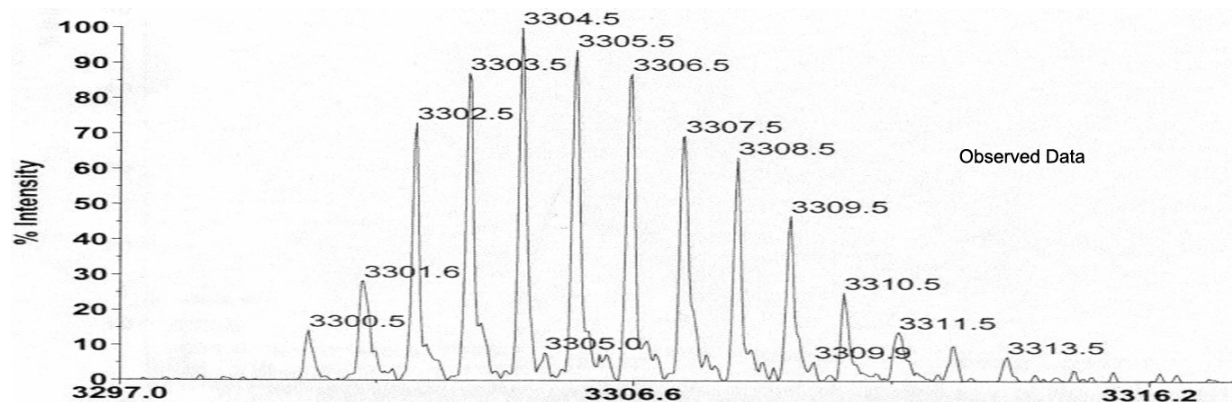
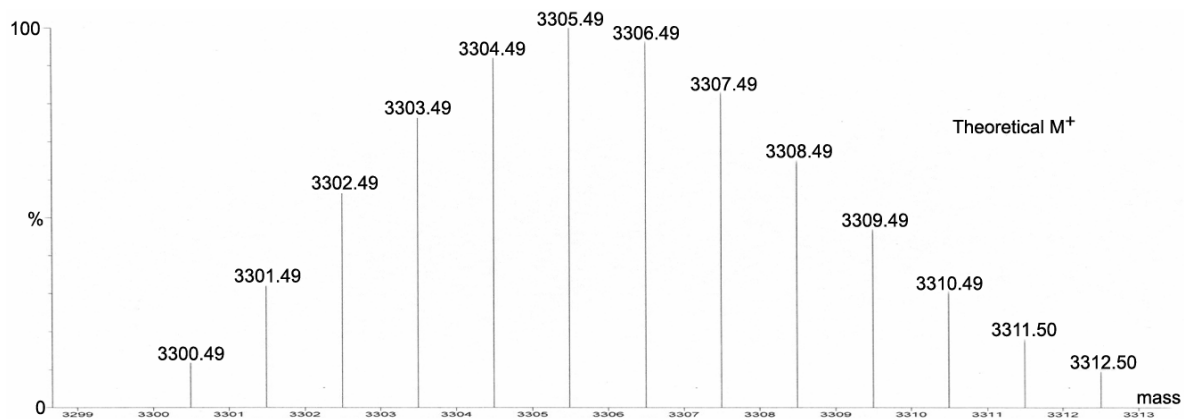
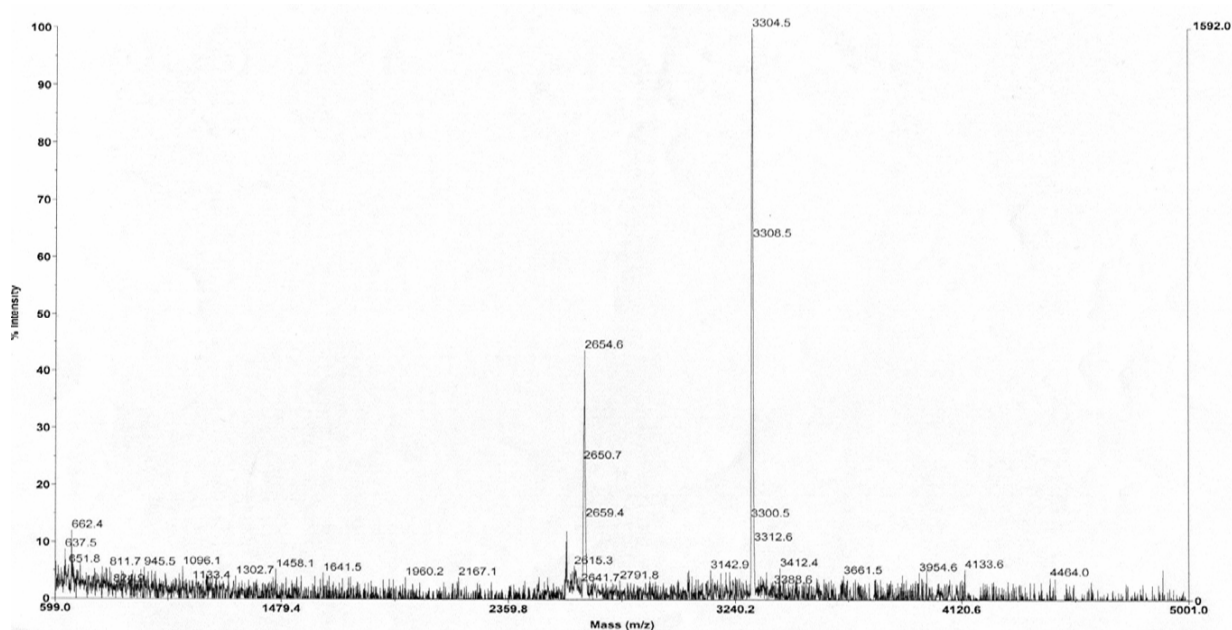
Matrix: Dithranol



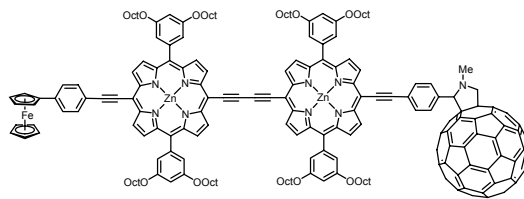
Si-P₂-C₆₀:



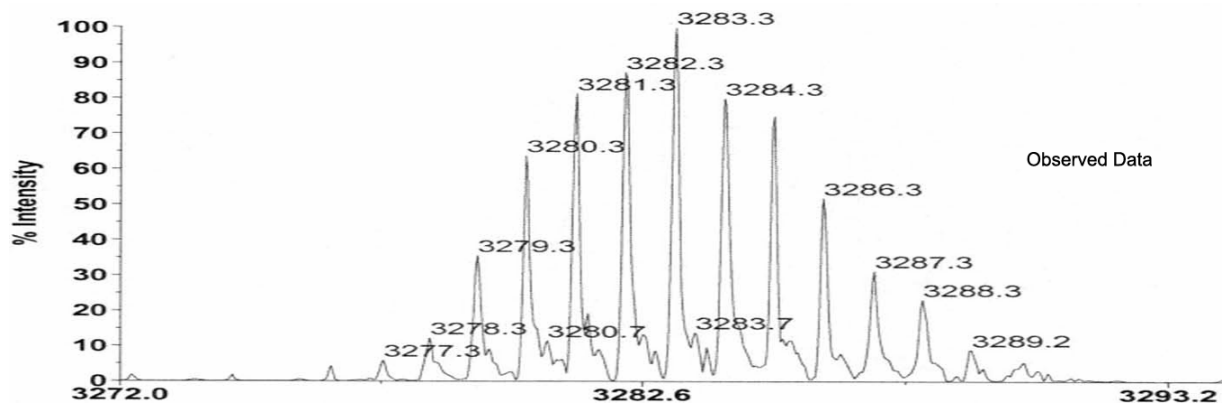
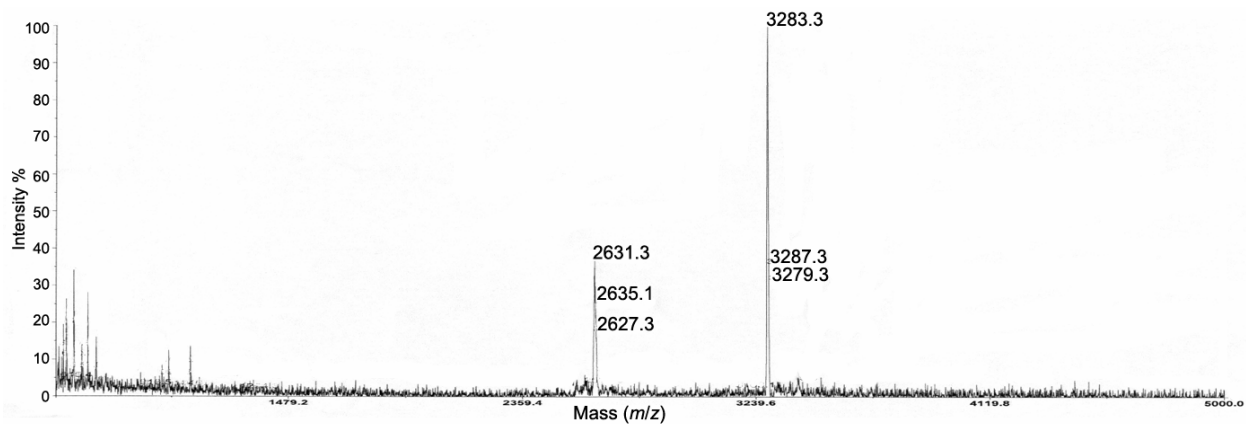
Matrix: DCTB



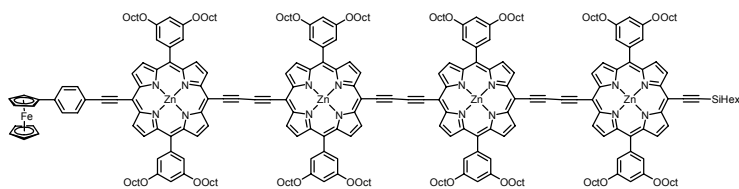
Fc-P₂-C₆₀:



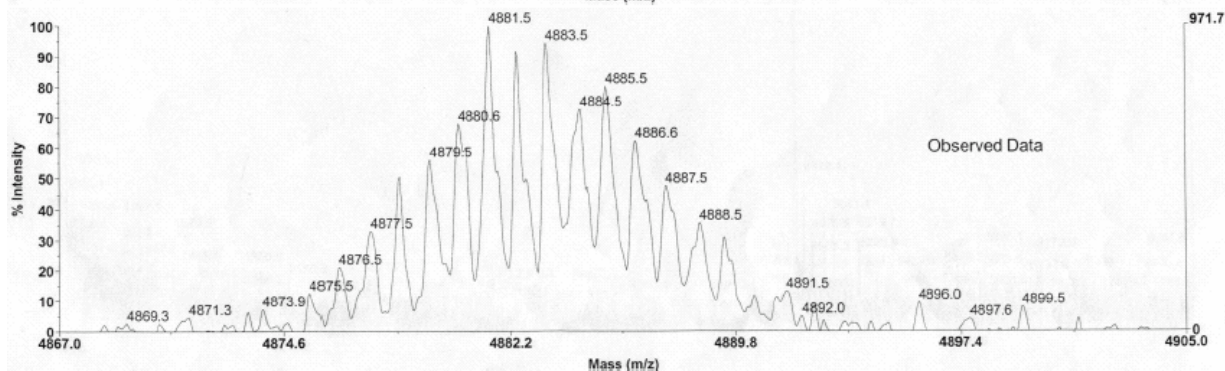
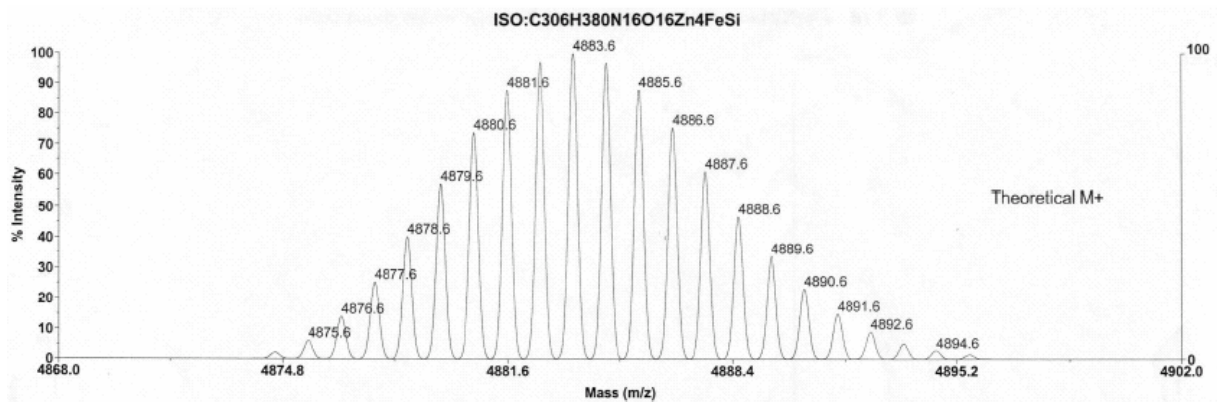
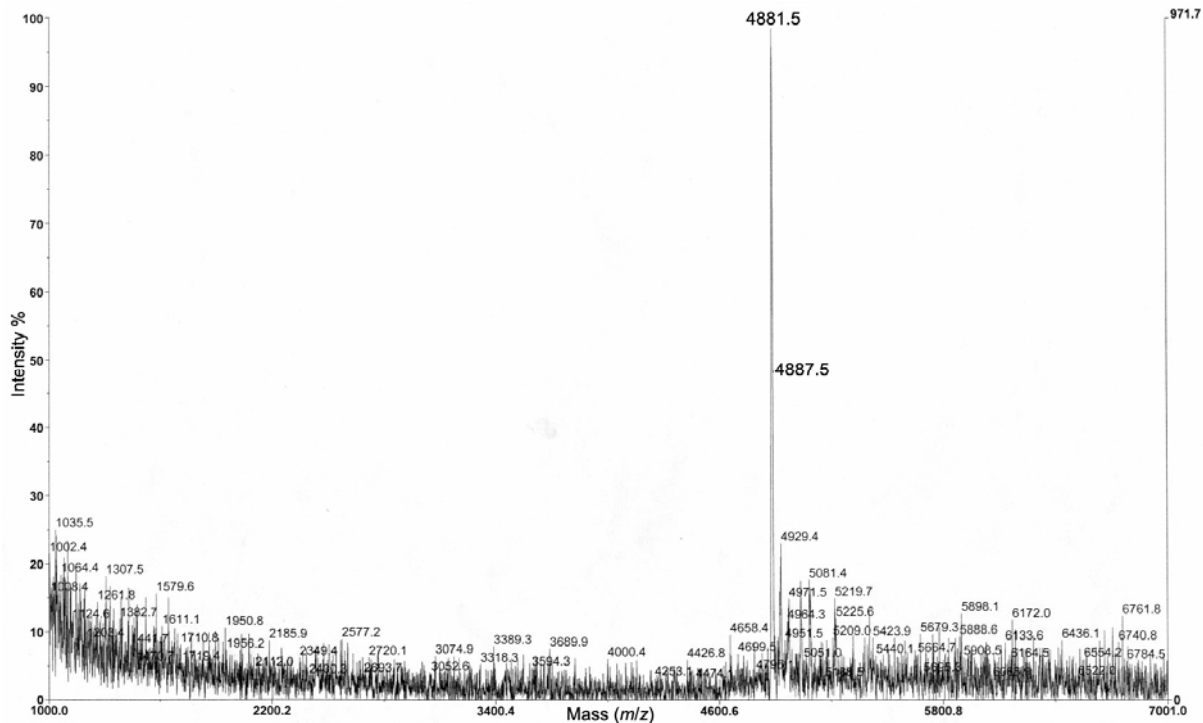
Matrix: DCTB



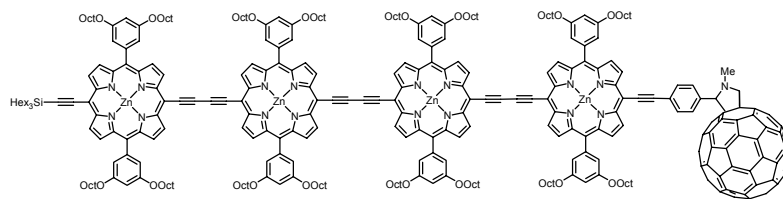
Fc-P₄-Si:



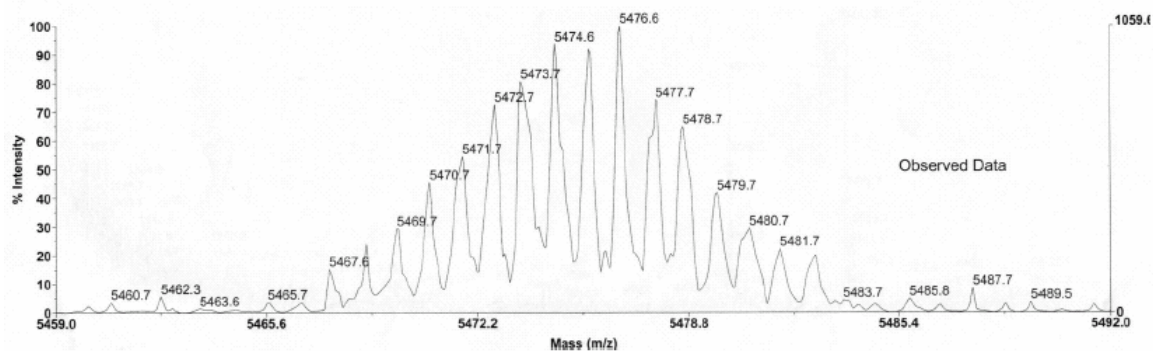
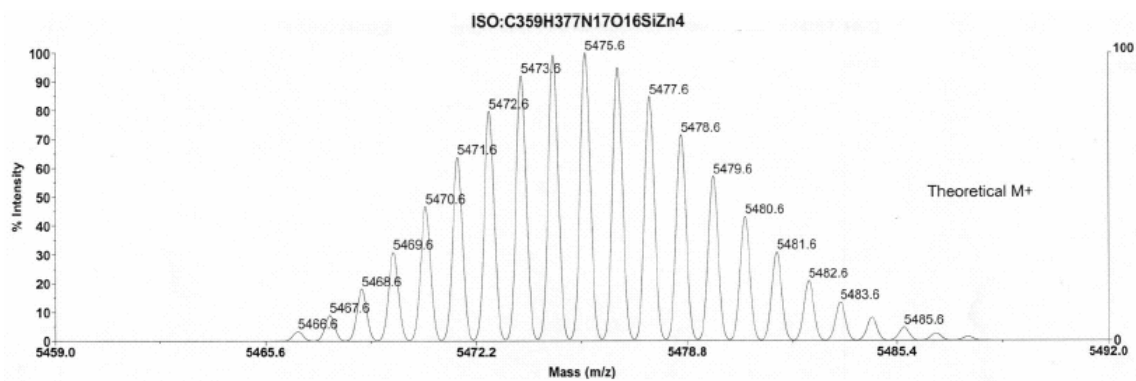
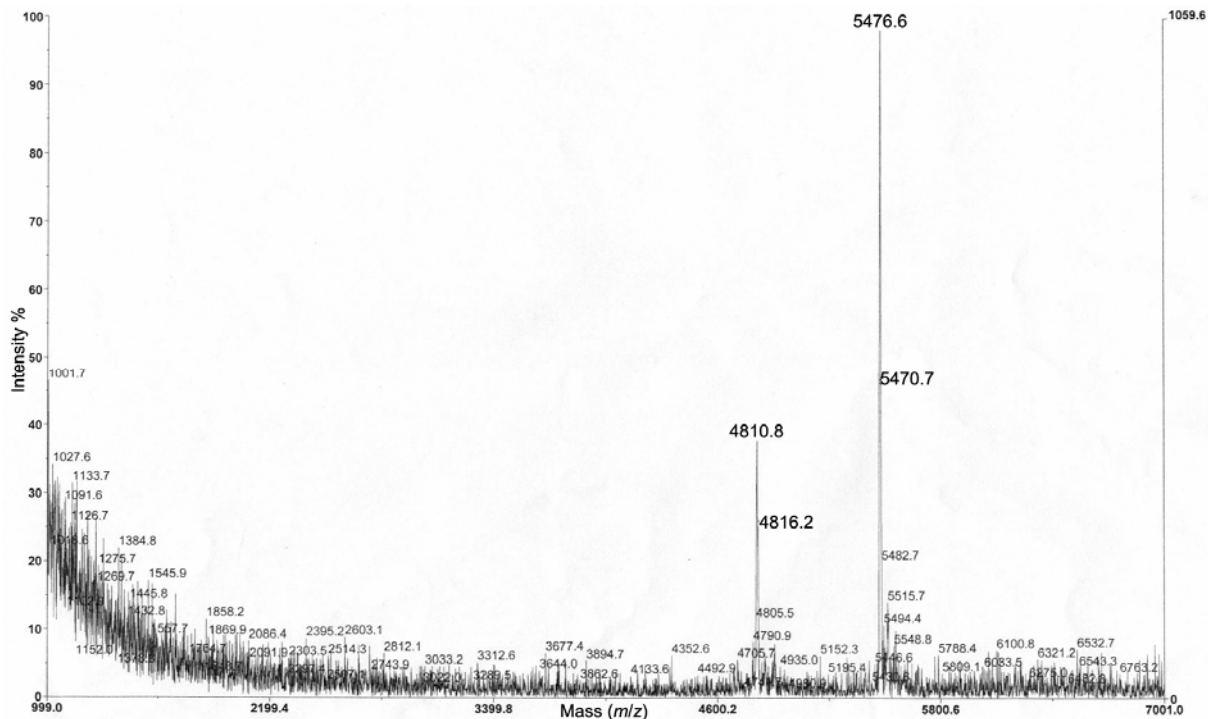
Matrix: DCTB



Si-P₄-C₆₀:

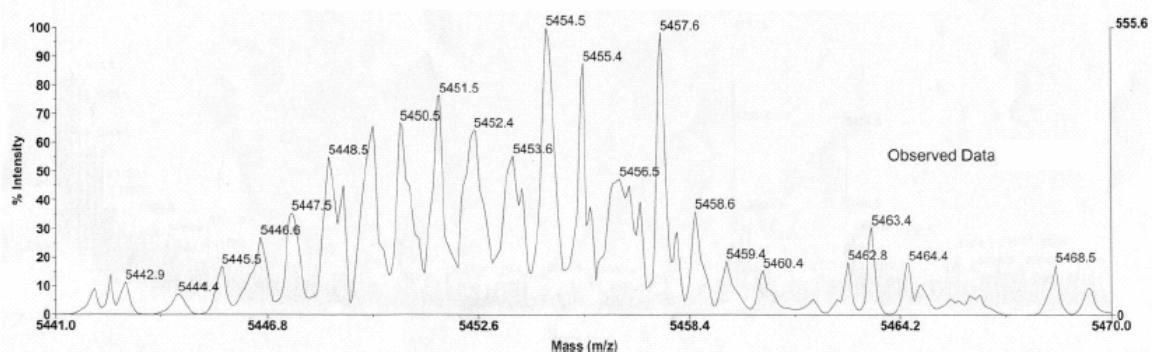
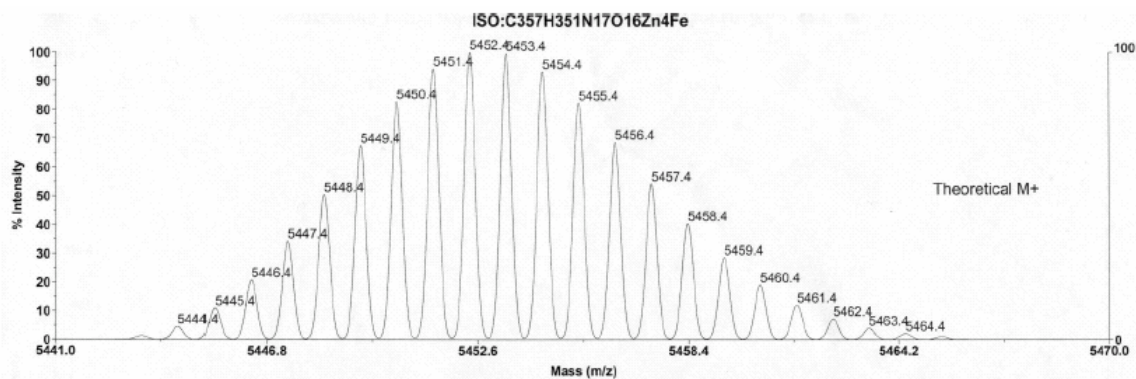
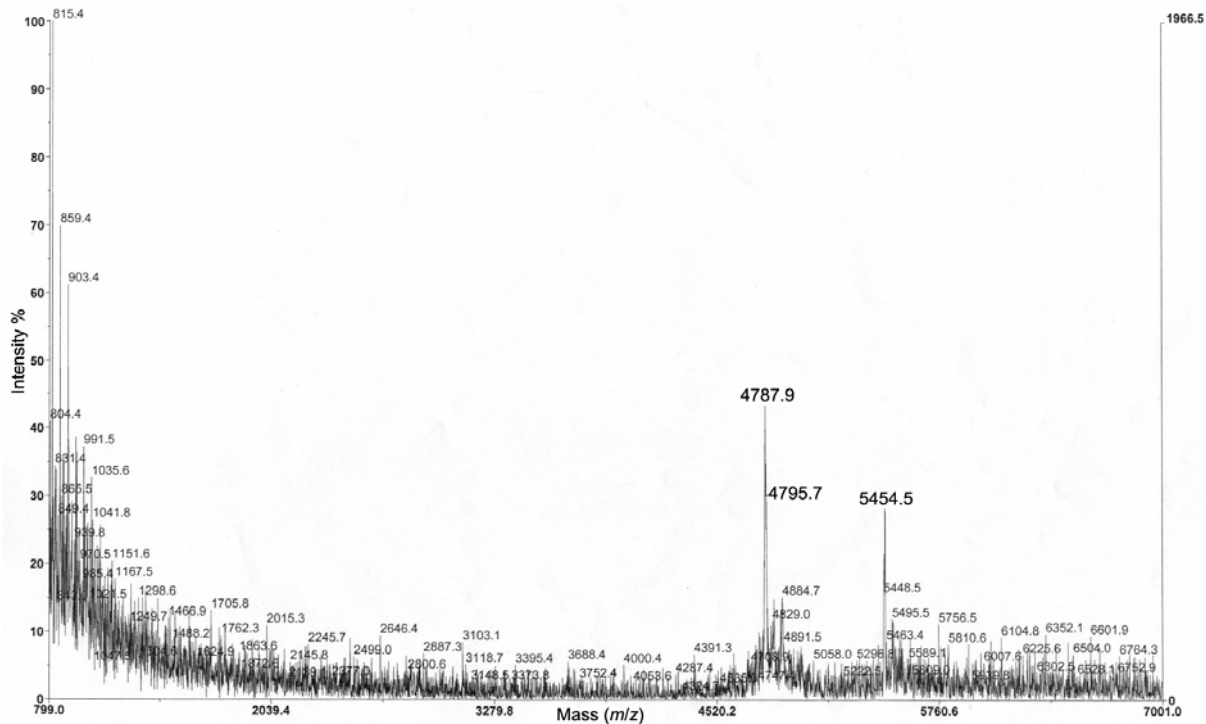
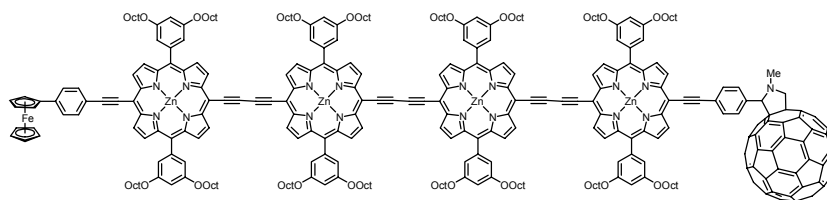


Matrix: DCTB



Fc-P₄-C₆₀:

Matrix: DCTB



Section 10: References

- (1) Rohmer, M. M.; Veillard, A.; Wood, M. H. *Chem. Phys. Lett.* **1974**, *29*, 466.
- (2) Armstrong, A. T.; Smith, F.; Elder, E.; McGlynn, S. P. *J. Chem. Phys.* **1967**, *46*, 4321.
- (3) Anderson, H. L. *Chem. Comm.* **1999**, 2323.
- (4) Taylor, P. N.; Huuskonen, J.; Rumbles, G.; Aplin, R. T.; Williams, E.; Anderson, H. L. *Chem. Commun.* **1998**, 909.
- (5) Dubois, D.; Kadish, K. M.; Flanagan, S.; Haufler, R. E.; Chibante, L. P. F.; Wilson, L. J. *J. Am. Chem. Soc.* **1991**, *113*, 4364. Stinchcombe, J.; Penicaud, A.; Bhyrappa, P.; Boyd, P. D. W. Reed, C. A. *J. Am. Chem. Soc.* **1993**, *115*, 5212. Khaled, M. M.; Carlin, R. T.; Trulove, P. C. Eaton, G. R.; Eaton, S. S. *J. Am. Chem. Soc.* **1994**, *116*, 3465.
- (6) Wilson, G. J.; Arnold, D. P. *J. Phys. Chem. A* **2005**, *109*, 6104.
- (7) Arnold, D. P.; Hartnell, R. D.; Heath, G. A.; Newby, L.; Webster, R. D. *Chem. Commun.* **2002**, 754.
- (8) Arnold, D. P.; Heath, G. A.; James, D. A. *J. Porphyrins Phthalocyanines* **1999**, *3*, 5.
- (9) Kuimova, M. K.; Hoffmann, M.; Winters, M. U.; Eng, M.; Clark, I. P.; Collins, H. A.; Balaz, M.; Tavender, S. M.; Wilson, C. J.; Albinsson, B.; Anderson, H. L.; Parker, A. W.; Phillips, D., manuscript in preparation
- (10) Ishimura, K.; Hada, M.; Nakatsujii, H. *J. Chem. Phys.* **2002**, *117*, 6533.
- (11) Ambroise, A.; Wagner, R. W.; Rao, P. D.; Riggs, J. A.; Hascoat, P.; Diers, J. R.; Seth, J.; Lammi, R. K.; Bocian, D. F.; Holten, D.; Lindsey, J. S. *Chem. Mater.* **2001**, *13*, 1023.